AD-A239 274

DOCUMENTATION PAGE

Form Approved
OMB No. 0704-0188

1. AGENCY USE ONLY (Leave blank)	2. REPORT DATE	3. REPORT TYPE AND DATES COVERED
		THESIS/DISSERTATION

4. TITLE AND SUBTITLE
Retrofit Strengthening of a Seismically Inadequate Reinforced Concrete Frame Using Pre-stressed Cable Bracing Systems and Beam Alteration

5. FUNDING NUMBERS

6. AUTHOR(S)
James E. Welter, Captain

7. PERFORMING ORGANIZATION NAME(S) AND ADDRESS(ES)
AFIT Student Attending: University of Oklahoma

8. PERFORMING ORGANIZATION REPORT NUMBER
AFIT/CI/CIA-91-020

9. SPONSORING/MONITORING AGENCY NAME(S) AND ADDRESS(ES)
AFIT/CI
Wright-Patterson AFB OH 45433-6583

10. SPONSORING/MONITORING AGENCY REPORT NUMBER

11. SUPPLEMENTARY NOTES

12a. DISTRIBUTION/AVAILABILITY STATEMENT
Approved for Public Release IAW 190-1
Distributed Unlimited
ERNEST A. HAYGOOD, 1st Lt, USAF
Executive Officer

12b. DISTRIBUTION CODE

13. ABSTRACT *(Maximum 200 words)*

91-07318

14. SUBJECT TERMS	15. NUMBER OF PAGES 190
	16. PRICE CODE

17. SECURITY CLASSIFICATION OF REPORT	18. SECURITY CLASSIFICATION OF THIS PAGE	19. SECURITY CLASSIFICATION OF ABSTRACT	20. LIMITATION OF ABSTRACT

THE UNIVERSITY OF OKLAHOMA

GRADUATE COLLEGE

RETROFIT STRENGTHENING OF A SEISMICALLY INADEQUATE REINFORCED CONCRETE FRAME USING PRESTRESSED CABLE BRACING SYSTEMS AND BEAM ALTERATION

A THESIS

SUBMITTED TO THE GRADUATE FACULTY

in partial fulfillment of the requirements for the

degree of

MASTER OF SCIENCE

By

JAMES E. WELTER

Norman, Oklahoma

1991

RETROFIT STRENGTHENING OF A SEISMICALLY INADEQUATE REINFORCED CONCRETE FRAME USING PRESTRESSED CABLE BRACING SYSTEMS AND BEAM ALTERATION

A THESIS

APPROVED FOR THE SCHOOL OF

CIVIL ENGINEERING AND ENVIRONMENTAL SCIENCE

BY

Thomas D Burch Jr

Benjamin Wallace

W. R. Tal

Dedicated to My Three Girls

Leslie, Amber, and Ashleigh

ACKNOWLEDGMENTS

The author expresses his heartfelt gratitude to Dr. Thomas D. Bush for his instruction, ideas, guidance, insight, and advise during the course of this research effort. Sincere appreciation is expressed to my committee members, Dr. Benjamin J. Wallace, and Dr. M. R. Tahari as well as Dr. A. Kukreti and Dr. M. Harajali who all offered advise and suggestions when they were needed most.

Special thanks goes to the United States Air Force and the Air Force Institute of Technology for making this experience possible by selecting the author to pursue a M.S. in Civil Engineering. The Air Force provided the time and financial support required to complete this work. Equally important to the author was the support of his wife, Leslie. Written words cannot adequately convey how much her hard work, understanding, companionship, and love contributed to the author throughout the pursuit of this degree as well as every day of his life.

Finally, the author wishes to thank the Lord God for sitting in the chair beside him and never getting up until it was all finished.

TABLE OF CONTENTS

LIST OF TABLES

LIST OF FIGURES

ABSTRACT

The primary objective of this thesis is to study analytically the effectiveness of prestressed cable bracing systems in conjunction with beam alteration as a viable retrofit strengthening scheme for seismically inadequate reinforced concrete structures. The prototype building studied features a strong beam-weak column lateral force resisting frames. The failure mechanism is non-ductile and dominated by shear failure of the reinforced concrete short columns. The analytical study is carried out using DRAIN-2D, a general purpose computer program for dynamic or static incremental analysis of inelastic plane frame structures.

In the first part of the study the effectiveness of prestressed cable bracing on the response of a single story subassemblage of the prototype frame is re-examined. The concept of beam alteration is then introduced. A parametric study is conducted to examine how systematically weakening the spandrel beams affects the frame's failure mechanism. The response of unstrengthened, braced-unaltered and braced-altered subassemblages are studied under both monotonic and cyclic incremental displacements.

The focus of the second part of the research is on the behavior of a six story subassemblage of the prototype frame to retrofit strengthening. The response of unstrengthened, braced-unaltered, and

braced-altered unique single story subassemblages are studied and compared to the response predicted by a six story subassemblage. The retrofit schemes are evaluated with respect to their adequacy for meeting current building code seismic strength requirements.

In the third part of the thesis some practical aspects of designing and installing prestressed cable bracing systems are discussed. Several connection details are presented which illustrate conceptually how prestressed cable braces might be attached to a structure in a retrofitting operation.

It was concluded analytically that prestressed cable bracing and beam alteration used in combination can be an effective retrofit strengthening scheme. For the prototype frame studied significant improvements in strength, ductility, and failure mechanism were achieved in the retrofitted frame over that of the original frame.

RETROFIT STRENGTHENING OF A SEISMICALLY INADEQUATE REINFORCED CONCRETE FRAME USING PRESTRESSED CABLE BRACING SYSTEMS AND BEAM ALTERATION

CHAPTER 1

INTRODUCTION

1.1 GENERAL

A tremendous outpouring of knowledge has been gained in the last twenty years concerning the behavior of structures to seismic loads. This increased understanding of seismic behavior has lead to a significant improvement in our ability to design and build new structures which are adequately equipped to resist significant seismic loads. Extensive investigation of failed structures in the aftermath of recent earthquakes, as well as knowledge derived from numerous experimental laboratory investigations, have led to new seismic design codes which guide engineers in designing new structures. However, surprisingly little attention has thus far been directed toward improving the seismic performance of existing structures to future earthquakes.

Studies made following some recent major earthquakes suggest that a large number of existing structures may not perform satisfactorily in an earthquake and therefore are probably not safe. Many reinforced concrete frame structures built in seismically active areas are likely to fail in future earthquakes. For safety sake, such structures should be replaced, demolished, or modified. In many cases it is not economically feasible or desirable to replace or demolish such

structures. It then becomes important to look at methods of modifying or retrofitting these structures to resist seismic loads. Much new research is needed to devise effective, practical, economical and aesthetically pleasing methods of seismic retrofitting.

The goal of any retrofitting scheme is to improve the structure's performance in future earthquakes. This can be done by improving the structure's strength, stiffness, ductility, or some combination of the three. More often than not, it is the structure's lack of ductility which is the primary concern. Ductility is the ability to maintain strength under large deformations in the inelastic range. The structure's failure mechanism is also of prime concern. The structure may be able to resist quite large lateral displacements; however, when its ultimate capacity is reached, the failure could be very sudden and catastrophic. It is thus apparent that strength, ductility and failure mechanism must be considered in the development of any viable retrofitting scheme.

The most likely candidate for seismic retrofitting is a building which is adequate to carry its intended gravity loads but is inadequate to carry the lateral seismic design loads. Such structures may be deficient in lateral capacity for several reasons, such as:

1. The seismic code design loads may have been increased since the building was constructed.
2. The building may have undergone damage in a previous earthquake.

3. Design or construction errors have been discovered or suspected.
4. Changes in the building's original intended use have occurred.

There are generally four major retrofitting techniques available today to improve the seismic performance of existing reinforced concrete structures. They are steel bracing systems, shear walls, wing walls, and column strengthening. Each of these techniques is discussed briefly below.

1. **Steel bracing systems.** A simple steel bracing application is shown in Fig. 1.1a. A steel bracing system is most feasible if it is attached to the exterior of a building's exterior frames. Column strengthening, wing walls, and shear walls often require significant alteration to the interior of the building. This is typically not true for steel bracing systems. The fact that steel bracing systems can be installed with minimal disruption to the building's current function and its occupants is a major advantage over other retrofitting techniques.
2. **Shear walls.** Application of shear walls is illustrated in Fig. 1.1b. Shear walls are created by infilling certain bays, usually the bays of interior frames. Shear walls are an efficient method of strengthening and stiffening a building.

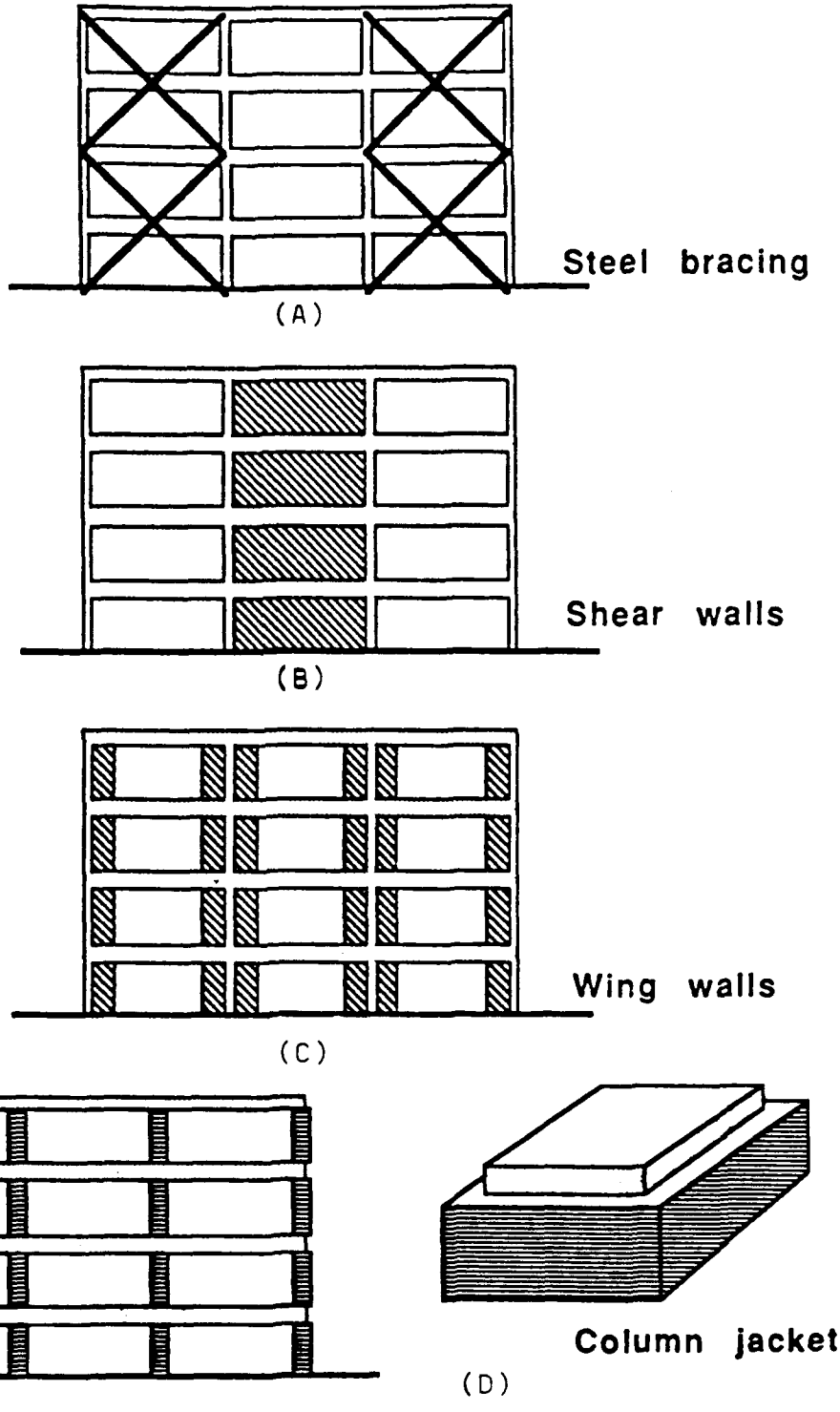

Fig. 1.1 Seismic retrofitting techniques [3]

3. **Wing walls**. A simple application of wing walls to an existing frame is shown Fig. 1.1c. In this technique one strives to strengthen the columns and improve overall ductility. Improvement in structural ductility can be achieved by ensuring the beams yield before the columns. Cast-in-place or precast walls are added to each side of the columns. This in essence adds cross sectional area to the columns thus increasing column strength and stiffness.
4. **Column strengthening**. The concept of column strengthening is indicated in Fig. 1.1d. In this technique, the columns are strengthened by encasing the columns with steel or reinforced concrete. As with wing walls, a designer may be successful in not only improving the lateral strength of the columns but in improving the failure mechanism of the entire structure as well. This is done by increasing the lateral capacity of the columns to such a level that the beams yield before the columns. The end effect is that overall structural ductility of the frame is improved.

The focus of this study is prestressed cable bracing systems which can be classified as a special case of traditional steel bracing. One significant disadvantage of traditional steel compression braces under cyclic loading is the problem of destructive inelastic buckling. Once a steel brace buckles in the "compression" portion of a loading cycle, the capability of the brace to dissipate energy in subsequent cycles is

greatly reduced. The shape of the hysteresis curves become narrow or pinched. Even if the structure survives large inelastic deformations during an earthquake, the steel bracing system may be permanently damaged. Inelastic buckling of the steel bracing can be reduced or eliminated entirely by designing the braces with either very low or very high slenderness ratios.

Braces with low slenderness ratios yield in compression before buckling. They maintain good hysteretic behavior; however, such sections can become very stocky, expensive, and unsightly.

Cables, on the other hand, have very high slenderness ratios (kl/r approaching infinity). Cables have the advantage of eliminating destructive inelastic buckling altogether. Cables simply go slack under compressive loading and then pick up load again when subjected to tension. Because the buckling load of the cables is nil only the tension members resist load. However, if a pretension force is applied to the cables, all cables will resist load within a given loading cycle even under "compression". This is true up to some critical drift at which the prestressing force in the cables subjected to "compressive" load is relieved and the cables finally go slack.

Relatively little research has been conducted concerning prestressed cable bracing systems. In this study, previous research efforts using prestressed cable braces will be re-evaluated and extended. In particular, application of prestressed cable braces to a specific class of reinforced concrete frame structure commonly constructed in California in the 1950's and 1960's will be examined. The prototype frame to be studied features reinforced concrete short

columns. Thus, the frame contains a weak column-strong beam configuration. Such a frame is likely to fail in a very undesirable mode. The weak columns may fail in shear before the beams yield in flexure. Such a failure can be sudden and catastrophic.

Bracing a weak column-strong beam frame with prestressed cable braces cannot in itself guarantee satisfactory behavior under large inelastic lateral deflection. Although the lateral capacity of the frame is improved, the ultimate failure mode of the frame may remain unchanged.

Beam alteration is a technique aimed at moving failure away from the columns and into the beams. This can be accomplished by weakening the beam just enough to guarantee that the beam will yield in flexure before the columns fail in shear. Complementing a prestressed cable bracing system with beam alteration on a subassemblage of the prototype frame is studied in chapter 4. The focus of chapter 5 is the behavior of single story and multi-story subassemblages of the prototype frame to various prestressed cable bracing schemes with and without beam alteration.

1.2 OBJECTIVE

The objectives of this research are threefold:

1) To study analytically the combined effects of prestressed cable bracing and beam alteration to the response of a reinforced concrete frame subassemblage. Can beam alteration improve the failure mechanism of the structure?

What is the effect of combining prestressed cable bracing and beam alteration to the monotonic and cyclic response of a single story subassemblage of the prototype frame? How are strength, stiffness, ductility, and failure mechanism effected?

2) To compare the response curves of unique single story subassemblages to a multi-story subassemblage of the prototype frame retrofitted with prestressed cable bracing and beam alteration. Is similar response predicted by both models? Can the retrofit strengthening scheme of an entire frame be engineered by considering the response of a single generic single story subassemblage?

3) To consider some practical aspects of retrofitting existing structures with prestressed cable bracing systems. Is it practical to attach prestressed cable bracing systems to the exterior frames of buildings? What are some of the design considerations? Conceptually, how might some typical connections look?

1.3 SCOPE

This research is limited in scope to the reinforced concrete structural frame studied experimentally and analytically by researchers at the University of Texas at Austin, and the University of Oklahoma [7, 2, 3]. For the purpose of studying the combined effects of a prestressed cable bracing system and beam alteration, a subassemblage of

the structure's exterior frame will be utilized. The subassemblage consists of a column and two beams, braced with two prestressed cable braces. It will be assumed that the subassemblage column will maintain its capacity to carry gravity loads up to large drifts despite potential shear failure of the column.

For the purpose of studying the response of an entire frame, it will be necessary to design the remainder of the prototype frame making use of design details available of the prototype experimental frame [3], and appropriate code provisions available at the time such structures were originally designed [10, 11, 12]. A multi-story subassemblage of the prototype frame will be developed and used to represent the response of the complete frame. The behavior of the unbraced and braced frame to static lateral monotonic and cyclic loadings will be examined by using DRAIN-2D, a Fortran program developed previously for the dynamic inelastic analysis of plane frame structures [1].

CHAPTER 2

BACKGROUND AND LITERATURE REVIEW

2.1 NEED FOR RETROFIT BRACING IN EXISTING STRUCTURES (STRONG BEAM-WEAK COLUMN DESIGNS)

The aim of any retrofitting scheme is to modify a structure in such a way that the overall performance of the building in an earthquake is improved to an acceptable level. This should be accomplished for the least cost and the least disruption to the existing function of the facility. In many cases it is the deficiency in ductility that can be expected to result in excessive structural damage. Post earthquake observations have indicated that severe damage to reinforced concrete structures has been due primarily to the instability of columns under large lateral deformation, and shear distress of short columns. Columns failing in shear must be avoided if possible. Two examples of short column failure under seismic loading are shown in Fig. 2.1. Such failures are non-ductile, sudden, and can be catastrophic. As will be discussed, short columns exhibit unstable hysteretic behavior as well as degrading stiffness and strength when subjected to cyclic loading. For the purpose of this discussion, a short reinforced concrete column is defined as one whose clear height to depth ratio is less than 3.

Short columns are many times unintentionally designed into a structure. Often their existence results from the placement of nonstructural exterior walls as shown in Fig 2.2. Masonry or other infill walls effectively reduce the clear height of the column from L_c to L'_c. Columns of this type, are called "captive" columns and

Fig. 2.1 Seismic damage to short columns, Japan [3]

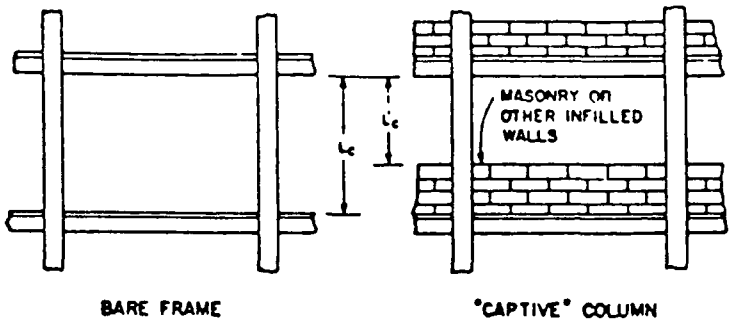

Fig. 2.2 "Captive columns" [2]

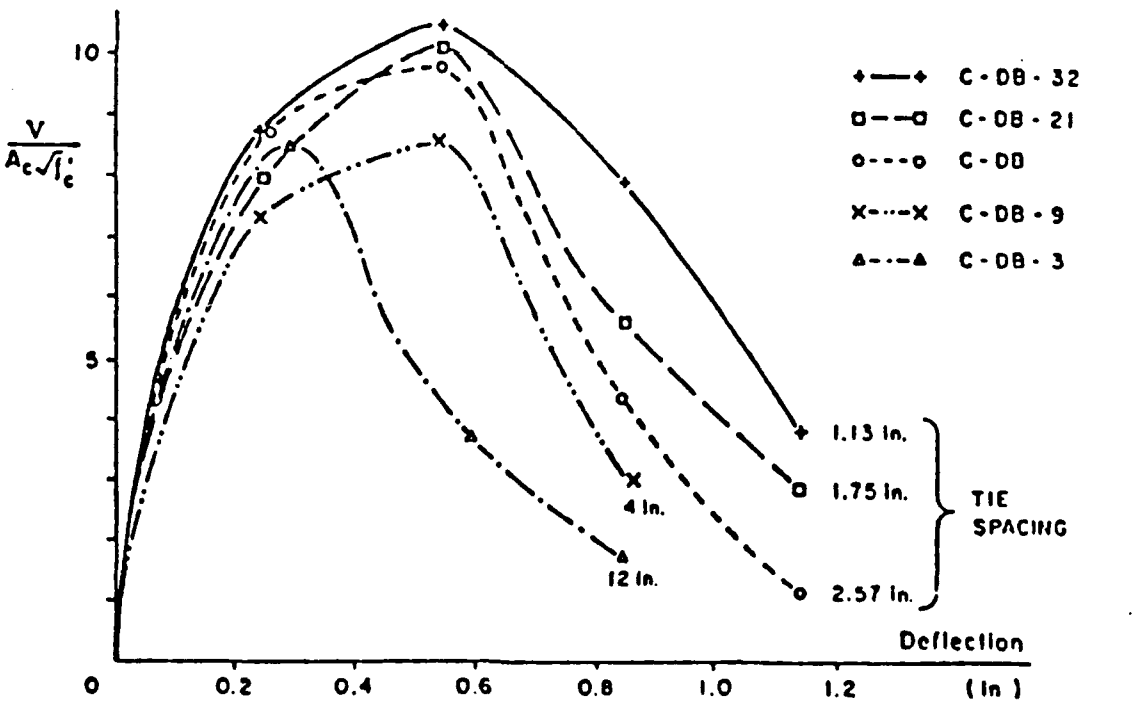

Fig. 2.3 Experimental load-deformation curves for short columns [2]

generally fail in shear. Failures of captive columns have been reported following several earthquakes such as the 1985 Mexico City earthquake [3].

If a beam-column frame is subjected to lateral loads, the columns will bend in double curvature. It is reasonable to assume that the columns will develop a point of inflection at or near mid height. The shear in the column is proportional to the magnitude of the end moments. In fact the shear is equal to the sum of the end moments divided by the clear length of the column. For joint equilibrium, the sum of the beam moments must equal the sum of the column moments. If the capacities of the beams are very large as compared to the capacities of the columns, such that the beams will not fail in flexure or shear (strong beam-weak column configuration), it is possible that relatively large end moments will be transferred to the columns. Short columns will develop tremendous shear stresses under these conditions. Typically the short columns will reach their maximum capacity before the beams and then fail in shear. As mentioned earlier, shear failure of short columns is non-ductile and occurs without much warning. In the interest of public safety, such weak column-strong beam situations should be corrected where possible. Therefore, strong beam-weak column structures are prime candidates for retrofit strengthening.

2.2 BEHAVIOR OF REINFORCED CONCRETE SHORT COLUMNS SUBJECTED TO CYCLIC LATERAL LOADS

Extensive experimental work has been undertaken concerning the behavior of short columns under lateral loads. The most notable work

was carried out by Jirsa, Woodward, and Umehara at the University of Texas at Austin [5, 6]. Experimental load-deformation curves for short columns are shown in Fig 2.3. Researchers were able to draw several important conclusions from such experimental results. They are as follows:

1. After the short column reaches its maximum shear capacity, the lateral load carrying capacity of the column is reduced with increasing lateral deflection as idealized in Fig. 2.4. As indicated in the figure, the ultimate shear capacity of the column, V_u, is reached at a relatively low lateral deflection.
2. The short column exhibits negative stiffness for drift levels exceeding that corresponding to the column's ultimate shear capacity. This negative stiffness can be observed as the negative slope region in Fig. 2.4.
3. The behavior of the column is dependent on the span to depth ratio, 2a/d, the magnitude of axial compression, N, and the amount of confinement provided by the transverse reinforcement.
4. Under cyclic lateral loading, Umehara concluded a compressive load on a short column increases the shear strength of a column; however, it also accelerates the strength degradation of the column after shear failure. In short, an axially loaded column is stronger in shear but less ductile than the same column without axial load.

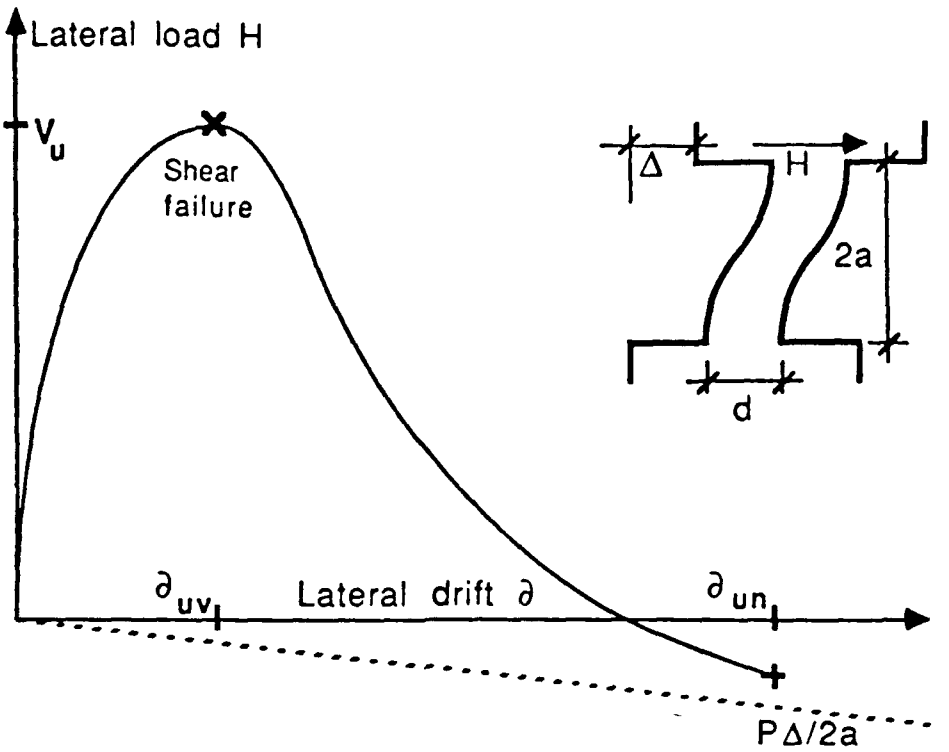

Fig. 2.4 Typical load-deformation curve for a reinforced concrete short column [3]

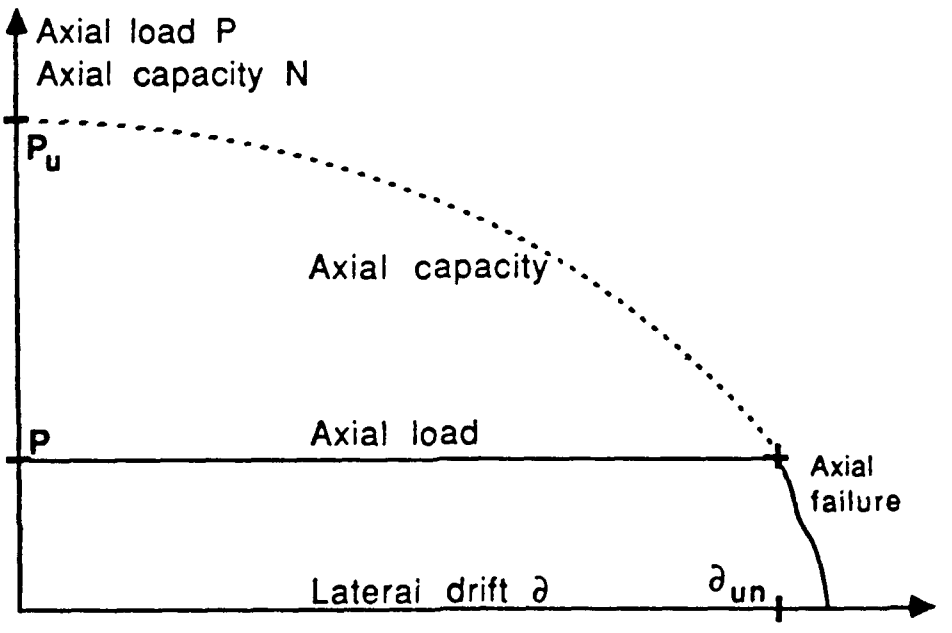

Fig. 2.5 Axial failure of a short column deformed laterally [3]

As a result, the hysteretic behavior of the short column is very poor and the column dissipates very little energy.

In an unbraced frame subjected to lateral loads, the columns may fail in shear for low values of drift. Even though it is possible that the columns could carry additional vertical load, the frame is considered to have failed. In a braced frame, however, the bracing system can be designed to carry most, if not all, of the lateral force, thus allowing the braced frame to carry the vertical gravity loads up to a much greater drift. It can be expected, however, that at some unknown lateral drift, the columns will be incapable of carrying their intended axial load. This concept is illustrated in Fig. 2.5. Very little research has been conducted to date which would enable prediction of the lateral drift at which the axial load carrying capacity of the column is affected. Tests on axially loaded short columns submitted to lateral drift have focused on the shear strength and were stopped when the lateral capacity deteriorated to a given level. For the purposes of this research, it is assumed that the columns will maintain their axial load carrying capacity up to very large drifts. With this assumption the focus of the study will be concentrated on the task of improving the frames lateral strength through retrofit bracing.

2.3 EXPERIMENTAL AND ANALYTICAL STUDIES FOCUSING ON RETROFIT STRENGTHENING OF REINFORCED CONCRETE FRAME STRUCTURES

Much of the original research on seismic retrofitting was conducted in Japan following several destructive earthquakes [3]. Many reinforced concrete buildings were retrofitted to repair damage suffered by

earthquakes while others were retrofitted to guard against damage in future seismic events. Most applications involved the use of cast in place infill walls for low rise structures. Wing walls and column strengthening were used in most other applications. Very few applications of steel bracing systems were undertaken primarily because of lack of confidence and design data available for such systems. Research programs were undertaken to evaluate the various retrofitting applications in place.

Of particular interest to this study is a series of tests conducted by Sugano and Fujimura [8]. Tests were conducted on third scale, one story single bay frames retrofitted with several strengthening schemes. The frames were subjected to static cyclic lateral loading and the load deformation response curves plotted. The test results are summarized in Fig. 2.6. Examination of this figure reveals that the frame infilled with concrete proved to be the strongest and stiffest scheme; however, it provided the least ductility. The steel diagonally braced frames performed very well providing significant increases in both strength and ductility. The "X" pattern braces were observed to perform superior to "K" or "Diamond" bracing patterns. Also of note was that a retrofitting scheme making use of tension braces displayed the largest energy dissipation capacity (not shown in the figure).

Recent experimental and analytical studies conducted at the University of Texas at Austin have focused attention on methods of retrofit strengthening of reinforced concrete frames for seismic loading on structures featuring short columns [3, 7]. Bush conducted experimental tests on a prototype building typical of a class of

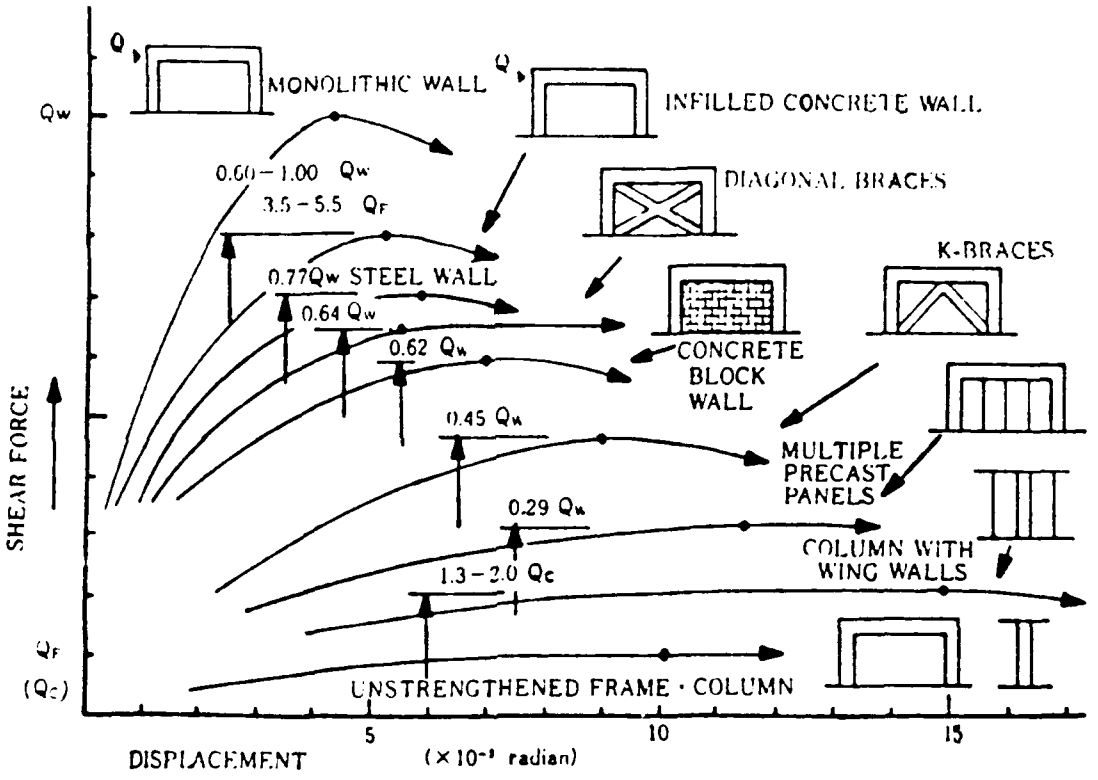

Fig. 2.6 Typical load-displacement relationships for different retrofitting techniques [3]

buildings commonly constructed in California about 30 years ago for commercial and residential use. A plan and elevation of the prototype structure are shown in Fig. 2.7. In this type of structure, almost the entire lateral load resisting capacity of the building in the long direction is provided by the exterior frames. The exterior frames are characterized by deep spandral beams and short columns. Tests were conducted on a two-thirds scale frame which represented a portion of the prototype building's exterior frame. The test frame modeled two bays of the prototype frame between the third and fifth levels. Sketches of the test set up and the applicable boundary conditions are shown in Fig. 2.8. The model frame was subjected to monotonic and cyclic loads before strengthening, and after strengthening with two different retrofitting schemes.

A related analytical study was performed by Badoux making use of the same prototype frame. The experimental test results were duplicated in the analytical study. Badoux also examined complementing the steel bracing system studied with application of beam alteration techniques. DRAIN-2D was utilized to model a subassemblage of the prototype frame and to analyze the response of the subassemblage to monotonic and cyclic loading. A complete description of the subassemblage is presented in Sec. 2.4.1 and a description of the program and its current capabilities is found in Sec. 3.1.

Two important conclusions were drawn from this research as it applies to the present study:

First, Badoux suggested that further research should be conducted to study the effectiveness of cable bracing systems. Bracing with

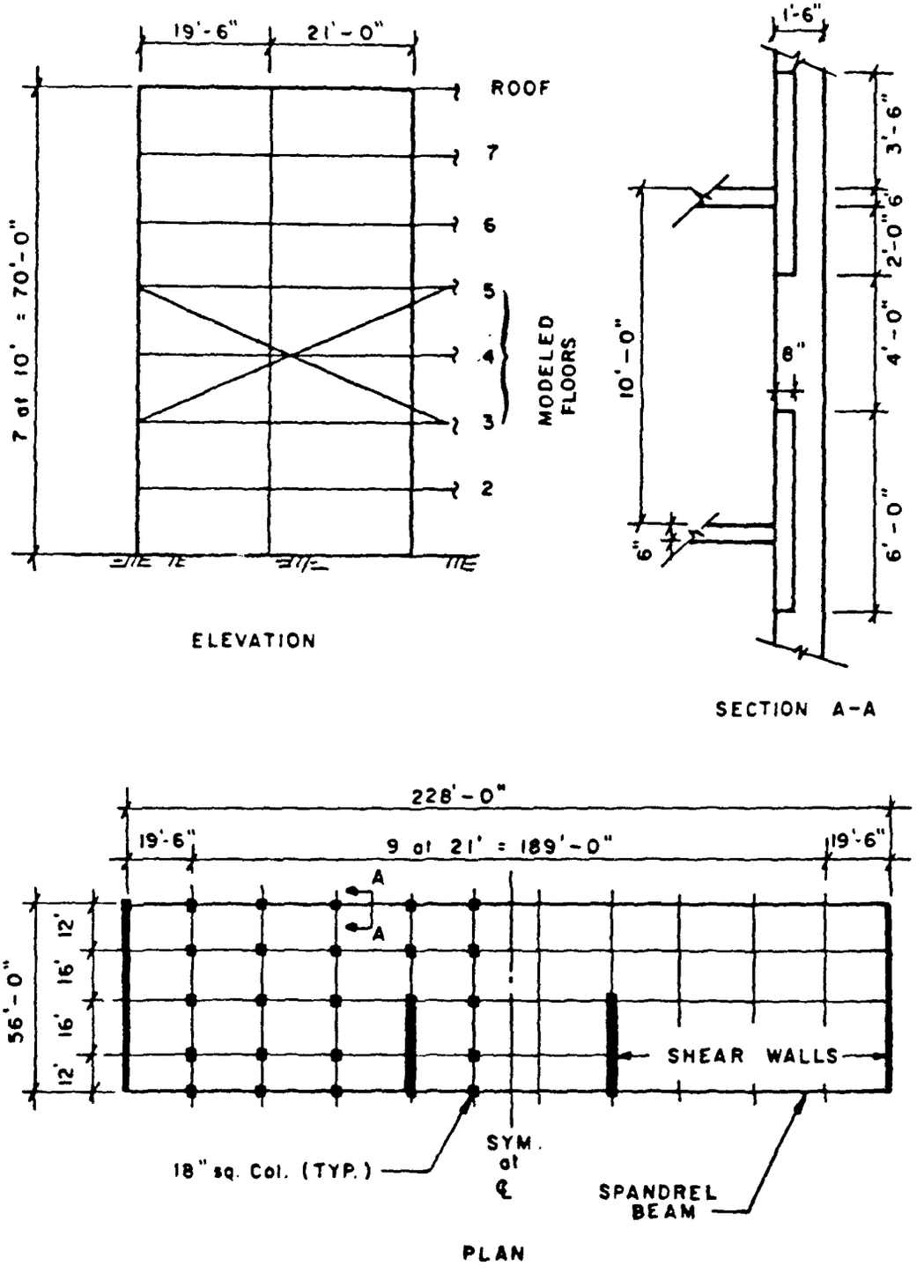

Fig. 2.7 Plan and elevation of prototype building [3]

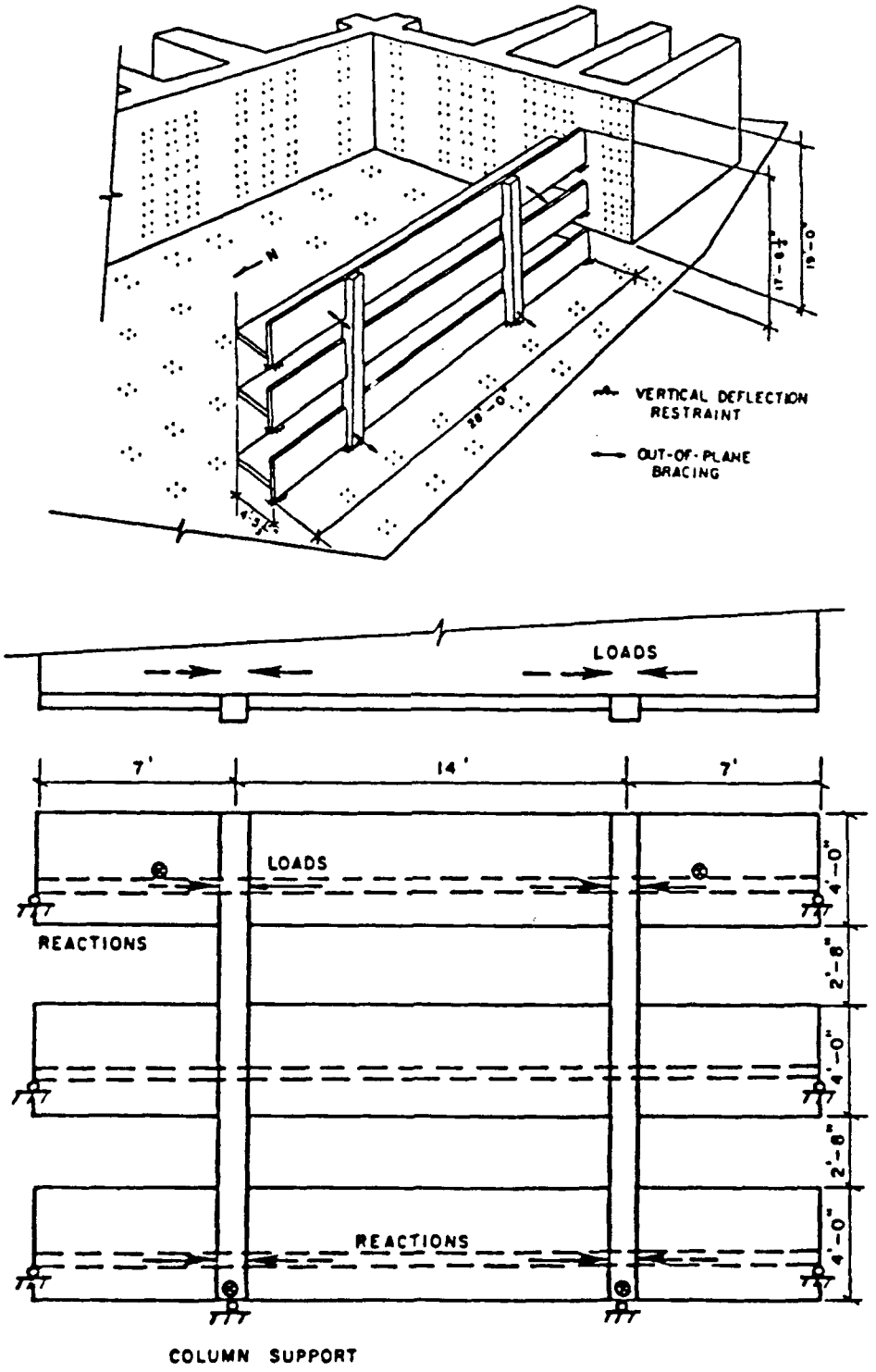

Fig. 2.8 Frame model, boundary conditions of the test set up [7]

cables eliminates the deteriorating effects of inelastic buckling of braces. He suggested that energy dissipation and level of prestressing of cable braces should be studied.

Secondly, his research showed that beam alteration was effective in altering the failure mechanism of the prototype frame. Additionally, when beam alteration was applied in conjunction with a steel bracing system, the result was a braced frame with greatly improved lateral strength and ductility.

2.4 SUMMARY OF PRESTRESSED CABLE BRACING SYSTEMS RESEARCH

Masroor [2] studied the application of prestressed cables as a viable retrofitting scheme for reinforced concrete frame structures with short columns. His work comprised a first extension of Badoux's research with application of prestressed cable braces. Masroor's analytical research revolved around the same prototype frame introduced in previous research at the University of Texas at Austin. Masroor limited his investigation to the behavior of the subassemblage studied previously by Badoux.

2.4.1 Analytical Model Of The Frame Subassemblage

The subassemblage consisted of a column, two beams and two prestressed cable braces. The subassemblage was chosen so as to represent a typical braced interior column of the prototype building as shown in Fig. 2.9. The subassemblage geometry and members were modeled from the prototype frame. The analytical model of the subassemblage is depicted in Fig. 2.10. The spandral beams of the subassemblage were

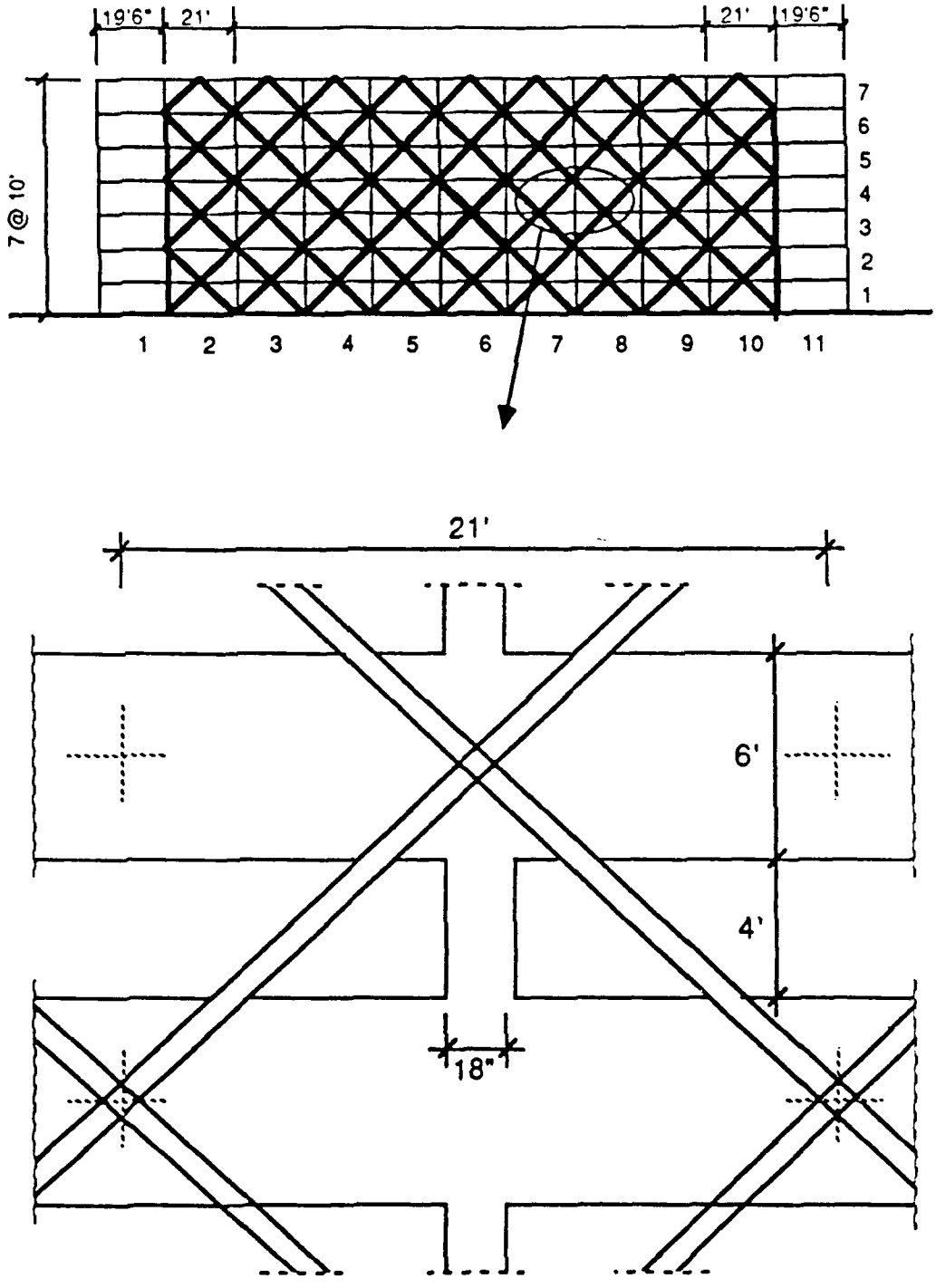

Fig. 2.9 Braced column of the prototype frame [3]

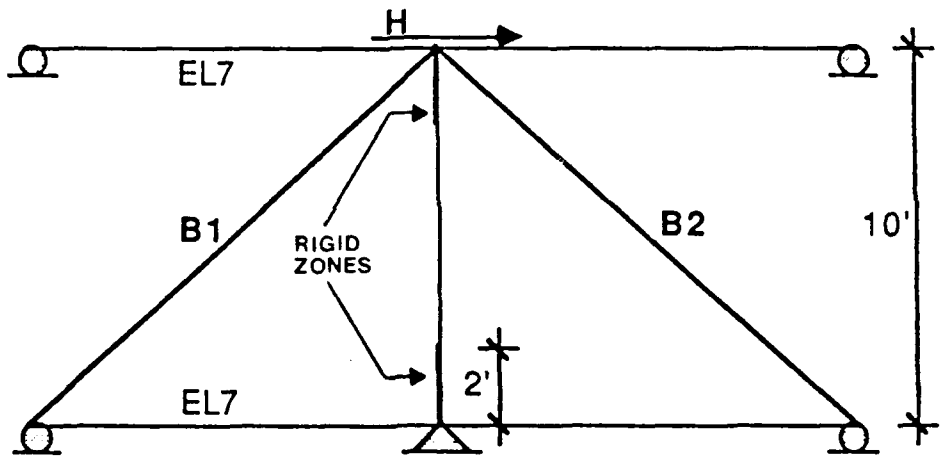

Fig. 2.10 Analytical model of the subassemblage [3]

roller supported at their mid-span. The rollers represented the existence of inflection points which occur near mid-span in beams of a laterally loaded frame. The upper beam-column joint was assumed to be free to displace horizontally and vertically as well as to rotate. Thus three degrees of freedom were established for this joint. Lateral loads were applied at this joint in the analytical study. The lower beam-column joint was restrained against horizontal and vertical displacement. The prestressed cables were assumed to be connected at one end at the upper beam-column joint and the other end to the roller support. The effect of column axial load due to the weight of upper stories was introduced implicitly into the model. This was accomplished through the inherent characteristics of the column's moment-rotation backbone curve input into the computer program. The structural properties of the subassemblage elements are discussed in Sec. 3.5.

The subassemblage was retained from the previous studies for the following reasons. First, it offered both conceptual and computational simplicity. Secondly, it was hypothesized that the global behavior of the reinforced concrete frame could be inferred from the behavior of the subassemblage alone. Thirdly, the subassemblage can be used as a model unit for future experimental and analytical research for devising new retrofitting techniques. And finally, results from previous research is available for which one can compare the effectiveness of the prestressed bracing to traditional bracing systems [3, 7].

2.4.2 Parameters Examined in Previous Study on Prestressed Cable Bracing Systems

Masroor studied the behavior of the subassemblage under two types of static incremental displacements, monotonic, and cyclic. The monotonic loading condition was undertaken to help in understanding the basic behavior of the unstrengthened frame, the bracing system, and the braced frame. The failure sequence of the members of the subassemblage was derived from the response of the subassemblage to the monotonic loading. The monotonic response formed a basis for the incremental cyclic loading. The monotonic response provided a basic envelope for the subassemblage within which cyclic loading behavior was expected to occur. The purpose of applying the cyclic loading is to reproduce the main character of an earthquake.

The monotonic and cyclic load cycles were held constant while the following parameters were varied and studied for their overall effect on the response curves for the subassemblage:

1) Optimum level of prestressing (0.25Py, 0.50Py, and 0.75Py).
2) Area of the cable braces.
3) Inclination of the cable braces.

1) Optimum level of prestressing. One of the most important benefits of using high strength cables for braces is that a prestressing force can be applied. It is not effective to prestress conventional mild steel braces. The behavior of the cable bracing system, and in turn the overall response of the braced frame is dependent on the level

of initial prestressing force applied to the cables. The amount of prestress force, P, applied to a cable was specified as some percentage of the cable yield force, P_y.

In order to determine the prestress force which optimized the response of the cable bracing system, Masroor studied three levels of prestress force: $0.25P_y$, $0.50P_y$, and $0.75P_y$. With the application of the initial prestressing force, the braces have an apparent buckling strength of $0.25P_y$, $0.50Py$, and $0.75P_y$ respectively. Similarly the cables can carry tension forces of $(P_y-0.25P_y)$,$(P_y-0.50P_y)$, and $(P_y-0.75P_y)$ respectively. Cables are not normally capable of carrying any load in compression; however, it is interesting to note that such is not the case with prestressed cables. The prestressed cables in "compression" participate in resisting the lateral displacement of the structure through a reduction in their initial tensile force as the deformation of the frame occurs.

2) Area of the cable braces. Two non-dimensional design parameters, n, and m, were introduced which are dependent on bracing cross-sectional area. Design parameters n and m were used to facilitate the comparison of the design strength of the bracing system and the effective lateral strength of the retrofitted structure. **Design ratio n** is a measure of the increase in strength desired in the design of the bracing system. The definition of n varies slightly depending on the design approach used. The two design approaches examined were ultimate design and serviceability design.

The **ultimate design approach** is applicable when the main objective of the retrofitting is to simply increase the lateral strength of the

frame to some desired level. Limiting interstory drift is not a primary concern. In the ultimate approach, the retrofitted frame may reach its ultimate lateral capacity at a drift at which the columns have previously failed in shear. It is assumed that the vertical capacity of the columns is maintained up to a high drift even though the columns may have failed in shear. For the ultimate approach, the design parameter n is defined as the ratio of the design lateral strength for a given story of the retrofitted structure, H_r, to the ultimate lateral strength for a given story of the unstrengthened structure, V_u,

$$n = H_r/V_u \tag{2.1}$$

The design lateral strength of the retrofitted structure is specified at the drift at which the isolated prestressed cable bracing system reaches its maximum strength.

A bracing system designed under the serviceability design approach will reach its desired lateral design strength at a specified drift level. The specified drift, for example, might correspond to shear failure of the columns in the prototype structure introduced in Sec. 2.3. The design ratio n is defined in the same way as for the ultimate design approach; however, the design strength of the retrofitted structure, H_r, is specified at the drift level desired rather than the drift at which the bracing system attains its maximum strength.

A value of n equal to 1 means that no strengthening of the frame is required. The original frame has sufficient strength to carry all the lateral load. A value of n between 1 and 2 indicates some light

strengthening is required. If n is between 2 and 3, the structure requires significant strengthening. More specifically, an n ratio of 2 means that the lateral strength of the retrofitted structure is twice that of the unstrengthened structure.

The n values are controlled by varying the cable cross-sectional area, A_c. The relationship between cross sectional area, A_c, and design ratio n for this study are given below for the two design approaches and $0.5P_y$ prestress force:

For the ultimate design approach:

$$A_c = [(n-.05)V_u]/[(f_y)(\text{Cos}\theta)] \qquad (2.2)$$

where A_c - area of each cable brace

n - design strength ratio

V_u - the ultimate shear capacity of the story being braced in the unstrengthened structure

f_y - the yield stress of the prestressed cable braces (230 ksi in this study)

θ - inclination of the braces to horizontal

Equation 2.2 is not a general equation. Equation 2.2 applies only to the prototype structure introduced in Sec. 2.3.

For the serviceability design approach:

$$Ac = [(n-1)(V_u)(L)]/[(C)(E)(\Delta_{fu})(\text{Cos}^2\theta)] \qquad (2.3)$$

where L - the length of the cable braces

C - the number of braces per story

E - modulus of elasticity of the cable braces (taken as 26,000 ksi for this study)

Δ_{fu} - drift at which the unstrengthened story reaches its ultimate strength

Equation 2.3 is general and is derived from the stiffness method. An increase in the cable brace cross-sectional area brings about a corresponding increase in the strength of the retrofitted frame and design ratio n. Design ratios of 2 and 3 were studied by Masroor.

Load ratio m for any story of the frame, is the ratio of the lateral capacity at any drift to the ultimate strength of the unstrengthened structure. Therefore, the maximum value of m for the unstrengthened structure is 1. The m ratio is simply a way of normalizing the lateral strengths of the unstrengthened and braced structures for simplified comparison.

3) **Inclination of the cable braces**. Two cable inclination patterns were studied for their effect on the response of the subassemblage. In the first type, the braces were considered to extend from the beam-column joint centroid of one story to the centroid of the beams of the story below. In the second configuration the braces were attached to the beam-column joint at every story level. The inclinations of the cable braces for the two types were calculated as 43.6^{o} and 25.4^{o}, respectively.

2.4.3 Conclusions From Previous Study On Prestressed Cable Bracing Systems

Four main conclusions were derived from Masroor's research [2]:

1. Optimum cable pretension force is 0.50Py.
2. Peak strength of the braced subassemblage is independent of the strength of the original unstrengthened structure.
3. The responses of the braced system and the original frame are not well matched in attaining maximum strength at specific drifts.
4. Prestressed cable bracing alone does not effect the overall failure mode of the subassemblage.

The optimum level of initial prestressing force for the cables is equal to half the yield strength of the cable brace. For the subassemblage of Fig. 2.10, the 0.50Py level of prestressing leads to simultaneous yielding and slackening of cable braces B1 and B2. The response of the braced subassemblage to $0.25P_y$ and $0.50P_y$ prestressing forces respectively is illustrated in Fig. 2.11. It should be noted that the response curve for the $0.75P_y$ prestress case is identical in shape to the $0.25P_y$ prestress curve, and therefore is not plotted on this figure. From Fig. 2.11 the following observations are made:

a) The braced system prestressed to 0.50Py maintains its elastic stiffness up to a much higher drift level (approximately 0.88% interstory drift at point a) over the

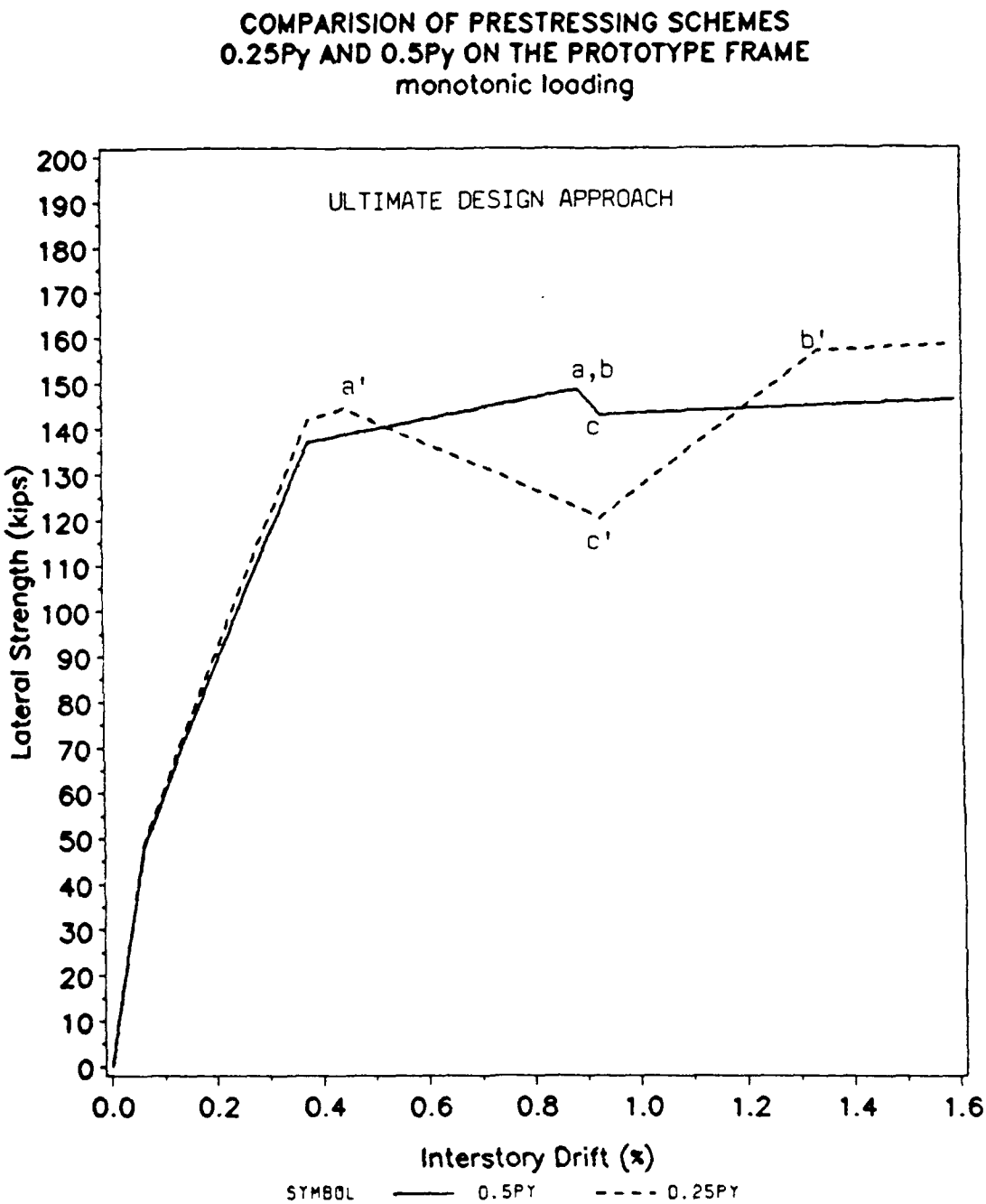

Fig. 2.11 Braced frame under monotonic loading, n=2, and 0.25Py and 0.5Py prestressing forces

system prestressed to $0.25P_y$ or $0.75P_y$ (.44% interstory drift at point a').

b) The braced frame prestressed to $0.50P_y$ reaches its maximum capacity at a lower drift level (point b verses point b') which helps in matching the strength of the unbraced frame to the bracing system. This feature is particularly important if using the serviceability design approach.

c) The system prestressed to $0.50P_y$ reaches and maintains its strength in a more desirable manner. The capacity of the 0.50Py prestressed frame gradually increases with drift up to its ultimate capacity at point b. If prestressing of $0.25P_y$ and 0.75Py are used, the capacity of the braced frame reaches an initial peak at point a' then decreases over a large interval of drift due to the negative stiffness of the column. The system finally regains positive stiffness again at point c'. Strength increases up to its ultimate capacity at b'.

The effectiveness of the prestressed cable bracing system becomes clear in Fig. 2.12. The response curves for the unbraced subassemblage, the bracing system by itself, and the braced subassemblage are shown in Fig. 2.12. The ultimate design approach was used with n=2. The peak additional strength brought about by the bracing system is independent of the unbraced frame. Study of the figure reveals that lateral capacity of the subassemblage is reduced to essentially zero at drift 1'' corresponding to the peak strength of the braced subassemblage.

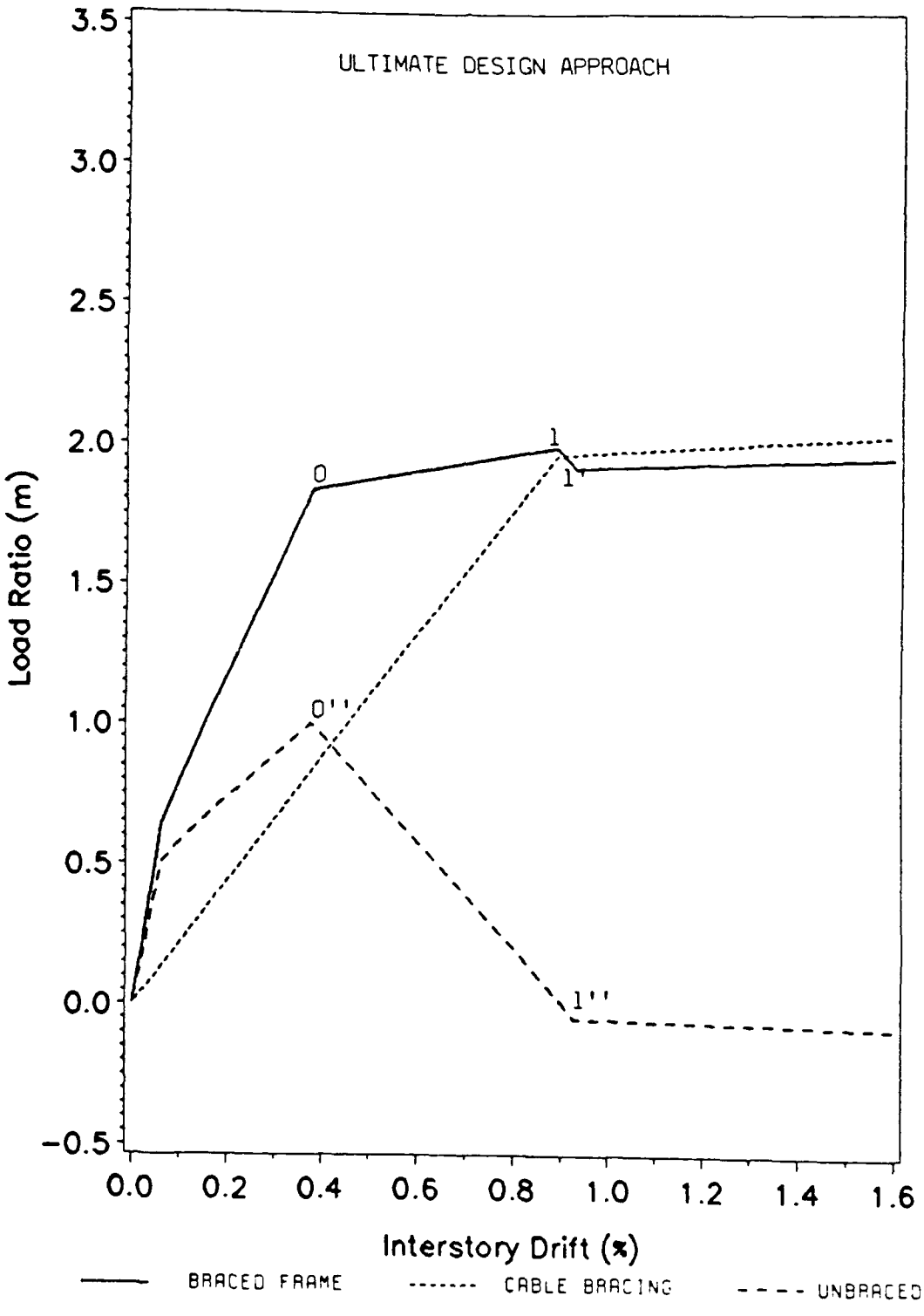

Fig. 2.12 Unbraced frame, bracing system, and braced frame under monotonic loading, n=2, and 0.5Py prestressing force

Nearly all the lateral strength of the frame at this drift is provided by the cable bracing system alone. Therefore, the desired design strength of the braced frame can be achieved by choosing an appropriate design ratio, n, for the bracing system. The strength and stiffness of the bracing system can be designed according to the ultimate design approach (i.e. so as to prevent collapse), or the serviceability design approach (i.e. to limit drift and to prevent excessive damage to the structure).

Also observable from Fig. 2.12 is that the response of the unbraced subassemblage and the bracing system are not well matched. The unbraced frame reaches its maximum strength at drift 0'' while the bracing system does not develop maximum capacity until drift 1'. This situation can only be remedied by using the same cable area as a conventional mild steel bracing system. If the ultimate strength approach is used, the lateral strength of the unbraced frame is negligible at the drift corresponding to the maximum strength of the bracing system. For this situation the bracing system must be designed to carry the entire design lateral loads.

Finally, although the strength and ductility of the braced subassemblage is greatly improved over that of the unbraced subassemblage, the basic mode of failure remains unaltered. Failure is still initiated by shear failure of the short column at drift 0. A complete discussion of the failure mechanism will be discussed in detail in Sec. 3.7.

CHAPTER 3

MODELING THE PROTOTYPE FRAME AND BRACING SYSTEM USING DRAIN-2D

3.1 SELECTION AND GENERAL DESCRIPTION OF THE COMPUTER PROGRAM

DRAIN-2D is a general purpose computer program for dynamic analysis of inelastic plane frame structures. The original program was developed at the University of California at Berkeley in 1973 [1]. The principal authors of the program are Amin E. Kanaan and Graham H. Powell. The program is written in Fortran IV programming language and is generally intended for use with a mainframe computer. The popularity and flexibility of the program have lead to many revisions over the years. The version of the program used in this research project has been altered from the original program by researchers at the University of California at Berkeley [1], the University of Michigan at Ann Arbor [4], the University of Texas at Austin, [3], and the University of Oklahoma, [2]. The Appendix of this report is a revised user's guide complete for the main program and the two elements used in this research study, Elements EL7 and EL1(m). The revised user's guide incorporates all previous revisions and does not require the user to refer to previous outdated user's guides for portions of the input data requirements.

The popularity of the program is due in part to its structure. The main program and the element library are so connected that new element subroutines can be added or old ones modified without any significant changes being required in the main program. The program consists of a number of base subroutines making up the main program. The main program subroutines read and print the structural geometry and loading data,

carry out a variety of bookkeeping operations, assemble the structural stiffness and loading matrices, and determine the displacement history of the structure. All data reading and printing operations as well as stiffness calculations are carried out within the element subroutines and returned to the main program. Elements EL7 and EL1(m) used in this research study are examples of new and revised subroutines respectively which have been added to the original program.

The program is generally intended for the dynamic analysis of structures. The current version of the main program has been modified, however, to allow for control of the structure's response history through the application of incremental lateral displacements rather than forces. This feature is necessary for the current research because the negative stiffness behavior exhibited by the reinforced concrete short columns at large drifts makes application of unique static incremental forces impossible (see discussion in Sec. 2.2). Additionally, the behavior of the structure will be easier to discuss in terms of specified drifts rater than specified loads.

The structure to be analyzed is idealized as a planar assemblage of discrete elements. Analysis is by the direct stiffness method, with nodal displacements as unknowns. Each node possesses up to three degrees of freedom, as in a typical plane frame analysis.

DRAIN-2D is not well suited for commercial application. The program requires an extensive formatted data input. Phenomenological models are used for the columns, beams and braces. Much of this data is not readily available when designing or analyzing a structure. Phenomenological models are based on simplified hysteretic rules that

mimic observed behavior. These hysteresis rules must be derived from test data available on test specimens which possess similar geometries, material properties and loading histories. New commercial software packages are available for the analysis of structures subject to dynamic loading. Such packages require less data input, are far more user friendly, and can be operated on personal computers. DRAIN-2D is still a very complete program, however, useful for conducting analytical research and aiding the researcher in understanding nonlinear behavior of structures subjected to complex dynamic or static incremental loading.

3.2 DESCRIPTION OF THE FRAME ANALYZED

The reinforced concrete frame used in this analytical study is modeled after the prototype building analyzed experimentally and analytically in previous research studies conducted at the University of Texas at Austin, [3, 7], and at the University of Oklahoma, [2]. These research studies were summarized in Sections 2.3 and 2.4. The prototype building was originally chosen because it represents a classic example of a building in need of seismic retrofitting. The prototype building is typical of a class of reinforced concrete structure built in California in the 1950's and 1960's. An example of a building similar to the prototype building is shown in Fig. 3.1. The perimeter frames of such a building provide the primary lateral strength of the structure in the long direction. The perimeter frames are characterized by deep spandrel beams and short columns. A plan and elevation of the prototype building was given in Fig. 2.7. The original prototype frame is seven

Fig. 3.1 Example Building [3]

stories high and eleven bays long [3]. Each of the two perimeter frames of the prototype building provide half the total lateral strength and stiffness of the entire structure. Reinforcement details typical for the third, fourth, and fifth levels of the prototype frame modeled in the experimental study [7] are given in Fig. 3.2.

The prototype building is seismically inadequate for two main reasons. First, the prototype frame was designed using the 1955 edition of the Uniform Building Code for seismic design loads, and Building Requirements for Reinforced Concrete (ACI 318-51), 1951 edition, for seismic reinforcement and detailing requirements. Seismic design loads have more than doubled in more recent design codes and seismic detailing requirements have become more stringent as well. Second, the lateral failure mechanism of the perimeter frames is undesirable. As discussed in Sec. 2.1, the prototype frame contains a weak column-strong beam configuration and is thus likely to exhibit shear dominated failure in the columns. Such a failure is sudden and brittle. The energy dissipation capacity is likely to be very small. The prototype frame is thus deficient in both strength and ductility and is a prime candidate for seismic retrofitting.

The following assumptions will be made with respect to the prototype building for the purposes of modeling the structure with DRAIN-2D:

1. Lateral loads will be considered parallel to the longitudinal axis of the building only. Since there are no shear walls providing resistance in this direction, it

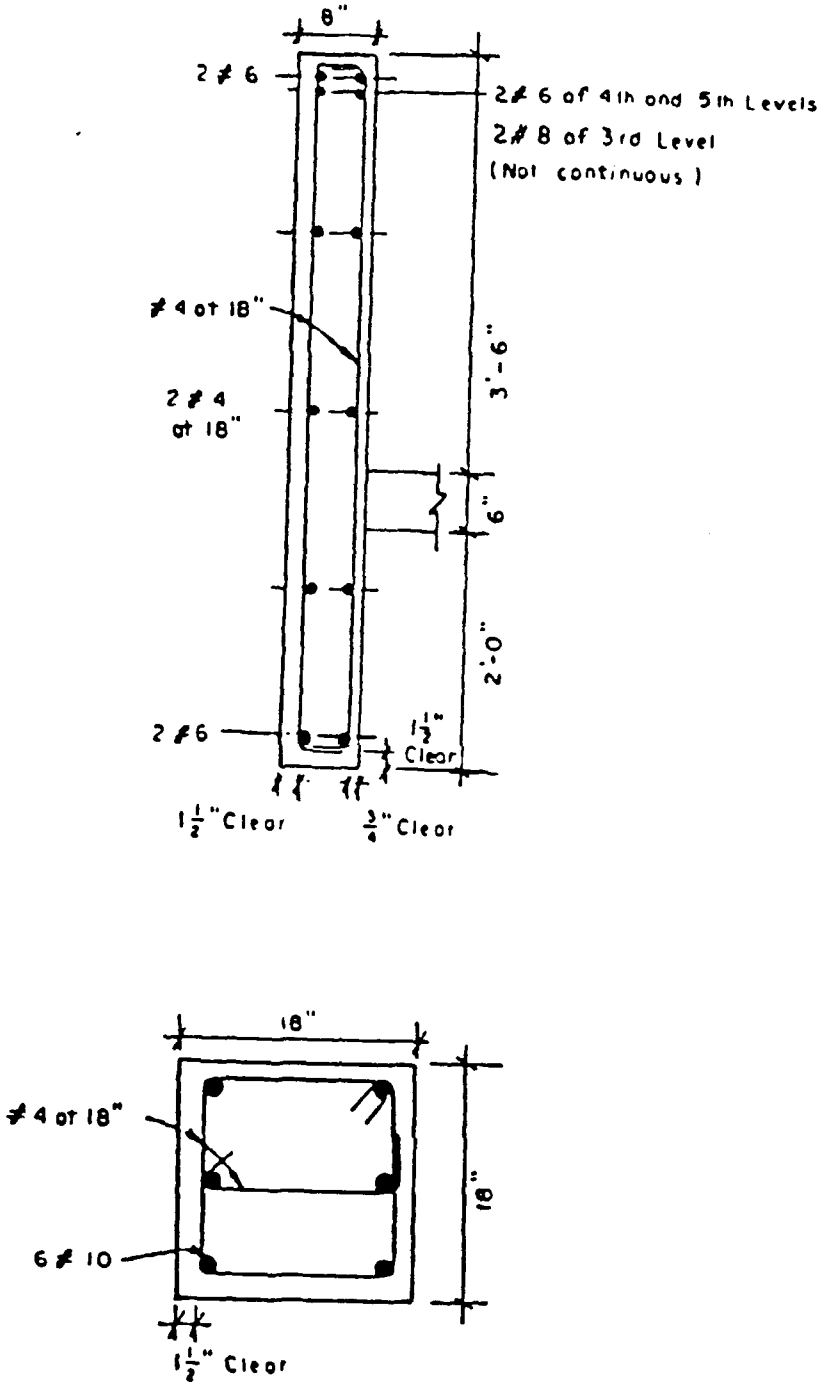

Fig. 3.2 Cross section of beam and column of prototype frame [7]

is assumed that all lateral resistance is provided by the perimeter frames.

2. The prestressed cable bracing system will be applied to the exterior frames only.
3. Axial inextensibility of the beams and columns will be assumed. This assumption will reduce the computer time required to solve the equilibrium equations as well as reduce the number of degrees of freedom. Therefore, there will be one horizontal degree of freedom per story and no vertical degrees of freedom.
4. A six story subassemblage will be modeled along a typical interior column line of the exterior frame. Because of the assumption of only one horizontal degree of freedom per story, it is reasonable to assume that the six story subassemblage will adequately represent the global behavior of the complete frame.

3.3 MODELING REINFORCED CONCRETE MEMBERS WITH ELEMENT EL7

For simplicity, the unbraced prototype frame will be modeled entirely with element EL7. Element EL7 is a reinforced concrete beam element with degrading stiffness. Element EL7 consists of a linear elastic beam element in series with two inelastic rotational springs, one at each end of the element as shown in Fig. 3.3. All nonlinear behavior and effects of stiffness degradation in the element are introduced into the system by means of the moment-rotation relationships of the inelastic springs. Since the inelastic behavior is reproduced by

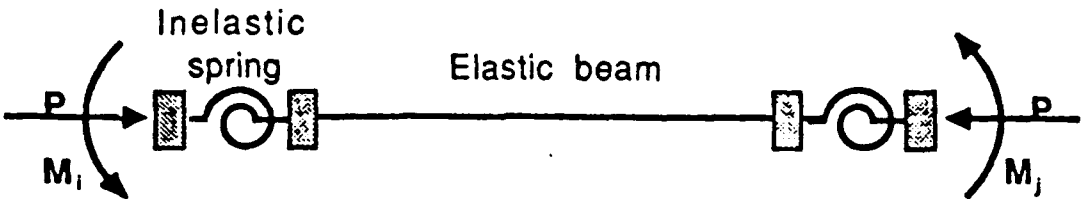

Fig. 3.3 Idealization of element EL7 [3]

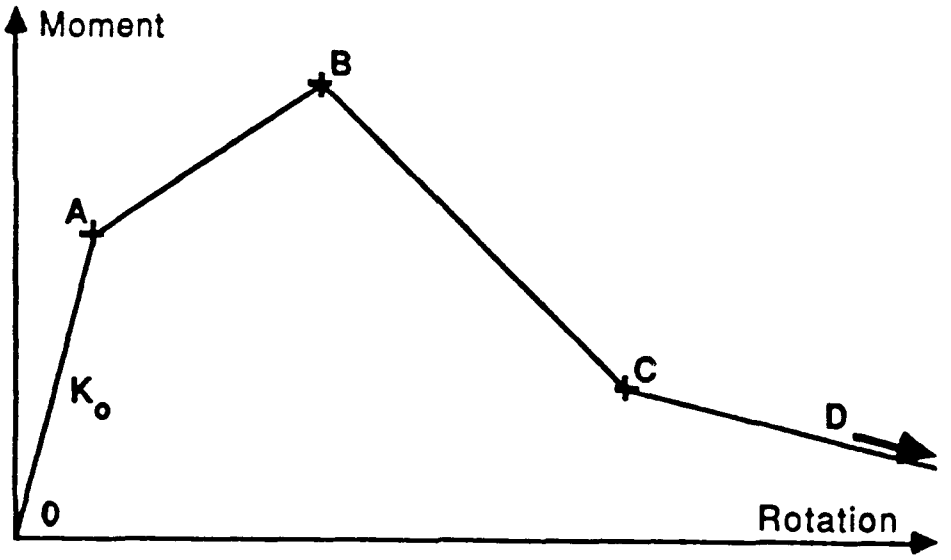

Fig. 3.4 Quadrilinear moment-rotation relationship for the inelastic spring [3]

the end rotational springs, the element's behavior is controlled through end moments rather than the shear. However, for a beam-column element bending in double curvature with the inflection point located at midspan, the end moments are proportional to the shear. As long as this assumption is true, the inelastic springs are satisfactory for modeling shear dominated behavior as in the case of a short column. EL7 also possesses flexural and axial stiffness; however, the moment-axial force interaction is not reproduced.

The element EL7 subroutine is capable of reproducing the stiffness degradation associated with cyclic loading [2]. As discussed in Sec. 2.2, a typical characteristic of reinforced concrete short columns is that once the column's maximum shear capacity is reached, the member exhibits negative stiffness with increasing drift (see Fig. 2.4). The shape of the moment-rotation relationship for the short column is assumed to be basically the same as the force-displacement curve shown in Fig. 2.4. For this reason, EL7 features a quadrilinear moment-rotation relationship as shown in Fig. 3.4. The length and slopes of segments OA, AB, and BC can be defined freely by the user. Thus the negative stiffness characteristic of a reinforced concrete short column can be reproduced by inputing a negative slope in segment BC. EL7 is very versatile in that the spring "backbone curve" can be tailored to match closely the experimental backbone curve of any test specimen with similar structural and material characteristics to that of the model element.

A phenomenological approach has been used to develop element EL7. A phenomenological model makes use of simplified hysteresis rules to

mimic experimental results. This modeling approach thus makes use of existing experimental data to define the hysteretic behavior of an element. Experimental work is often carried out on a component basis (i.e. columns, beams, joints, etc.) which produces the type of data needed for phenomenological models. The nonlinear hysteretic behavior of deep spandrel beams and short columns, similar in geometry, reinforcement, and material properties to the prototype frame, have been investigated experimentally.

The hysteretic behavior of the EL7 spring is based on the Takada model [14] and reflects observed experimental behavior for reinforced concrete components. The hysteretic rules are shown in Fig. 3.5. The relationships plotted in Fig 3.5a define the hysteresis rules for a flexure dominated element such as a beam. Note the slope of segments AB an BC are positive (i.e. positive stiffness throughout the loading cycle). The relationships plotted in Fig. 3.5b define the hysteresis rules for a shear dominated element such as the short column. Note the slope of segment BC is negative (i.e. negative stiffness in this portion of the load cycle). A reinforced concrete element submitted to inelastic cyclic loading loses stiffness. The hysteretic model reproduces this stiffness degradation as can be seen in subsequent cycles of Fig. 3.5a and b.

3.4 MODELING PRESTRESSED CABLE BRACES WITH ELEMENT EL1(m)

The original truss element, EL1, has been modified to model the behavior of prestressed cable braces [2]. The inelastic behavior of the modified truss element is shown in Fig. 3.6. As seen in the figure, the

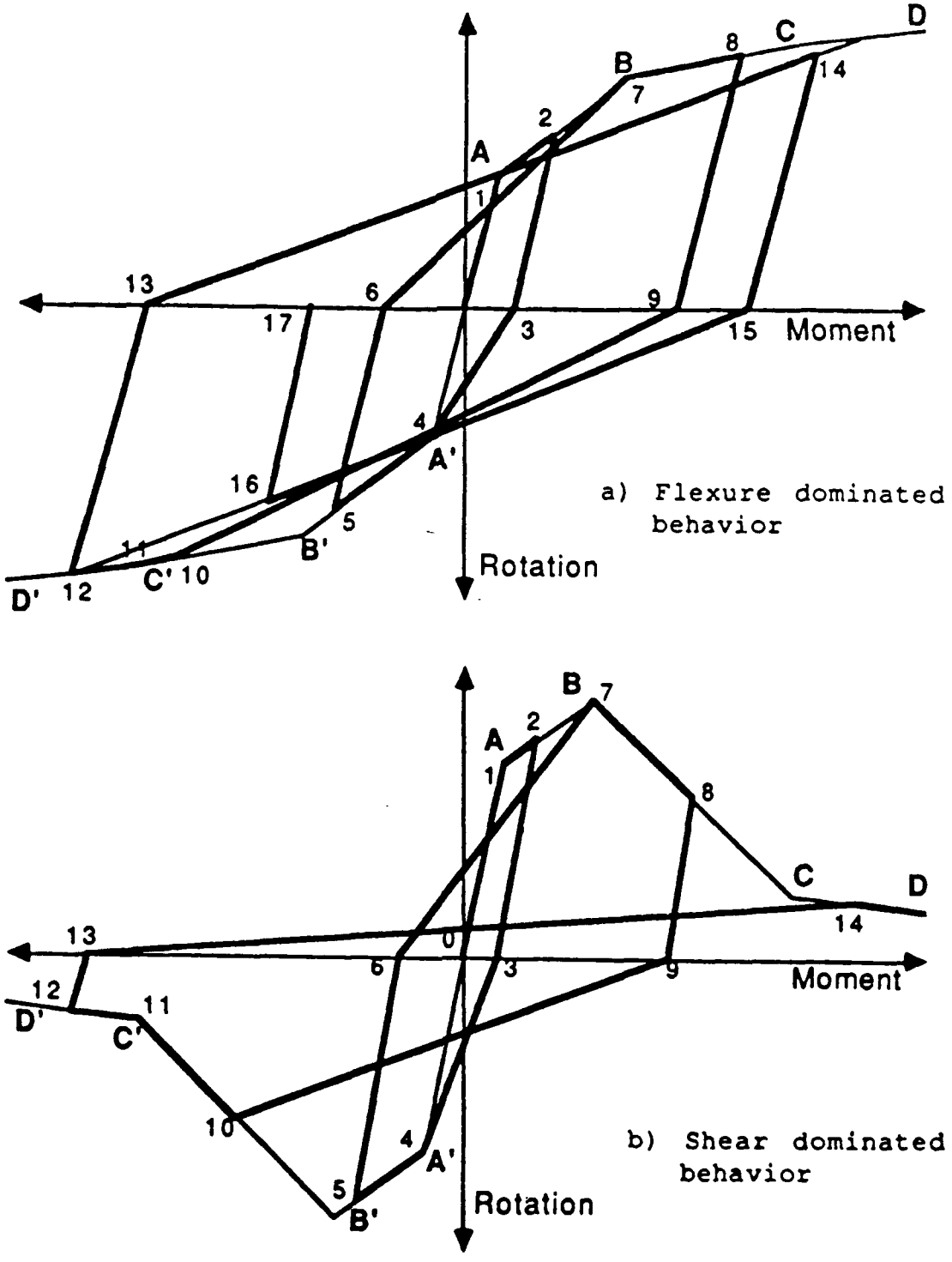

Fig. 3.5 Hysteretic rules for beam column element EL7 [3]

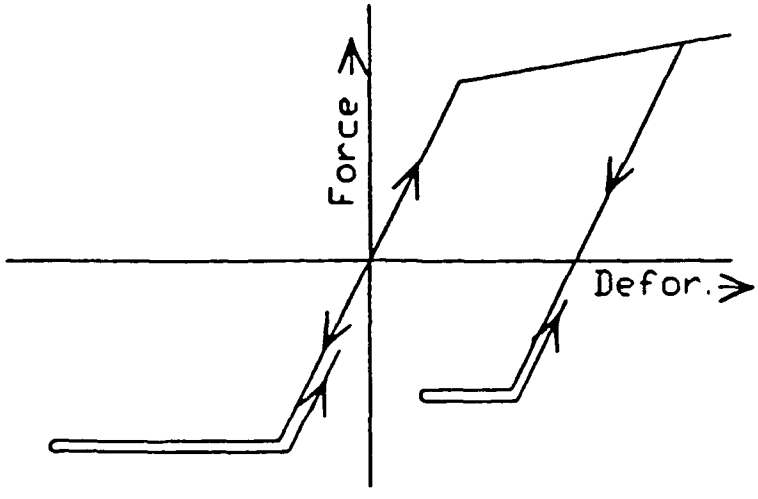

Fig. 3.6 Modified truss element [2]

cable brace yields during the tensile portion of the load cycle; however, it buckles with zero stiffness once the compressive force equals the initial pretension force in the cable. The prestressing force in the cables can be applied by specifying the initial tension force in the member.

3.5 MEMBER PROPERTIES USED IN THE ANALYTICAL MODEL

The member properties used in this analytical study are based on the structural properties of the prototype frame itself. Critical frame dimensions are contained in Fig. 2.7. Cross sections of the spandrel beam and short column reinforcement, in the third, fourth, and fifth levels of the prototype frame were given in Fig. 3.2. The beams and columns are modeled with element EL7 while the prestressed cable braces are modeled with element EL1(m). The structural properties of the columns, beams, rigid zones and braces of the prototype frame are described below.

COLUMNS. The dimensions of the column cross section shown in Fig. 3.2 are 18" by 18". The effective column width perpendicular to the plane of the frame is reduced from 18" to 10". This stems from the fact that the width of the column (18") is so much larger than the width of the spandrel beams (8") that moment is transferred to the column over a reduced column width. A column width of 10" gives good results with the experimental data [3].

Some curvature develops within the depth of the spandrel beam when the frame is subjected to lateral loading and was observed during the experimental study of the prototype frame [7]. This observation

significantly influences the length of the rigid zone, e_c, of the column which is input for the computer program. A rigid zone equal to two-thirds the spandrel depth was found to give close agreement between the analytical and experimental results. Each column is thus divided into three elements, a 72" column and two 24" rigid beam-column elements attached to the column ends. The interstory height remains 120". The column and the two rigid zones are illustrated in Fig. 2.10.

The ultimate lateral capacity of the column is needed for the analytical study. The shear strength of the columns is underestimated if calculated according to Chapter 11 of Building Code Requirements for Reinforced Concrete (ACI 318-83 code) [3]. The equation shown in Fig. 3.7 was developed for the lateral strength of an axially loaded short column. The equation is based on experimental results and applies for values of 2a/d between 2.0 and 5.0, and for axial compression lower than the balanced load. The first term in the equation represents the contribution of the compression strut which develops in the concrete. The contribution of the axial load to shear strength is in the second term. The third term represents the contribution of the column lateral reinforcement. As an example, the shear capacity of the subassemblage column is found to be 75 kips using the equation and the following properties:

a= 24"	A_s/A_g= 0.041	A_g= 180 in^2	N= 250 kips
d'= 16"	f'_c= 3 ksi	I= 4860 in^4	h= 18"
b= 10"	f_{ys}= 40 ksi	A_v= 0.60 in^2	S_h= 18"

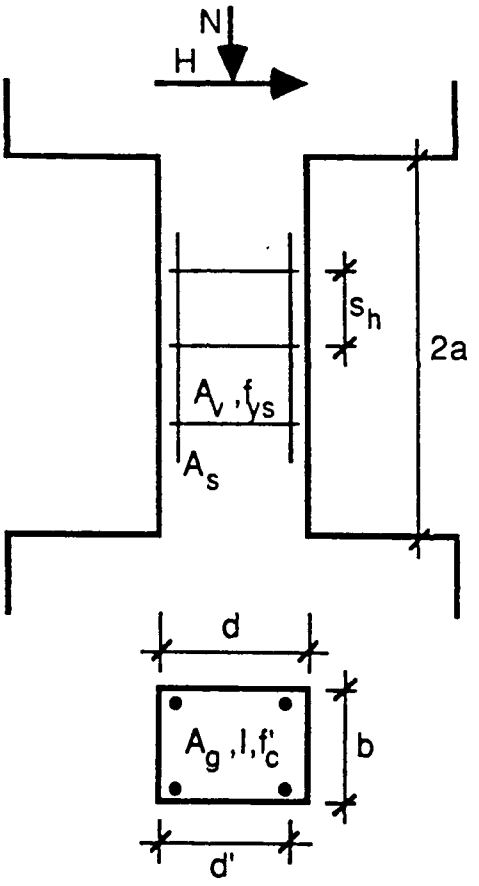

$$V_u = (7.3 - 2.6\ a/d' + 1.7\ \sqrt{A_s/A_g})\ bd'\sqrt{f'_c}$$

$$+ 2\ Nl/(aA_g h) + 0.61\ A_v\ f_{ys}\ d'/s_h$$

Fig. 3.7 Short column with strength equation [3]

As described in Section 3.3, the column will be modeled using element EL7. The phenomenological model used in EL7 will be based on experimental load-deformation curves. The load deformation curves used in this study are based on experimental work done by Woodward and Jirsa [6]. An experimental load-deformation curve similar to the subassemblage column in terms of reinforcement, depth to span ratio and level of axial load is shown in Fig. 3.8. It is thus reasonable to use this experimental backbone curve for the phenomenological model required for the subassemblage column. Fig. 3.8 is scaled for a column with 48 inch free height in Fig. 3.9. The assumption is made that the response of the subassemblage column will follow the behavior defined by the load deformation relationship shown in Fig. 3.9.

As mentioned in Section 3.3, element EL7 makes use of a quadrilinear backbone curve to define the moment-rotation relationship of the inelastic springs. In Fig. 3.9 it is shown how element EL7's quadrilinear backbone curve is "fitted" to the experimental load deformation curve. The moment-rotation relationship at a section at the end of the column is used to represent the overall flexural stiffness of the column in the computer model for element EL7. The moment rotation relation of the column is derived from the quadrilinear load deformation backbone curve of Fig. 3.9. Assuming an inflection point at mid height of the column, the end moment was obtained by multiplying the end shear by 1/2 = 72"/2. The corresponding rotation at the end of the column was taken to be the rigid body rotation of the chord connecting the end points of the column, $\theta = \Delta/l$.

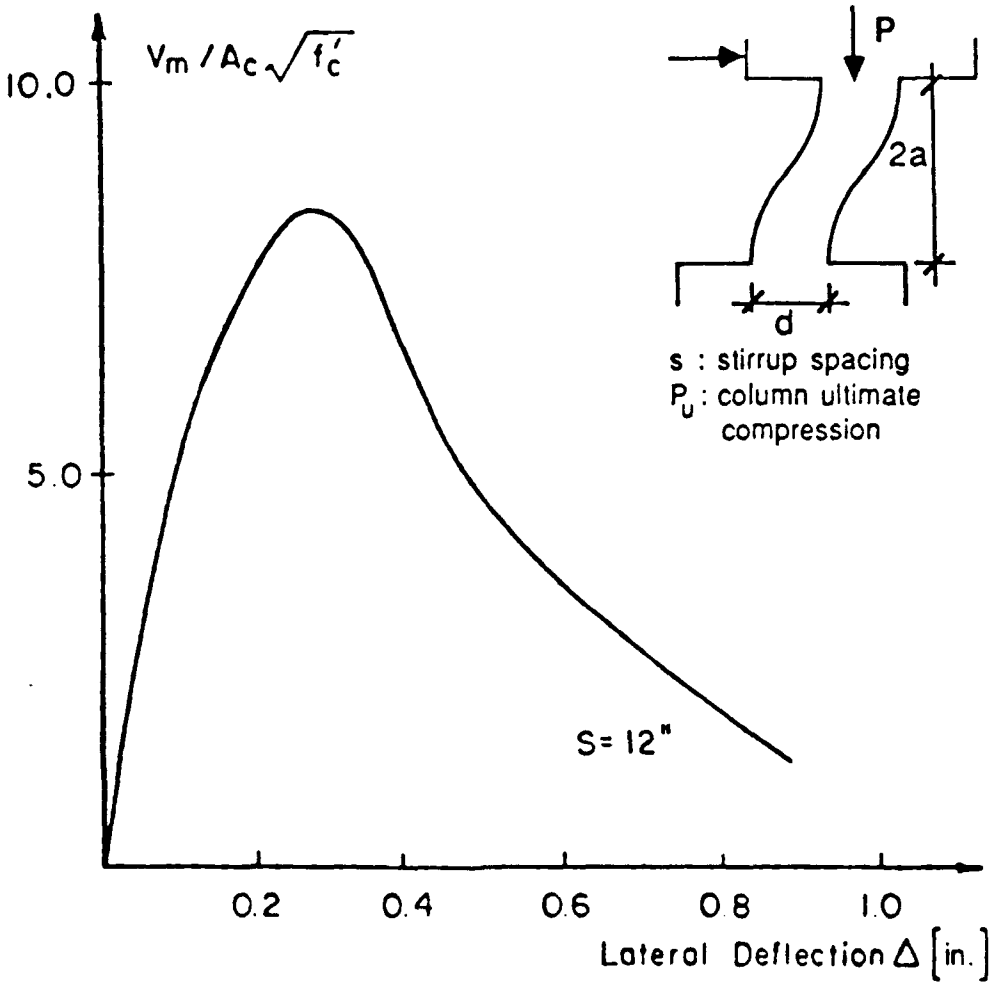

	2a/d	d/s	P/P_u
Woodward Test	36"/12" = 3	12"/12" = 1.0	$\frac{140}{880} = 1/6.2$
Subassemblege Column	48"/18" = 2.7	18"/18" = 1.0	$\frac{250}{1300} = 1/5.2$

Fig. 3.8 Experimental load-deformation curvefor a short column similar to the subassemblage column [2]

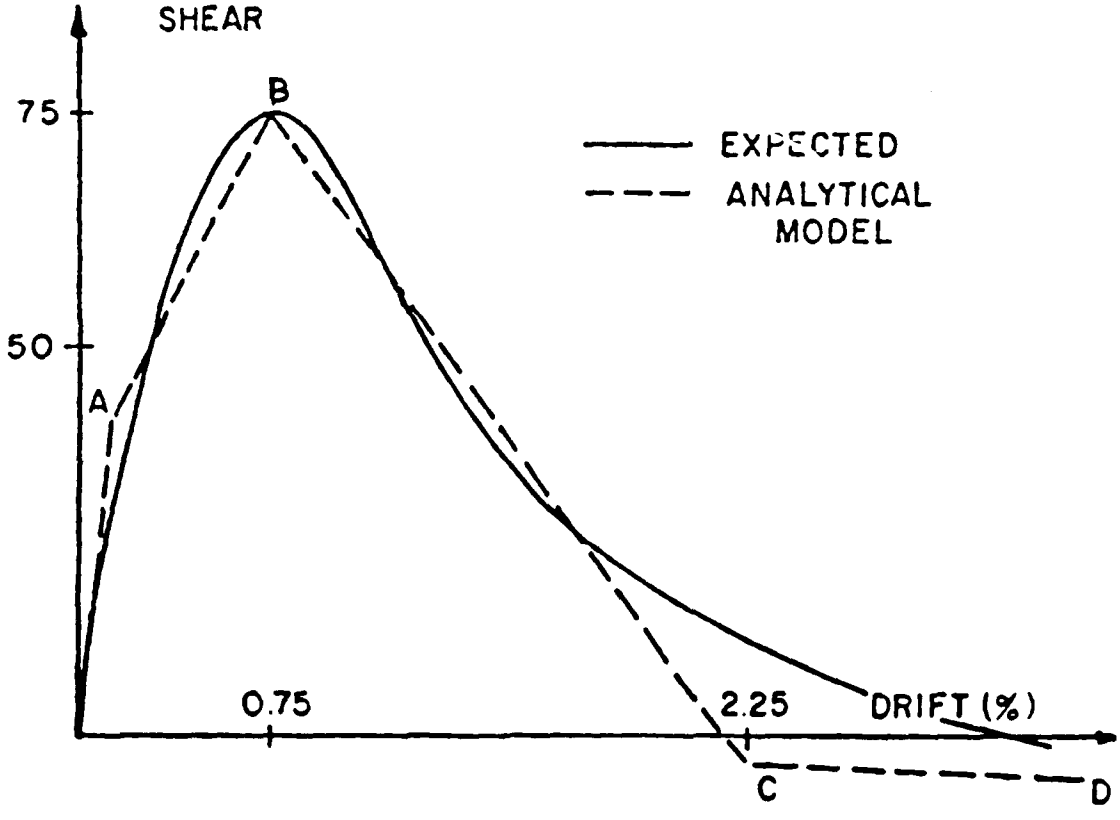

Fig. 3.9 Load deformation curve for the subassemblage column [2]

Recall from Sec. 3.3 that the column modeled by EL7 consists of a linear elastic beam element in series with two inelastic rotational springs, one on each end. The elastic beam has constant stiffness at all stages of loading. The stiffness of the rotational springs, however, is derived from the moment-rotational relationship of the overall column. Thus, all inelastic yielding in the element model is assumed to take place in the rotational springs.

Stiffness degradation is exhibited in short columns subjected to cyclic lateral loads. This phenomenon, discussed in Sec. 2.2., is modeled by altering the stiffness of the inelastic rotational spring. The rotational spring is given a very large initial stiffness by the program, $(E_cI_c \times 10^{8})$, where E_cI_c is the stiffness of the linear elastic beam element computed from

$$E_cI_c = (V)(L)^3/(12(\Delta))$$

Recall that the overall stiffness of two springs in series is taken as the inverse of the summation of the springs' reciprocal stiffnesses. Thus, a large initial spring stiffness guarantees the initial stiffness of the column element will be essentially the same as that of the elastic beam element, E_cI_c.

The initial column stiffness extends up to about 50% of the ultimate shear strength of the column element in the phenomenological model. This corresponds to segment OA in Fig. 3.9. The overall stiffness of the column reduces to about 15% of its initial stiffness once the ultimate shear strength is reached (refer to the slope of

segment AB in Fig. 3.9). The stiffness of the inelastic spring at point A is calculated internally by the program and correspondingly reduces to about 1.5×10^{-9} times the initial spring stiffness. The degrading segment of the load-deformation curve, segment BC, has a negative slope equal to -13.8% of the initial column stiffness. The stiffness of the inelastic spring in this part of the curve is internally calculated as -1.38×10^{-9} times the initial spring stiffness. Segment CD represents the portion of the curve where the lateral capacity of the column becomes less than the P-delta effects. The column has to "borrow" strength to carry the axial load, hence the capacity of the column becomes negative. The overall stiffness of the column in segment CD is -0.33% of the initial column stiffness while the spring stiffness is internally calculated as -3.3×10^{-11} times the initial stiffness of the rotational spring.

BEAMS. The critical dimensions and reinforcement detailing of the third, fourth, and fifth level beams of the prototype frame are shown in Figs. 2.5 and 3.2. The beams of the prototype frame deform in double curvature when subjected to lateral loading. The beam's capacity to resist positive and negative moment is, however, not symmetric. In calculating the moment curvature relationship for the spandrel beam, a 48 inch width of floor slab near the bottom of the beam is considered to carry moment along with the spandrel. The positive cracking moment is thus larger than the negative cracking moment. The negative yield moment and ultimate moment of the beams, however, are greater than the corresponding positive moment values because of the unsymmetrical reinforcement. The detail in Fig. 3.2 indicates twice as much negative

moment top steel than positive moment bottom steel. Different positive and negative moment-rotation relationships must therefore be derived for the spandrel beams.

Calculation of the moment-curvature relation for positive moment at the end of the beam produces a yield moment less than the cracking moment. Upon investigation, it was found that this phenomenon results partly from the fact that the spandrel beam is severely under reinforced. The percentage of steel provided is less than that required as a minimum in the 1951 version of the ACI Building Code [10]. For simplification M_{cr} was taken as M_u for schemes where $M_{cr} > M_u$. In those cases, the beam was assumed to transition directly from the elastic range to strain hardening. The moment-rotation relationship thus reduced to a bi-linear curve.

The Element EL7 subroutine allows the user to input different yield moment values for positive and negative moment. The user is constrained, however, to one set of stiffness ratios as input (refer to the user's guide in Appendix A). The same stiffness ratios must be applicable for both positive and negative moment. The stiffness ratios are used in the program along with the input yield moment values to define the moment-rotation relationship for the inelastic springs. This constraint becomes significant for sections such as the prototype spandrel beam which have different negative and positive moment-curvature relationships. The user is therefore not able to input the hand calculated positive and negative moment rotation relationships directly. A compromise moment-rotation relationship must be developed which contains one set of stiffness ratios applicable for both positive

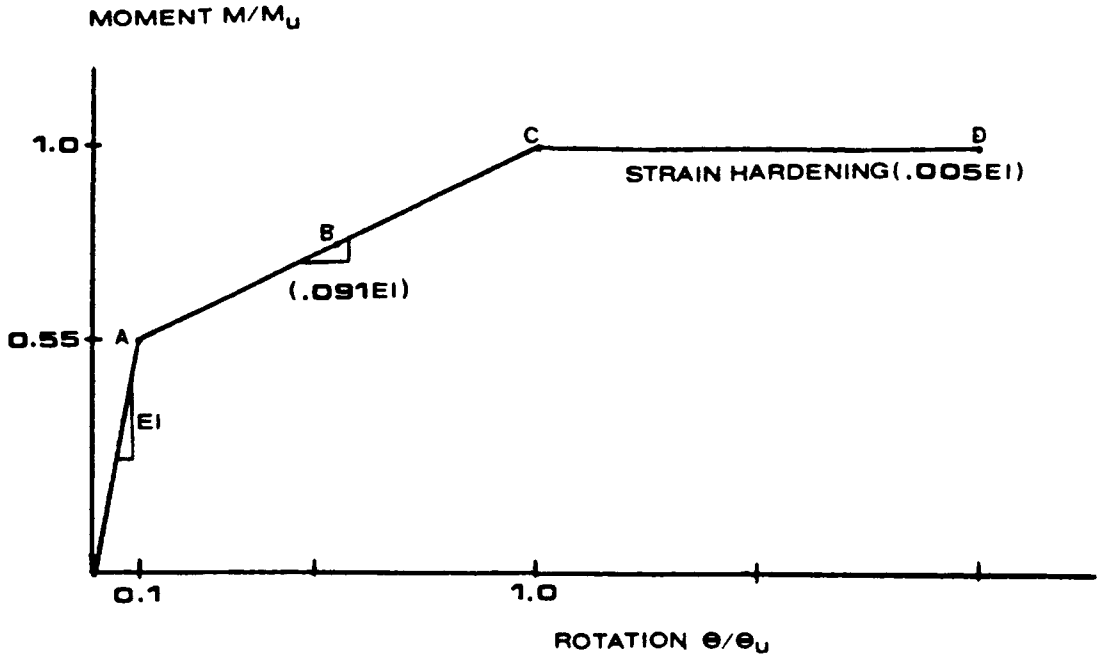

Fig. 3.10 Moment-rotation relationship for the beam

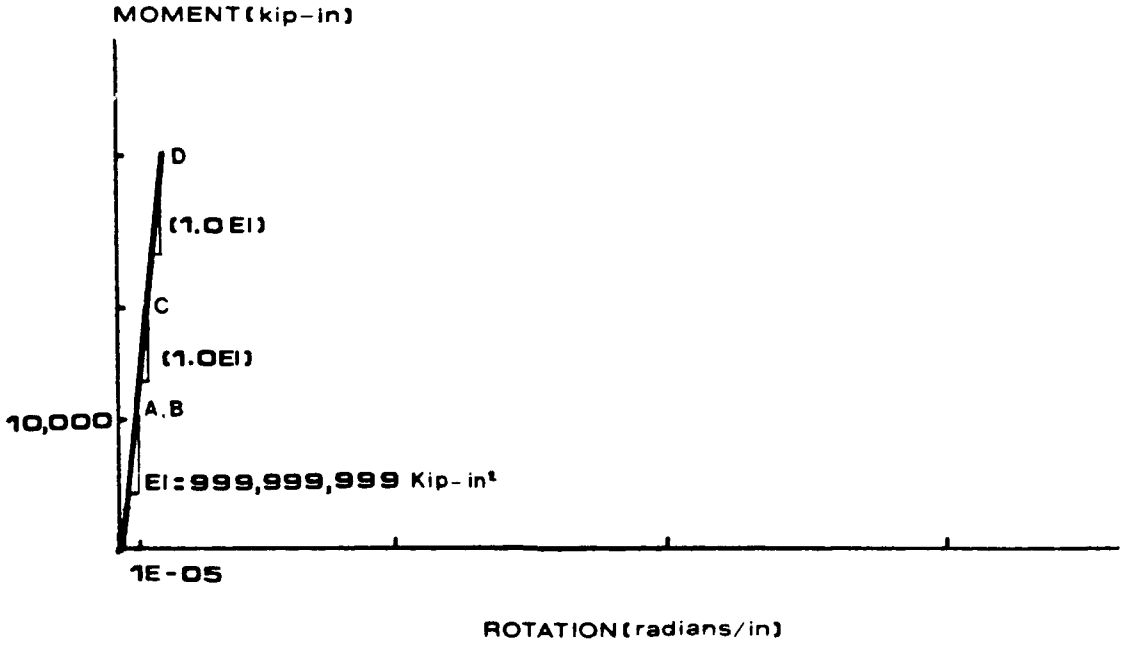

Fig. 3.11 Moment-rotation curve for a typical rigid element

and negative moment. Fig. 3.10 was developed by "averaging" the slopes of the positive and negative moment-rotation curves for the prototype spandrel. The resulting tri-linear moment curvature relationship is thus applicable for both positive and negative moment. Fig. 3.10 represents a compromise and was developed in an attempt to live within the constraints of the existing program. The resulting monotonic response obtained using this model compares well with experimental tests conducted on the prototype frame [3]. The moment-curvature relationship is first hand calculated at ultimate for both positive and negative moment at a section taken at the ends of the spandrel beam. The cracking moment is taken simply as 55% of the calculated ultimate moment. The yield moment is taken as the average of the ultimate and assumed cracking moment. Finally the resulting moment-curvature curves are converted to moment-rotation curves by multiplying the curvatures by d/2 (assuming the plastic hinge develops along a length d/2). It is assumed that the spandrel beam will behave in a ductile manner and that reduction of the cracking moment to a value below that obtained by hand calculation will not significantly affect overall frame response.

Similar to the approach used for the column, the initial stiffness of the inelastic spring is set very high at $E_c I_b \times 10^8$. $E_c I_b$ is the flexural stiffness of the beam element calculated from the section properties of the uncracked transformed section. For the beam section shown in Fig. 3.2, the uncracked stiffness was calculated to be 928,339,200 kip-in^2. The high initial spring stiffness ensures the initial stiffness of the beam element is the same as the elastic beam element in segment OA of Fig. 3.10.

The positive and negative ultimate moments for the section shown in Fig. 3.2 are 4030 and 6370 kip-inches respectively. Using the model in Fig. 3.10, the positive and negative cracking moments are 2215, and 3500 kip-inches respectively. At point A of Fig. 3.10 the concrete is assumed to have cracked and the stiffness of the spandrel beam reduces to 9.1% of the initial uncracked beam stiffness. Correspondingly, the stiffness of the inelastic rotational spring will reduce to 9.1×10^{-10} times the initial spring stiffness. The stiffness of the beam at point C corresponds to strain hardening in the beam, segment CD. The slope of segment CD reduces to 0.5% of the initial beam stiffness. The corresponding stiffness of the inelastic springs drops to 5×10^{-11} times the initial spring stiffness. The stiffness of the beam in the strain hardening region is taken as constant until failure.

RIGID ZONES. The 24" *rigid zones* at the beam-column joints shown in Fig. 2.10, are also modeled using element EL7. This element must behave elastically throughout the loading cycles. This is done by keeping the stiffness of the rotational springs constant for all segments of the quadrilinear moment-rotation curve. The idealized moment-rotation relationship for a typical rigid element is shown in Fig. 3.11. A very high value of flexural stiffness has been used, about twenty times the initial stiffness of the column.

BRACES. The prestressed cable braces are modeled using the modified truss element described in Sec. 3.4. The cable braces of the bracing system consist of individual steel strands wound together in such a way so as to form a complete cable. The number of strands in the cable depend, of course, on the magnitude of the lateral force to be

resisted. The cable material used in this study is assumed to be stress relieved ASTM A416, grade 270. The ultimate tensile strength is rated at 270 ksi and the yield strength is approximately 230 ksi. The modulus of elasticity used is E= 26,000 ksi. The prestressing force applied to the cables in the computer model is assumed to be the effective prestressing force, that is, the initial prestressing force minus losses. The cross sectional areas of the cable braces are calculated with either Eqn. 2.2 or Eqn. 2.3 depending on whether the ultimate or serviceability design approach is taken.

3.6 STATIC INCREMENTAL LOADING

During an earthquake, ground motion occurs in random fashion in countless directions. It is the horizontal component of these motions, however, which produces the most damage to structures. It is for this reason that most research is limited to lateral loads only. The response of the prototype frame is studied under two types of static incremental lateral loads, monotonic and cyclic.

3.6.1 Monotonic Loading

The prototype frame was subjected to monotonically increasing horizontal displacements. The purpose of examining the behavior of the frame under monotonic loading is to produce simplified response curves from which the basic failure mechanism of the unstrengthened, braced-unaltered, and braced-altered frames can be derived. The behavior of the frame to monotonic loading provides a response envelope within which the cyclic loading response is expected to occur.

The frame was loaded far into the inelastic range such that the capacity of the unbraced frame was reduced to essentially zero. The applied percentage drift was limited to 1.6%.

3.6.2 Cyclic Loading

The purpose of applying cyclic static incremental lateral loading is to reproduce the main characteristic of an earthquake. The response curves produced from the cyclic loading are called hysteresis loops. The area enclosed in the hysteresis loops is directly related to the capacity of the structure to effectively dissipate energy in a seismic event.

The cyclic loading history applied to the prototype frame was chosen in such a way that key frame behavioral events occurring when loaded in one direction are followed by the occurrence of the same event when loaded in the opposite direction. Such events might include cracking of the columns and/or beams, or shear failure of a column. A total of six cycles of increasing interstory drift were applied up to a maximum interstory drift of 1.8%. The cyclic loading history applied to the prototype frame is illustrated in Fig. 3.12.

3.7 RESPONSE OF THE UNBRACED AND BRACED SUBASSEMBLAGE

In this section the response of the unbraced and braced subassemblage to static incremental monotonic displacements is reviewed. The failure mechanism of the unbraced subassemblage is described and the

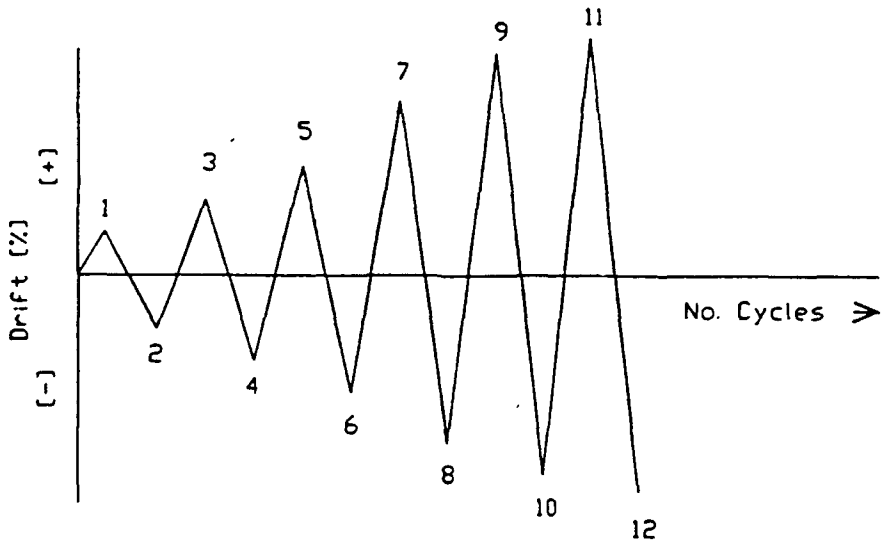

NUMBER OF CYCLE	PEAK INTERSTORY DRIFT δ %		LOAD REVERSAL
	POSITIVE δ %	NEGATIVE δ %	
I	0.075	-0.117	1 2
II	0.210	-0.225	3 4
III	0.510	-0.770	5 6
IV	1.200	-1.200	7 8
V	1.710	-1.710	9 10
VI	1.800	-1.800	11 12

Fig. 3.12 Loading history for the cyclic case [2]

effect of the prestressed cable bracing system on the total response is discussed.

3.7.1 Failure Sequence Of The Unbraced Subassemblage

The response of the unbraced subassemblage to monotonic loading is shown in Fig. 3.13. The failure sequence of the unbraced subassemblage is described below. Reference numbers are those of Fig. 3.13.

1-2 : The subassemblage behaves elastically.

2 : Columns crack in shear. Initial stiffness decreases. Interstory drift = 0.06%, H = 38k.

3 : Spandrels crack in flexure. Interstory drift = 0.15%, H=50.0k.

4 : Column fails in shear. Stiffness becomes negative for increasing interstory drift. Interstory drift = 0.39%, H=75k.

5 : Column lateral capacity drops to zero. Interstory drift = 0.90%.

5-6 : Column lateral capacity becomes negative. The column lateral capacity becomes less than the P-delta effects.

3.7.2 Response Of The Braced Subassemblage

The response of the braced subassemblage when subjected to monotonic loading is shown in Fig. 3.14. For this bracing scheme, the ultimate design approach was taken with a design strength ratio of n=2 (see discussion in Sec. 2.4.2 for the definition of n). The cable braces are considered to extend from the beam-column joint of one story to the center of the beams of the story below as shown in the figure.

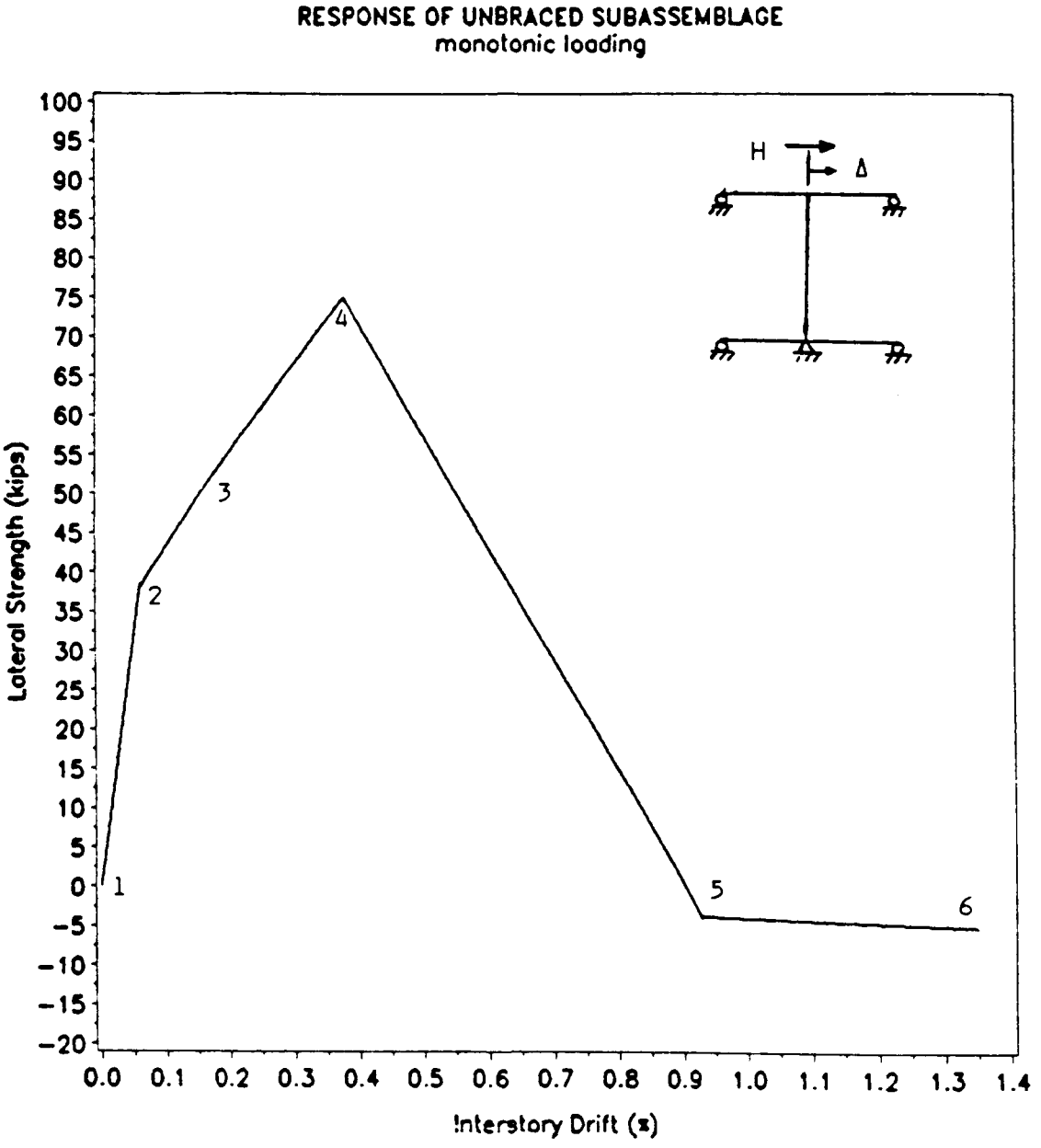

Fig. 3.13 Response of the unbraced subassemblage to monotonic loading

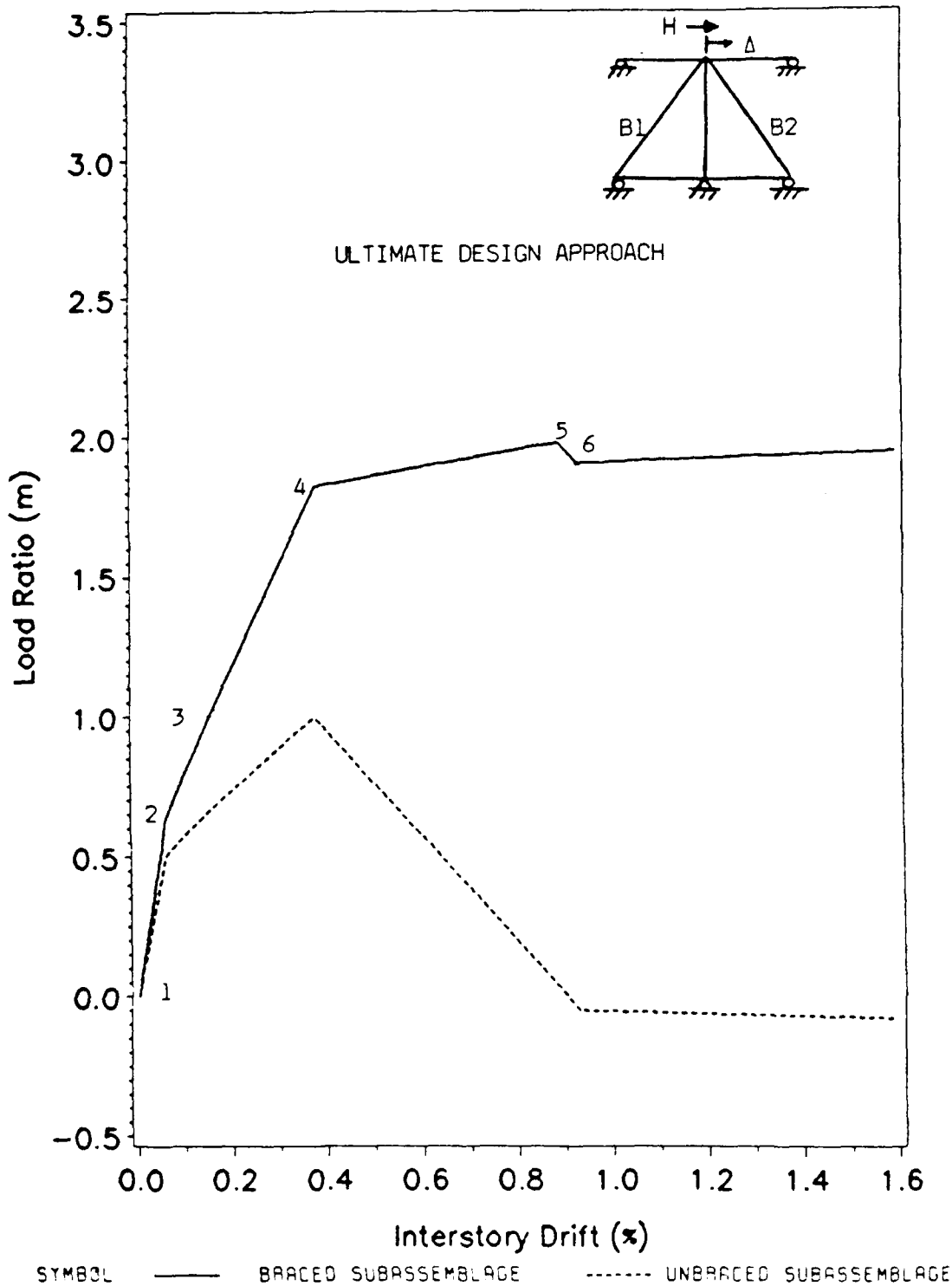

Fig. 3.14 Response of the unbraced subassemblage to monotonic loading, n=2, and 0.5Py prestressing force

An initial prestressing force of $0.5P_y$ is applied to the ASTM A416 grade 270 stress relieved cables. For comparison, the response of the braced subassemblage is superimposed over the response of the unbraced subassemblage. The failure sequence for the braced subassemblage is discussed below. Reference numbers are those of Fig. 3.14.

1-2 : The subassemblage behaves elastically.

2 : Columns crack in shear. Initial stiffness decreases. Interstory drift = 0.06%, H=47.3k, m=0.63.

3 : Spandrels crack in flexure. Interstory drift = 0.15%, H=75k, m=1.0.

4 : Column fails in shear. Interstory drift = 0.39%, H=138.8k, m=1.85.

5 : Simultaneous buckling and yielding of brace B1 and B2. Ultimate capacity of the braced subassemblage is reached. Interstory drift = 0.88% , H=150k, m=2.0. Stiffness becomes negative for increasing interstory drift.

6 : Lateral capacity of the unstrengthened subassemblage drops to zero Stiffness regains positive slope as the frame stiffness is now less negative.

From Fig. 3.14 it can be seen that although the response of the subassemblage has been substantially improved over that of the unbraced subassemblage, the overall failure mechanism has not been altered. The frame behavior is still dominated by shear failure in the short columns occurring at point 4. The overall effectiveness of the bracing system still depends on the response of the unbraced frame.

CHAPTER 4

EFFECTIVENESS OF BEAM ALTERATION IN CONJUNCTION WITH PRESTRESSED CABLE BRACES

4.1 BEAM ALTERATION IN FRAMES WITH WEAK COLUMNS-STRONG BEAMS

The overall effectiveness of any seismic design is measured not only in terms of the magnitude of the ultimate seismic resistance but on the nature of the failure mechanism which develops at this ultimate resistance as well. The unstrengthened prototype frame studied in this research project contains a weak column-strong beam configuration. As will be discussed in detail in Sec. 4.2, the failure mechanism of this frame is undesirable. The failure of the frame is controlled by shear failure in the short columns at relatively low horizontal drift. Beyond the drift at which the shear failure occurs, the frame rapidly loses lateral capacity and significant damage to the columns also degrades the frame's ability to carry vertical loads. Even if the frame is braced to carry current design lateral loads, the ultimate failure mechanism will remain unchanged. In the event of an earthquake which induces lateral loads on the frame exceeding the design loads, the failure will follow a brittle collapse type mechanism. The key to a favorable failure mechanism in a multi-story building is to move failure away from the columns and into the beams.

The difference between the lateral failure mechanisms of a strong column-weak beam frame and a weak column-strong beam frame is illustrated in Fig. 4.1. As is evident from the figure, the strong

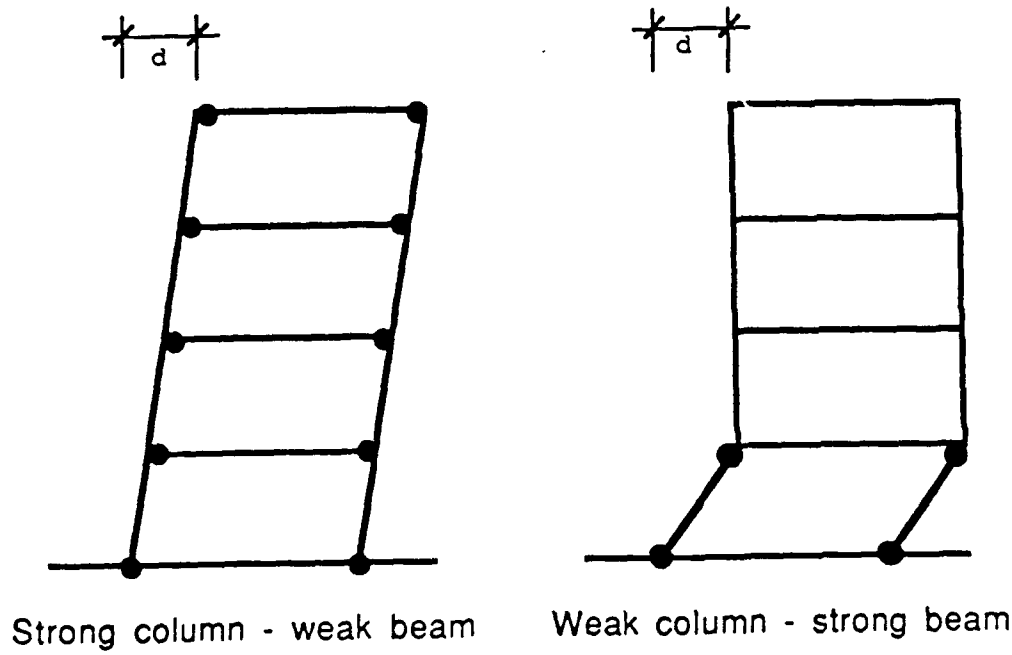

Fig. 4.1 Frame lateral failure mechanisms [3]

column-weak beam frame fails through the development of plastic hinges at the ends of the beams. Such a failure mechanism is very ductile and energy dissipation is quite significant. Since the inelastic behavior is limited to the beams, the columns are able to carry the vertical loads even under large lateral drifts. Most importantly, this mechanism does not typically result in collapse of the structure. A weak column-strong beam frame, however, can fail either through the development of plastic hinges at the ends of the columns or failure of the columns in shear. Such failure mechanisms are somewhat less ductile and typically dissipate less energy than beam hinge type mechanisms. Tragically, such mechanisms can result in collapse of one or more stories.

Beam alteration is a technique by which strong beams are physically altered in some manner so as to move failure away from the columns and into the beams. The aim of such techniques is to alter the ultimate failure mechanism of the structure to one that is more favorable. Applications of beam alteration are already in use countries such as Mexico and Japan. Beam alteration can be combined with some other type of seismic retrofitting technique such as steel bracing in order to improve the overall seismic performance of a structure [3].

In this study, the aim is to convert the weak column-strong beam frame to a strong beam-weak beam frame. This can be achieved by either strengthening the columns or by weakening the beams. The former has the advantage of simultaneously altering the failure mechanism and improving the lateral strength of the frame. It does not, however, make practical sense in this study because the prestressed cable bracing system can be

designed to provide all the lateral strength required. Weakening the beams may be easier and less expensive than column strengthening.

The concept of beam weakening involves reducing the flexural capacity of the beam just enough so that plastic hinges will form at the ends of the beams before column failure occurs. One way of achieving this result is to core or cut into the beam ends and sever some longitudinal reinforcement. The altered beam must still, of course, be able to develop sufficient moment to carry the gravity loads to the columns. Loss in the frame's lateral strength and stiffness, however, can be easily made up by the prestressed cable bracing system.

Badoux performed a parametric study on the prototype frame subassemblage introduced in Sec. 2.4.1 to investigate the effectiveness of combining beam alteration with a steel bracing system [3]. The objective in this chapter is to extend Badoux's parametric study to prestressed cable bracing systems. The idea of combining beam alteration with prestressed cable bracing systems to examine the overall improvement in seismic response of the prototype frame will be investigated. The scope of the investigation will be limited to the one degree of freedom subassemblage of the prototype frame introduced in Sec. 2.4.1.

4.2 INTRODUCTION OF BEAM ALTERATION PARAMETERS

4.2.1 The q And r Ratios

When altering a structure with the aim of achieving a more desirable failure mechanism, it is necessary to keep two strength

concepts in mind. First, the "brittleness" of individual members making up the frame, and secondly, the relative strength of the columns and beams at the joints under lateral loading. In this section these two strength concepts are defined as ratios q and r. These two ratios will aid in the discussion and facilitate the quantitative study of the beam alteration-prestressed cable brace retrofit scheme.

Ratio q. The first concept or ratio that should be kept in mind is the brittleness of the individual members in the frame. For a frame member submitted to double curvature as shown in Fig. 4.2, q is defined as

$$q = V_{us}/V_{uf} \tag{4.1}$$

where V_{us} is the shear leading to shear failure and V_{uf} is the shear leading to flexural failure. Thus q can be thought of as a measure of the member's brittleness. If q is less than 1.0, the failure in the member is shear dominated and will occur in a brittle fashion. The column in the subassemblage of the prototype frame has a q value of

$$q_c = 75k/133k = 0.56$$

This indicates brittle behavior and is expected in a frame with short columns. By contrast the q value for the spandrel beam is calculated as

$$q_b = 123k/44.4k = 2.77$$

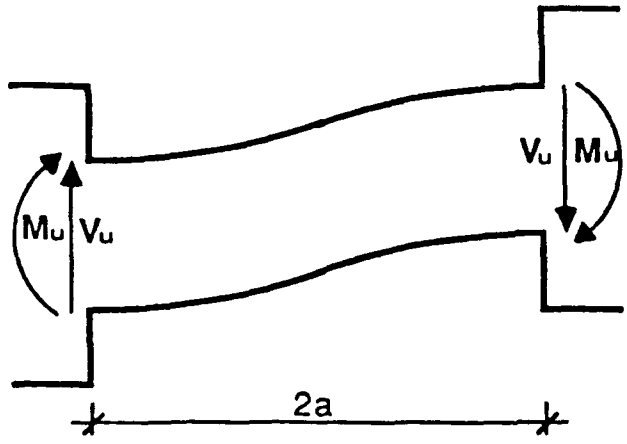

$$q = V_{us} / V_{uf}$$

$$V_{uf} = (M_{u+} + M_{u-})/2a$$

Fig. 4.2 Ratio q for a member in double curvature [3]

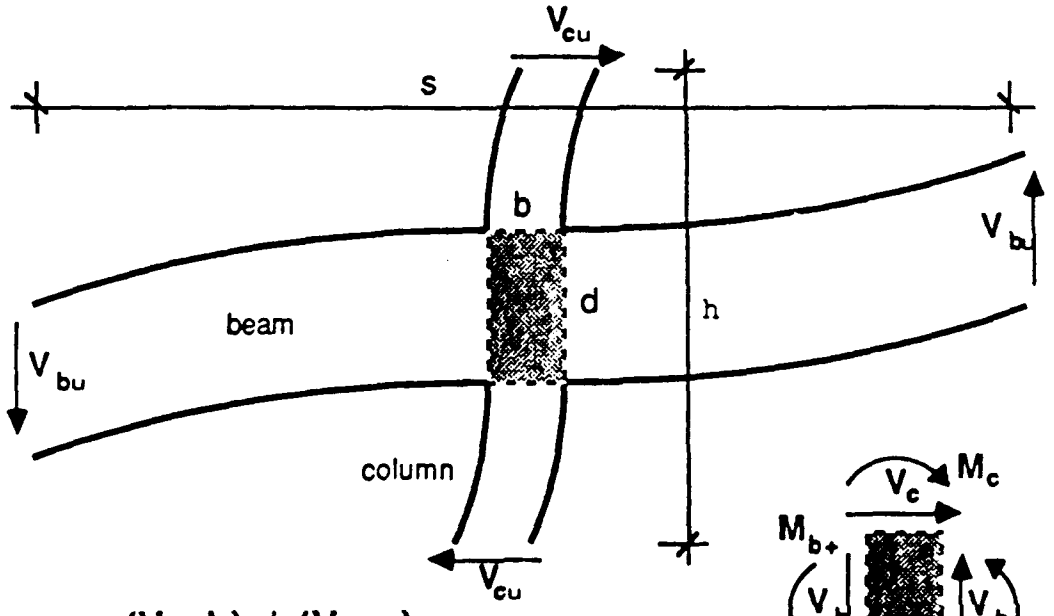

$$r = (V_{cu} h) / (V_{bu} s)$$

$$V_{buf} s = (M_{bu+} + M_{bu-}) s / (s - b)$$

Fig. 4.3 Ratio r for a beam column joint [3]

Ratio r. The second ratio is a measure of the relative strength of the beam and column at the frame's joints. A typical beam-column joint subjected to lateral loading is illustrated in Fig. 4.3. The ratio r is defined as

$$r = (V_{cu})h/(V_{bu})s \qquad (4.2)$$

where $(V_{cu})h$ is the ultimate moment which will cause column failure and $(V_{bu})s$ is the ultimate moment which will cause beam failure. As shown in Fig. 4.3, if q for the beam is greater than 1.0, then $V_{bu} = (M_{bu+} + M_{bu-})/(s - b)$, where M_{bu+} and M_{bu-} are the beam positive and negative moment capacities at the face of the joint. V_u is equal to V_{us} if q is smaller than one.

A value of r less than 1.0 indicates the columns framing into the joint are weaker than the beams. As discussed previously, favorable failure mechanisms will have beams failing in flexure before the columns fail in shear. In such mechanisms, the columns are stronger than the beams and thus r is greater than 1.0. The joints of the prototype frame yield:

$$r = (V_{cu})h/(V_{bu})s = (75k \times 120\ in)/(44.4k \times 252\ in) = 0.80.$$

The aim of the beam alteration-prestressed cable brace retrofit scheme is to raise column q values above 1.0 and r values of the joints well above 1.0. Section 21.4.2.2 of ACI 318-89 [9] requires the ratio of the

flexural strength of the columns framing into a joint to the flexural strength of the girders framing into that same joint shall not be less than 6/5 = 1.2. Expressed in terms of the r ratio (taking nominal rather than factored beam and column strength) the requirement becomes;

$$r > [(1.2)(.9)]/(.7) = 1.54$$

This requirement in part takes into account the contribution of slab reinforcement and strain hardening to beam strength.

4.2.2 Beam Weakening Parameters

The concept of beam alteration is illustrated in Fig. 4.4. As the frame reaches its ultimate capacity, the aim is for plastic hinges to develop in the beams rather than at the column ends. The plastic hinges will develop at the beam's ends where the magnitude of the moments induced by gravity loads and lateral displacements will be the greatest. To ensure such a mechanism, the flexural capacity of the beam at the ends must be reduced. This can be accomplished by cutting or coring into the beam. Typically, at least two cuts are made into the beam. The primary reduction in flexural capacity comes from severing the longitudinal reinforcement, but there is also a reduction in strength due to the change in effective section depth from d to (d - u - v) as shown in the figure.

The depth of the cut into the top of the beam is defined as parameter u. Similarly the depth of the cut into the bottom of the beam is defined as parameter v. The effective length of the cut along the

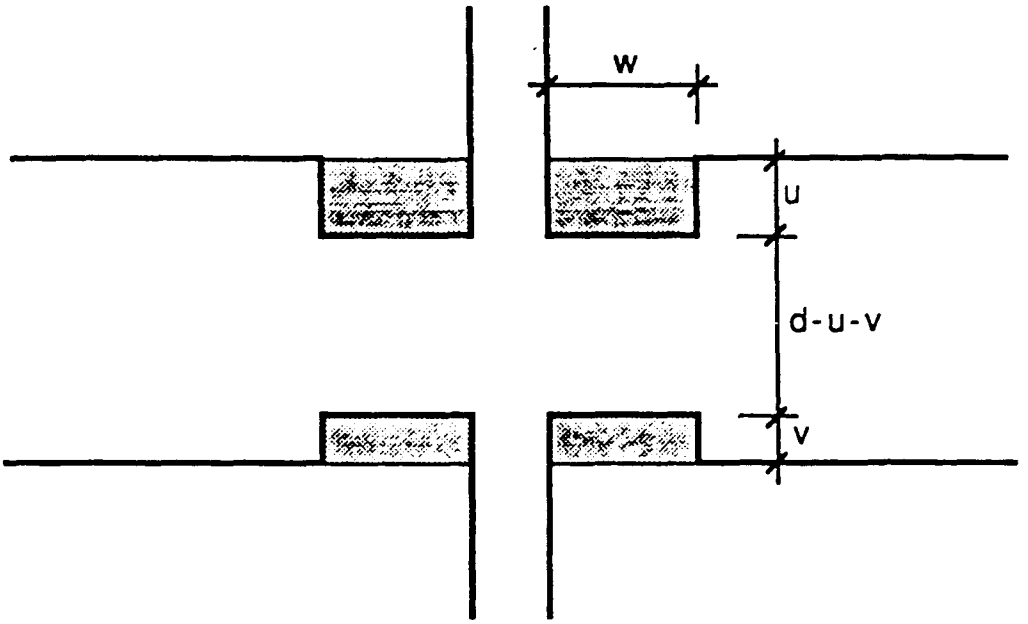

Fig. 4.4 Weakening parameters u, v, and w [3]

beam is defined as parameter w. The effective length of the cut, w, is greater than simply the distance between the two extreme cuts. This is due to the anchorage lengths which must develop as a result of severing the reinforcement. The length w is important in the development of the plastic hinge and the subsequent dissipation of energy. Plastic hinges at the ends of fixed beams are generally thought to form over a length of roughly 0.5 x the effective depth of the beam. If w is too small to allow the hinge to fully develop, yielding and cracking cannot spread and the rotation capacity of the hinge is limited. For this reason, w should be larger than the effective depth of the section, (d - u - v).

Cutting into the beam increases the effective free height of the columns. If the effective free height of the column is defined as 2a before beam alteration, weakening the beam in this manner will increase the effective free height of the column to (2a + u + v). As a direct benefit of this, the ratio q for the column is increased by a factor of (2a + u + v)/2a. Thus beam alteration appears to reduce the brittleness of the column. The strength of the column, however, is not reduced as V_{us} is not affected.

The designer must be careful in choosing weakening parameters u, v, and w. One must ensure foremost that the weakened beam is still adequate to perform its primary function which is to transfer the gravity loads to the columns. In the prototype frame, the capacity of the deep spandrel beams is more than enough to carry the gravity loads. In fact, there is sufficient positive moment steel in the section to allow the beam to carry the gravity loads as a simply supported beam. Theoretically, then, the moment capacity of the beam ends could be

reduced to zero. This is not entirely true as the section must still have sufficient effective depth to transfer shear force. Additionally, when cutting or coring the section, care must be taken to not disturb the shear reinforcement.

4.3 EVALUATION OF BEAM ALTERATION SCHEMES

In a parametric study conducted by Badoux, twelve beam weakening schemes for the subassemblage were evaluated in conjunction with a steel bracing system [3]. The weakening parameters u and v were varied to cover a wide range of possible weakening schemes. From the results of his study it was concluded that four of the twelve schemes result in significant alteration of the subassemblage's behavior. These four schemes have been retained for the present study and are summarized in Table 4.1. These schemes can be accomplished by either cutting or coring into the beam as shown in Fig. 4.5.

TABLE 4.1 Beam Alteration Schemes

Scheme #	U	V	W	qc	qb	r
1	3"	0"	36"	0.60	3.52	1.06
2	3"	3"	36"	0.63	4.00	1.59
3	6"	0"	36"	0.63	5.29	1.62
4	6"	6"	36"	0.70	5.47	3.08

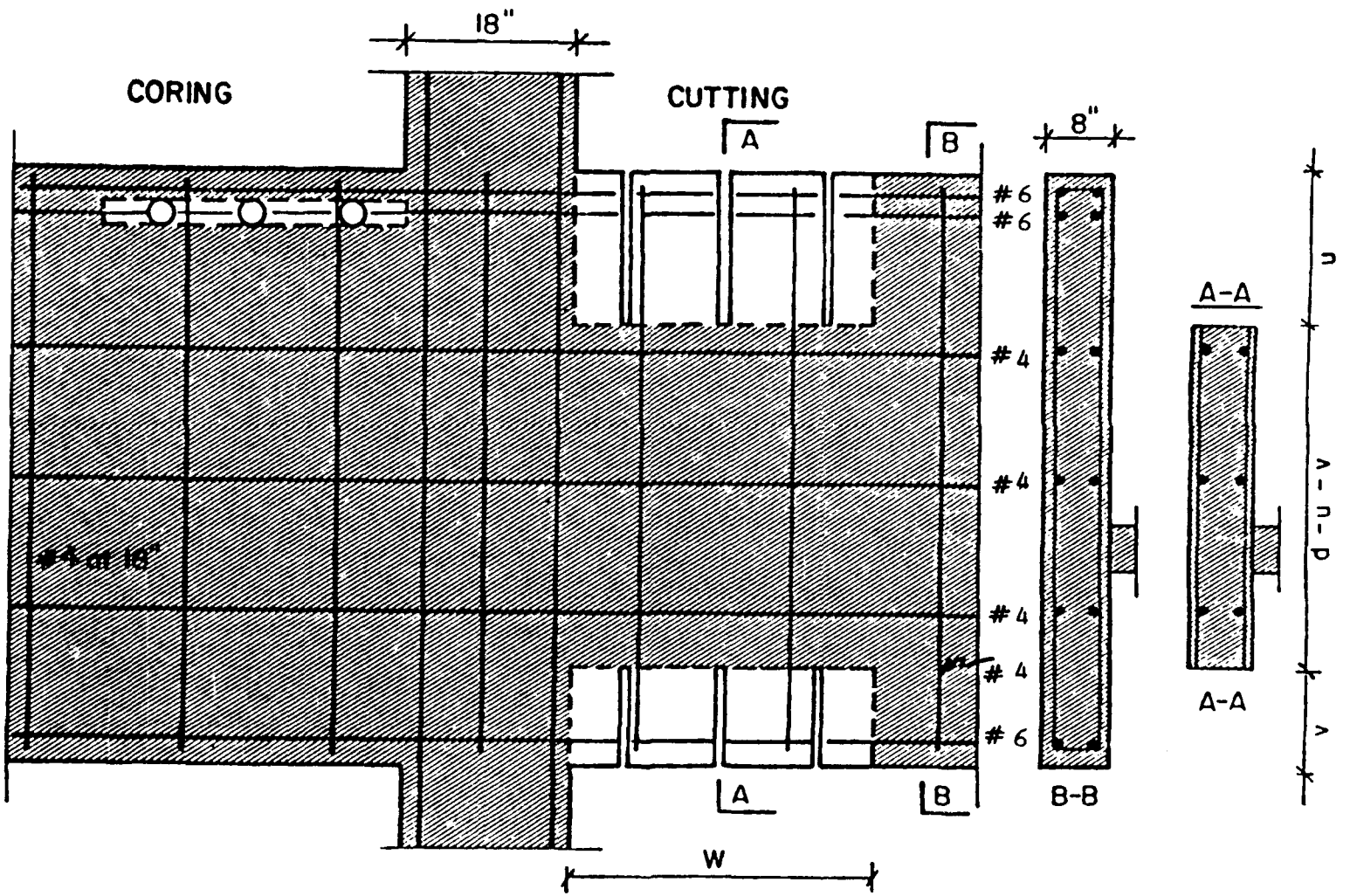

Fig. 4.5 Beam weakening schemes for prototype building

The effect of the four beam alteration schemes on the response of the unbraced subassemblage is shown in Fig. 4.6. In scheme 1 the top layer of negative reinforcement is cut (two #6 bars). The beam moment capacity is reduced by 24% and the factor of safety against column failure r is increased from 0.8 to 1.06. The overall lateral capacity of the unbraced subassemblage has been reduced from m = 1.0 to m = 0.87. The failure mechanism, however, has successfully been altered. At point 0 the weakened beam fails in flexure at a drift of about 0.3%. The brittleness of the column is improved as well from q = 0.56 to 0.60.

In scheme 2 the first layer of negative reinforcement (two #6 top bars) is cut as well as the first layer of positive moment reinforcement (two #6 bottom bars). The moment capacity of the beam is reduced by 49% and r is increased to 1.59. The failure mechanism of the altered subassemblage is as follows:

1-2 : Subassemblage behaves elastically

2 : Column cracks in shear. Interstory drift = 0.06%, m = 0.35.

3 : Beams crack in flexure. Interstory drift = 0.1%, m = 0.5.

4 : Plastic hinges develop in beam. Interstory drift = 0.175%, m = 0.59.

In scheme 3 the top two layers of negative moment steel are cut (four #6 top bars). For this scheme the moment capacity of the beam is reduced by 50.5% and the r ratio is further increased to 1.62. Finally, in scheme 4 both primary positive and negative reinforcement has been removed from the beam section. The moment capacity is reduced to 26% of

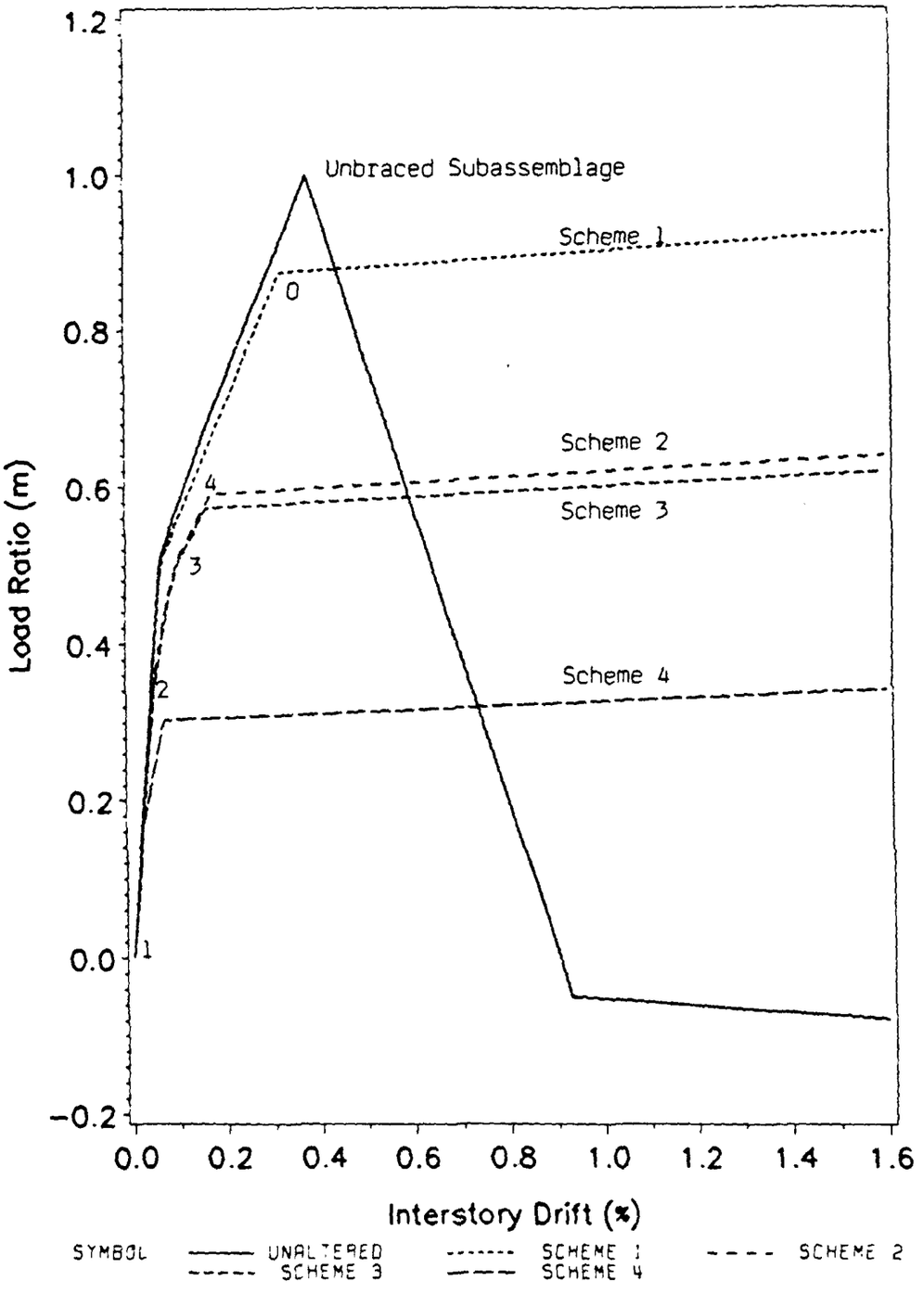

Fig. 4.6 Response of subassemblage to beam alteration schemes, monotonic loading

the beam's initial flexural capacity. The factor of safety against column failure is increased to 3.08.

The choice of beam alteration schemes depends upon the desired level of safety against column damage. In all four schemes examined, the r ratio was raised above 1. In scheme 1, however, the factor of safety, r = 1.06, is very slim. The contribution of the slab reinforcement and strain hardening in the beam reinforcement could increase the flexural capacity of the columns by as much as 10 - 15%. Scheme 1 does not provide a factor of safety of 1.54 as required by ACI 318-89 Sec. 21.4.2.2. Schemes 2, 3, and 4 all provide adequate factors of safety against column failure. The high safety levels provided by Schemes 2, 3, and 4 are particularly desirable because of the frame's short brittle columns (maximum q ratio achieved was only 0.7). Scheme 4 achieves an r = 3.08 which is unnecessarily high.

4.4 EFFECT OF BEAM ALTERATION ON CYCLIC RESPONSE

Cyclic Response of the Unbraced Subassemblage. The cyclic response of the unbraced subassemblage is charted in Fig. 4.7. The failure sequence is described below:

1 : Column cracks in the positive direction

2 : Column cracks in the negative direction

3 : Spandrel beams crack in positive direction

4 : Spandrel beams crack in the negative direction

5 : Column fails in shear in positive direction

6 : Column fails in shear in negative direction

7 : Column loses all lateral capacity in positive direction

8 : Column loses all lateral capacity in negative direction

9, 11 : Same as 7

10, 12 : Same as 8

The hysteretic behavior of the unbraced subassemblage is quite poor. Once the column's ultimate capacity is reached at points 5 and 6 respectively, the loss in stiffness and strength is very rapid. Pinching of the hysteresis loops become more severe until the area enclosed within the loops becomes zero at point 7 in the fourth loading cycle.

Cyclic Response of the Altered Subassemblage. The cyclic response of the subassemblage with beam alteration scheme 2 is shown in Fig. 4.8. The failure mechanism is as follows:

1 : Column cracks in the positive direction

2 : Column and spandrel beams crack in the negative direction

3 : Plastic hinge develops in the spandrel in the positive direction

4 : Plastic hinge develops in the spandrel in the negative direction

5,7,9,11: Same as 3

6,8,10 : Same as 4

The improvement in hysteretic behavior of the subassemblage due to the beam weakening is quite apparent from Fig. 4.8. The shape of the hysteresis loops are fat and open indicating an improved energy dissipating capacity in the subassemblage. Pinching of the loops

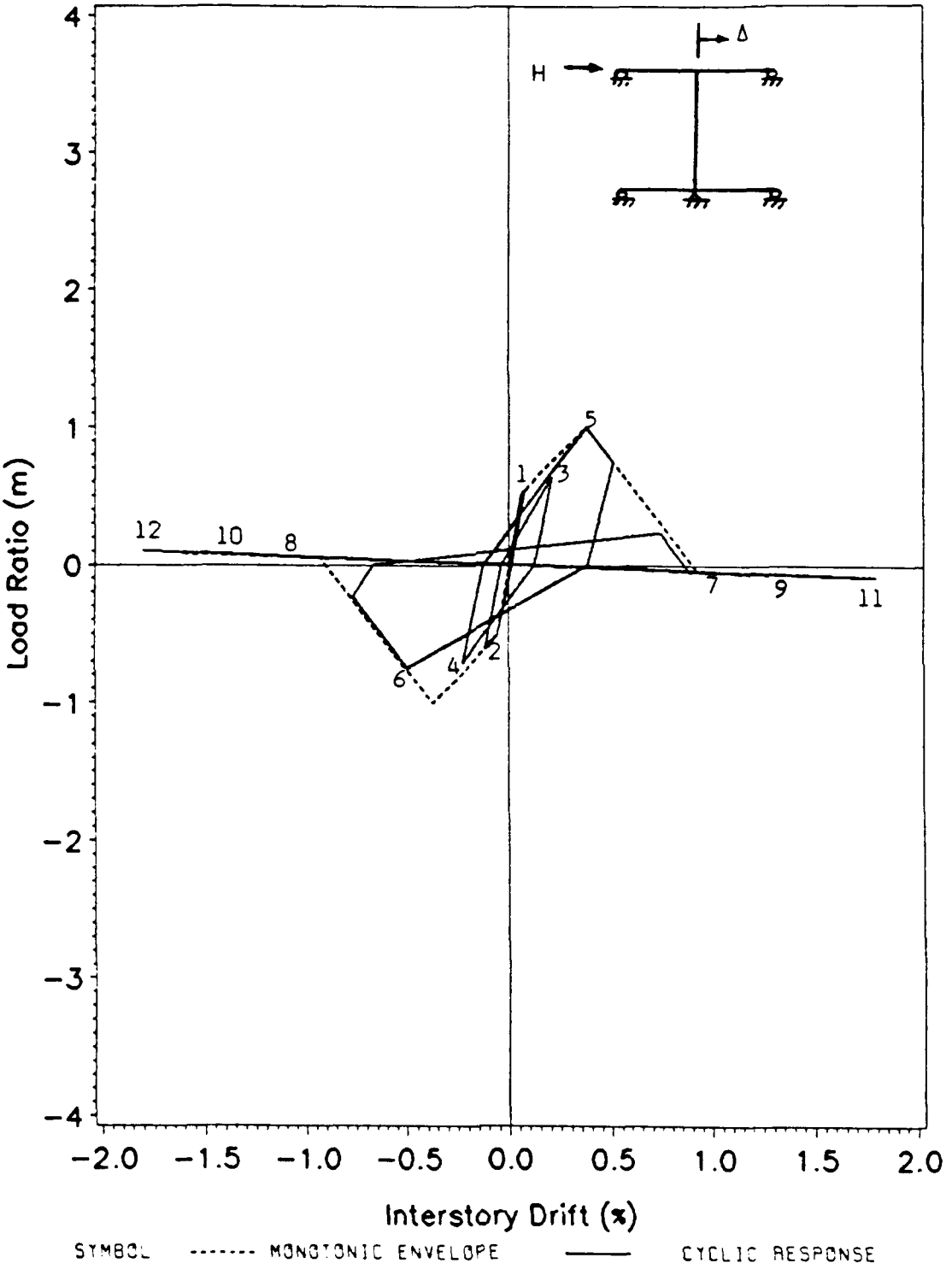

Fig. 4.7 Response of the unbraced subassemblage to cyclic loading

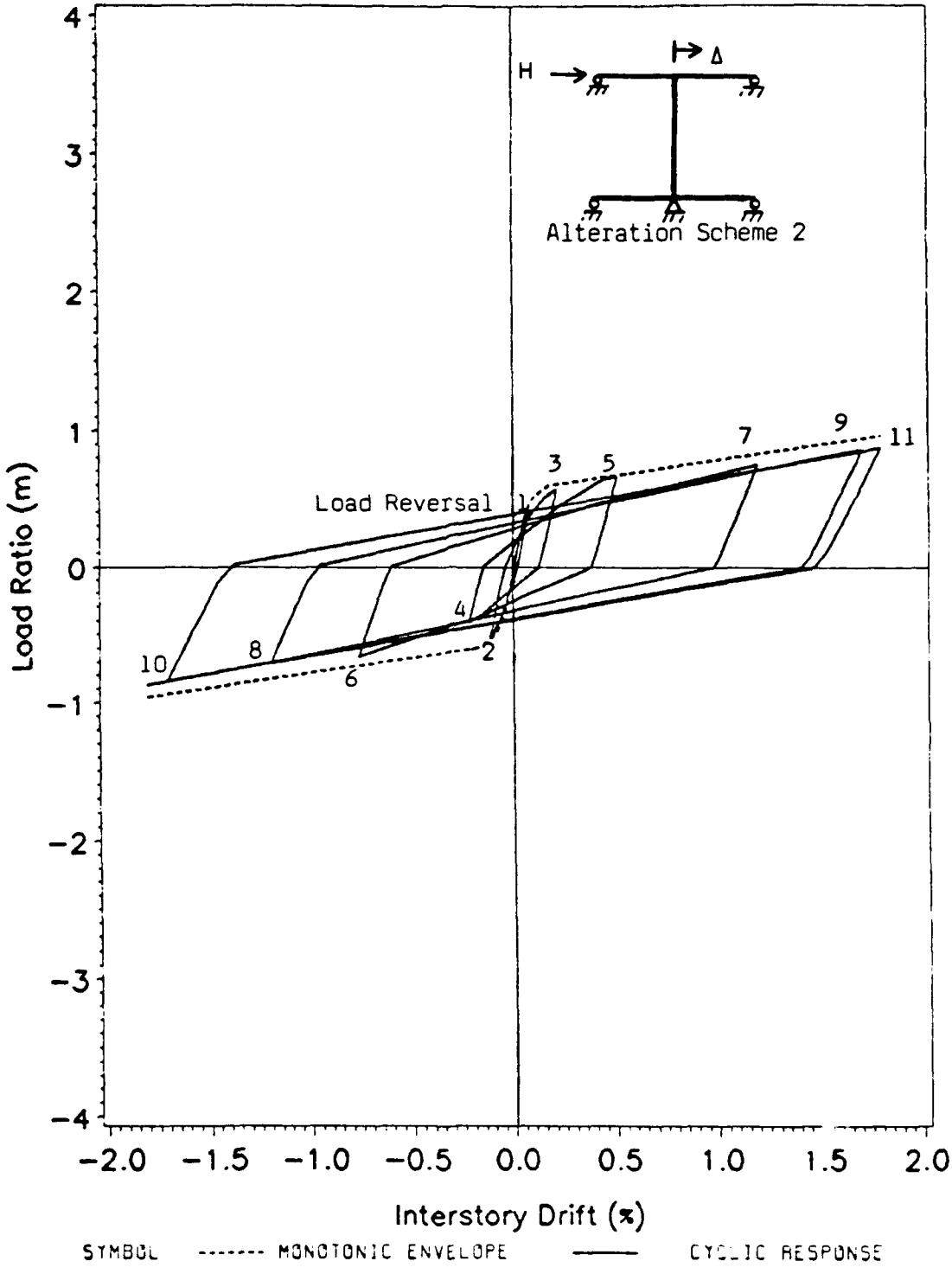

Fig. 4.8 Cyclic response of the subassemblage with beam alteration scheme 2

experienced in the later loading cycles of Fig. 4.7 is all but eliminated in the analytical model; however, some slight pinching can be expected in the actual structure due to the opening and closing of flexural cracks.

4.5 RESPONSE OF THE BRACED SUBASSEMBLAGE WITH BEAM ALTERATION

The influence of beam alteration in concert with prestressed cable braces on the response of the subassemblage is discussed in this section. Both the ultimate and serviceability design approaches for the prestressed cable bracing schemes will be investigated with n=2. Using equations 2.2 and 2.3, the cable brace areas used are 0.88 in^2 and 0.98 in^2 for the ultimate and serviceability design approaches respectively. The prestressed cable bracing is combined with beam alteration scheme 2 from Sec. 4.3. The subassemblage is subjected to both monotonic and cyclic incremental static displacements as presented in Sec. 3.6.

4.5.1 Monotonic Behavior

The monotonic response of the subassemblage with prestress cable bracing and beam alteration scheme 2 to monotonic loading are shown in Figs. 4.9 and 4.10 for the ultimate and serviceability design approaches respectively. The cable brace area used to obtain the braced-unaltered and braced-altered response curves of Fig. 4.9 was 0.88 in^2. The cable brace area used to obtain the braced-unaltered and braced-altered response curves of Fig. 4.10 was 0.98 in^2. The failure mechanisms of the unbraced-unaltered subassemblage and the braced-unaltered subassemblage are dominated by shear failure of the column at points 0"

and 0' respectively. Failure of the column does not occur in the braced-altered subassemblage. Failure has been shifted from the column and into the beams. The failure mechanism for the braced-altered subassemblage in Fig. 4.9 is presented below:

1-2 : Subassemblage behaves elastically

2 : Column cracks, m = 0.63, interstory drift = 0.06%

3 : Spandrel beams crack, m = 0.71, interstory drift = 0.1%

4 : Plastic hinge develops in the spandrel beam, m = 0.98, interstory drift = 0.175%

5 : Cable brace B1 yields and brace B2 goes slack, m = 2.56, interstory drift = 0.88%

A much higher ultimate strength is attained for the subassemblage if both prestressed cable braces and beam weakening are utilized. In Fig. 4.9, a 28% higher lateral strength is attained at an interstory drift of 0.9% over that provided by the cable bracing only. At this same drift the unbraced-unaltered subassemblage exhibits no lateral force resisting capacity at all. At lower drift levels, however, the results are somewhat mixed. The strength of the braced-altered subassemblage at 0.39% interstory drift is about 38% higher than the unbraced-unaltered subassemblage, but 24% less than the capacity of the braced-unaltered subassemblage at the same drift. Similar conclusions can be drawn using the serviceability design approach of Fig. 4.10.

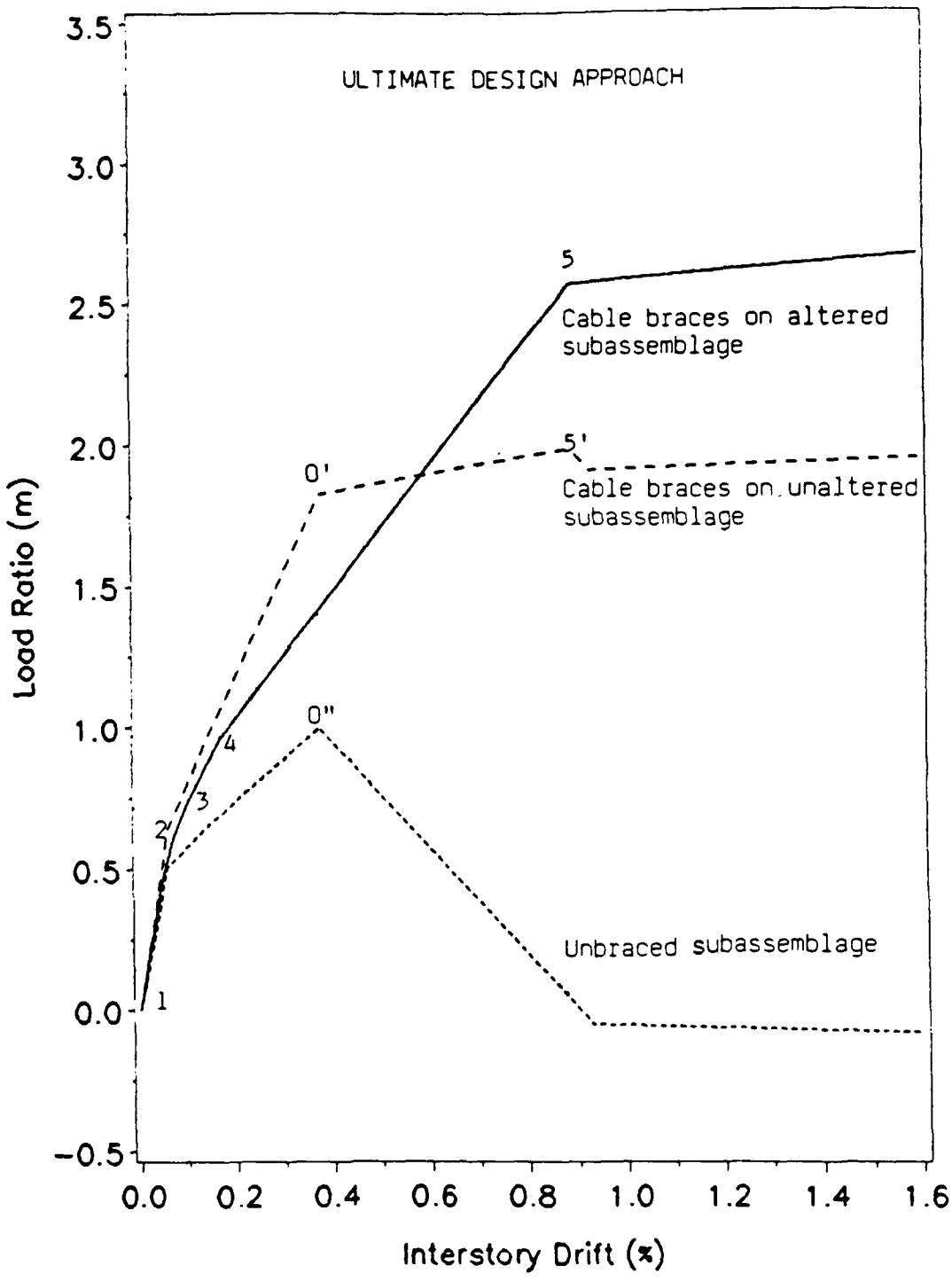

Fig. 4.9 Response of the subassemblage with prestressed cable bracing and beam alteration scheme 2, ultimate design approach with cable area = 0.88 in^2 and 0.5Py prestress force, n=2

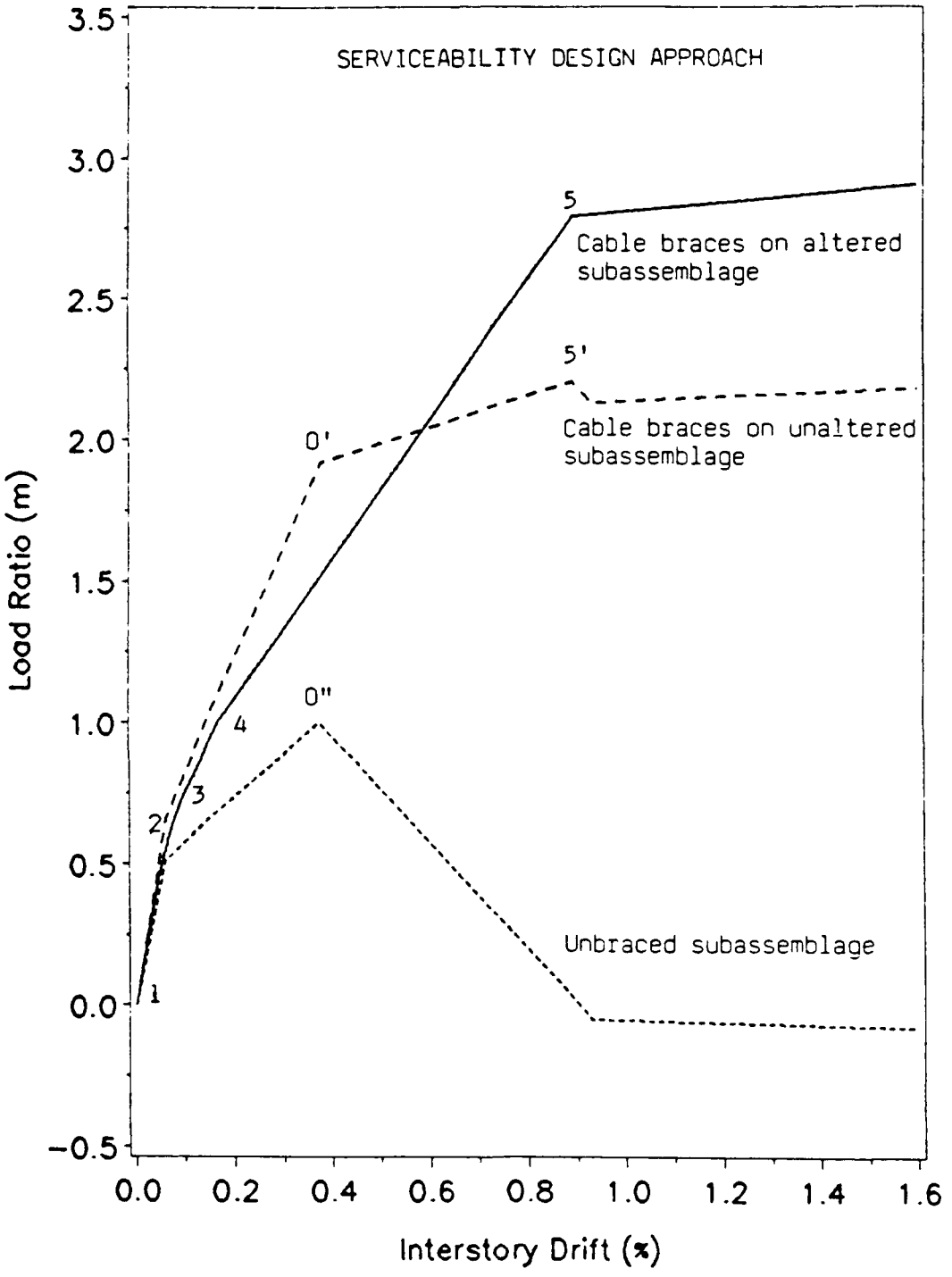

Fig. 4.10 Response of the subassemblage with prestressed cable bracing and beam alteration scheme 2. Serviceability design approach with brace area = 0.98 in² and 0.5Py prestress force, n=2

4.5.2 Cyclic Behavior

The cyclic response of the subassemblage retrofitted with prestressed cable braces only is shown in Fig. 4.11. The ultimate design approach for the cable braces is used with n=2 and $0.5P_y$ prestress force in the cables. The area of the cable braces is 0.88 in^2. The numbered points on the figure indicate the load reversal points defined in Fig. 3.12. The primed numbers on the figure indicate significant points on a particular loading cycle prior to the load reversal for that cycle. The failure sequence is as follows:

1 : Column cracks in shear in the positive direction

2 : Column cracks in shear in the negative direction

3 : Spandrels crack in flexure in positive direction

4 : Spandrels crack in flexure in negative direction

5 : Column fails in positive direction, effectiveness of the cable braces still intact

6 : Column fails in negative direction, effectiveness of the cable braces still intact

7 : Brace B1 yields and B2 goes slack, strength is now entirely dependent on the bracing system

8 : Brace B1 goes slack and B2 yields

9, 11 : Same as 7

10, 12 : Same as 8

The effect of beam alteration scheme 2 on the braced subassemblage using the ultimate and serviceability design approaches are shown in

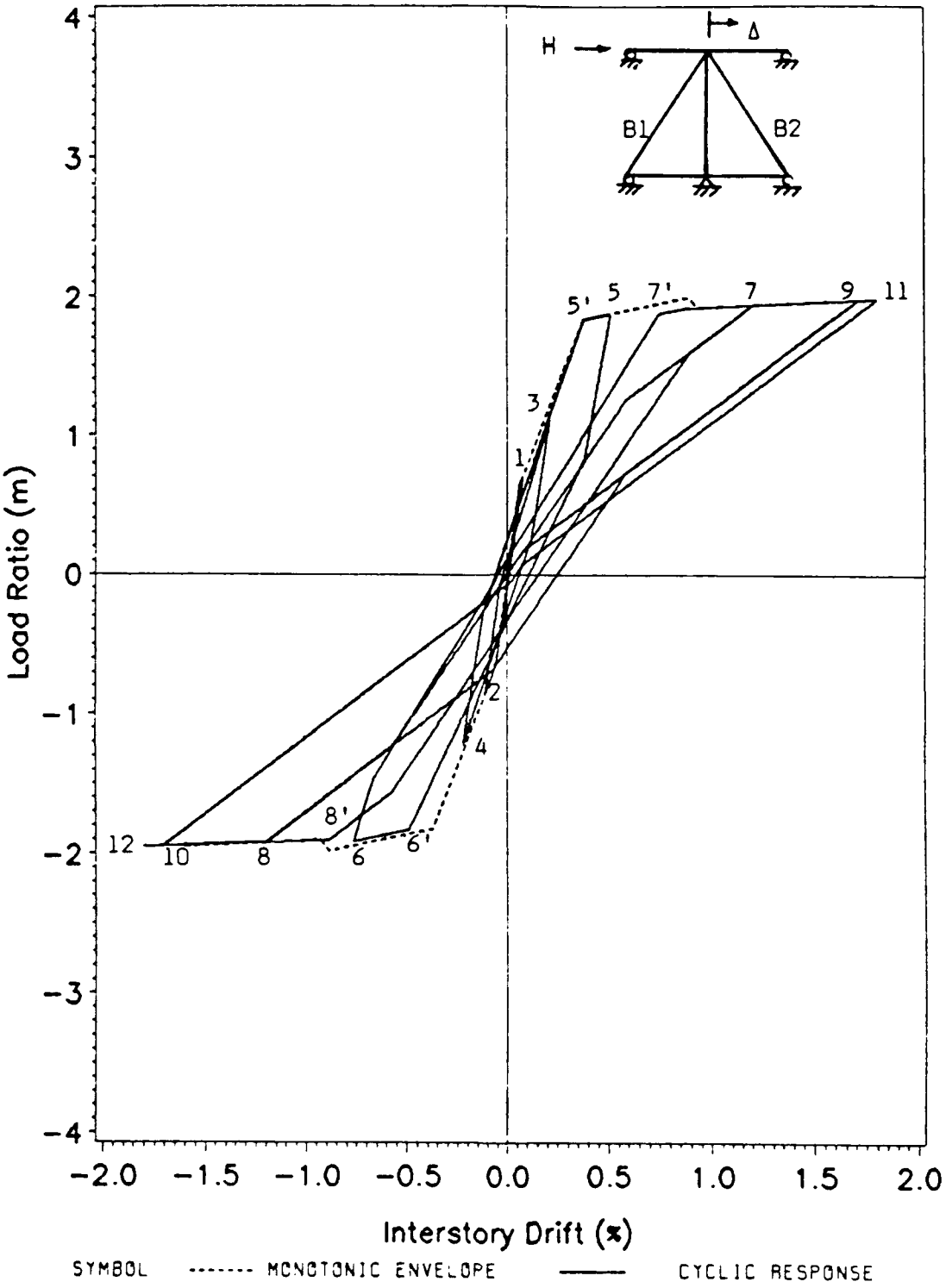

Fig. 4.11 Cyclic response of the subassemblage with prestressed cable braces only. Ultimate design approach with n=2, brace area = 0.88 in², and 0.5Py prestress force.

Figs. 4.12 and 4.13 respectively. The failure sequence for Fig. 4.12 is given below:

1 : Column cracks in the positive direction

2 : Column and spandrels crack in the negative direction

3 : Plastic hinge develops in the spandrels in the positive direction

4 : Plastic hinge develops in the spandrels in the negative direction

5, 7 : Same as 3

6, 8 : Same as 4

9, 11 : Same as 3

10, 12 : Same as 4

Improvement in the hysteretic performance of the braced-altered subassemblage is evident in Figs. 4.12 and 4.13 over the braced-unaltered subassemblage of Fig. 4.11. Responses of all the systems are dominated by the behavior of the prestressed cable braces in the later loading cycles. The hysteresis loops of the braced-altered subassemblages exhibit less pinching because of the development of the plastic hinges in the spandrel beams.

4.5.3 Variation Of Prestressed Cable Brace Area To Attain Desired Strength

As pointed out in Sec. 4.5.1, combining beam alteration with prestressed cable braces significantly increases the ultimate strength of the retrofitted subassemblage. Referring to Figs. 4.9 and 4.10, the

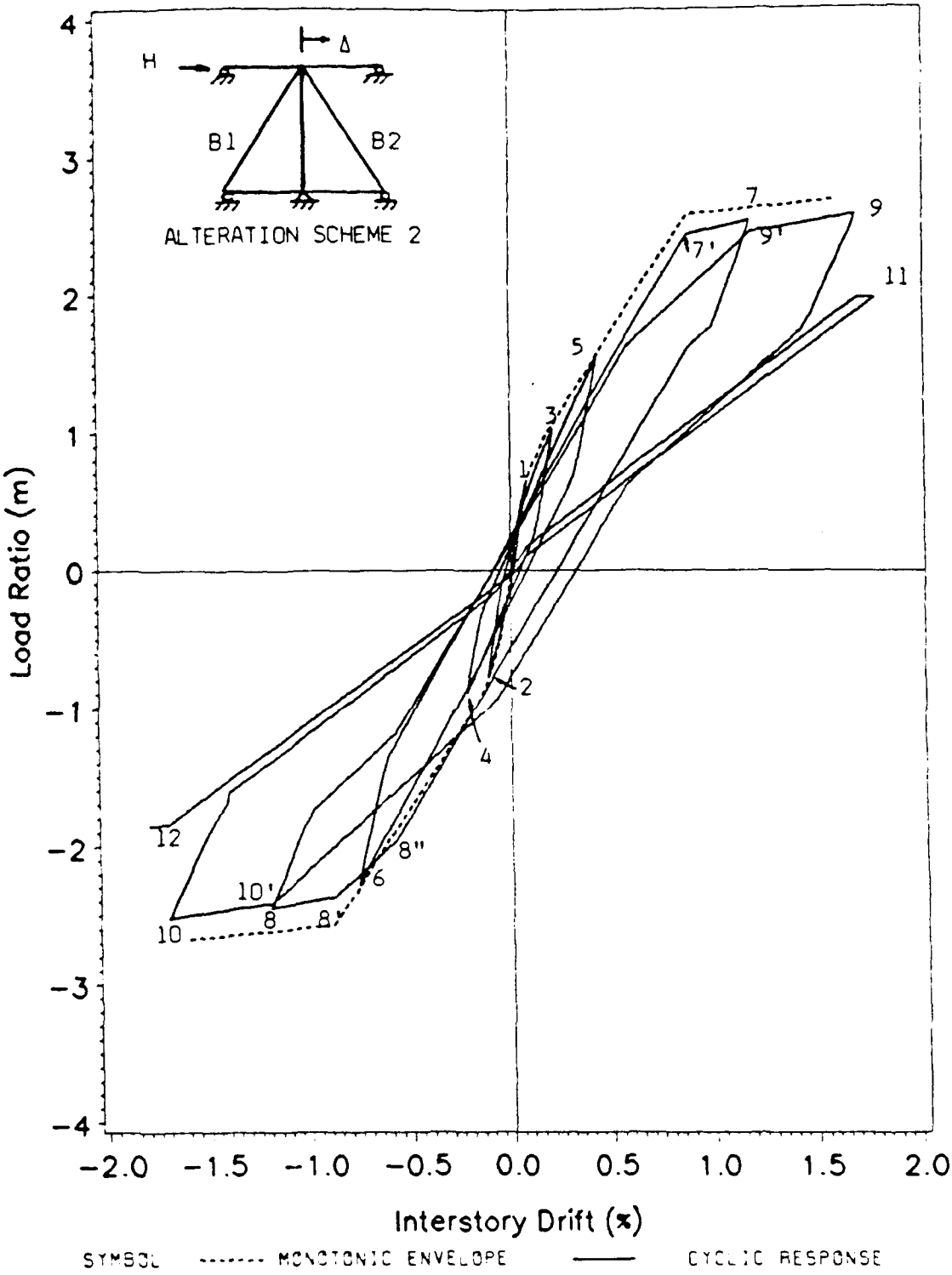

Fig. 4.12 Cyclic response of the subassemblage with prestressed cable braces and beam alteration scheme 2. Ultimate design approach with brace area = 0.88 in², and 0.5Py prestress force.

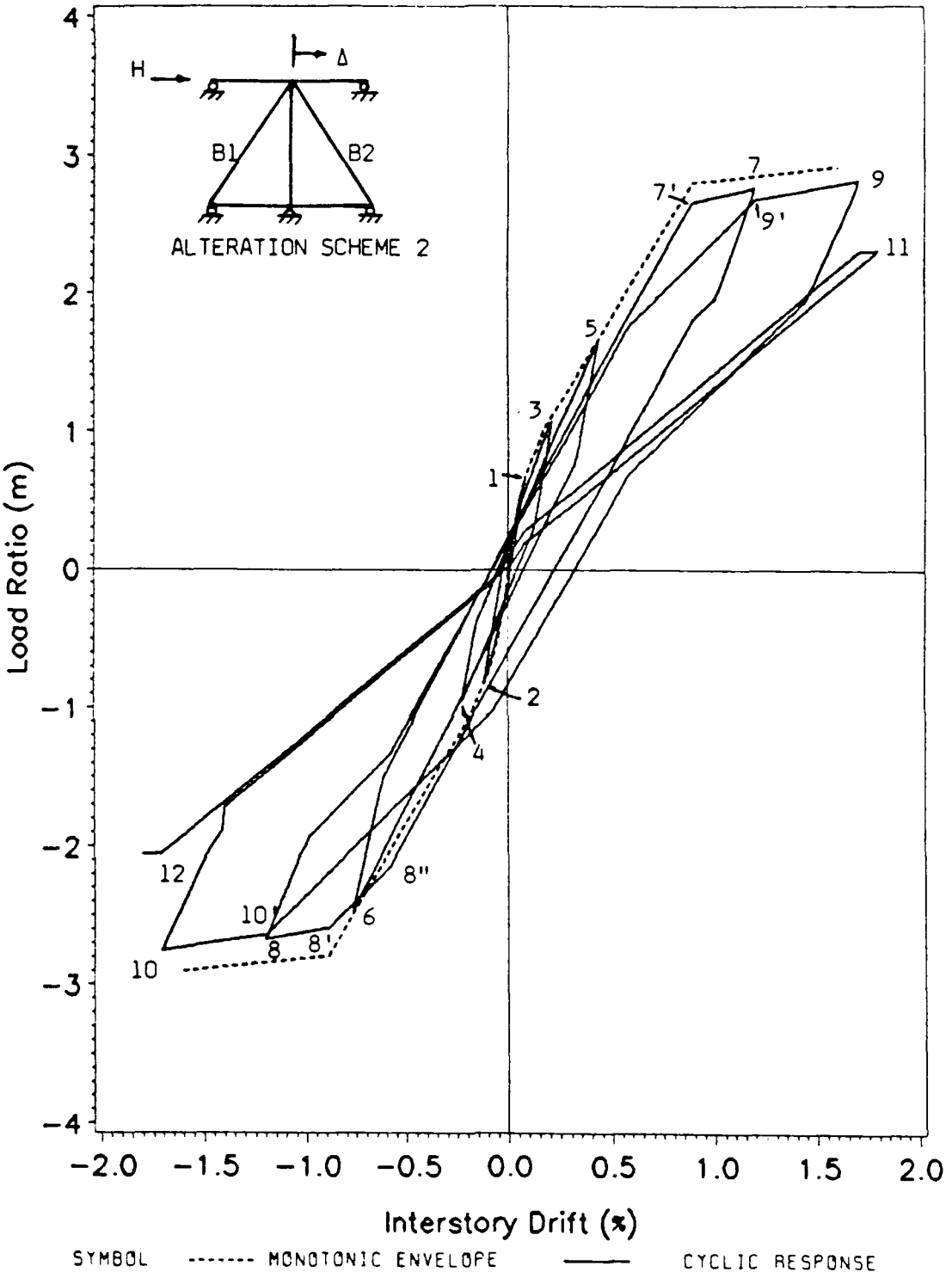

Fig. 4.13 Cyclic response of the subassemblage with prestressed cable braces and beam alteration scheme 2. Serviceability design approach with brace area = 0.98 in² and 0.5Py prestress force.

ultimate strength, however, is not reached until the structure reaches an interstory drift in excess of .9%. Possibly more significant to the designer might be the fact that the braced-unaltered subassemblage provides higher strength at low drifts than does the braced-altered subassemblage with the same cable brace area. Weakening the spandrel beams does, however, favorably alter the frame's failure mechanism. This important benefit of beam alteration cannot be overlooked. But is an improved failure mechanism worth sacrificing stiffness and strength at low drift levels ?

As discussed in Sec. 2.4.2, using the serviceability design approach, the designer strives to limit drift in the structure by designing the retrofitted frame to attain a desired strength at a specified drift level. In Fig. 4.10, the cable brace area was calculated using equation 2.3. The aim is to achieve a retrofitted strength of twice that of the original unstrengthened frame at a drift of 0.39%. This point is labeled 0' in Fig. 4.10. The cable brace area used is 0.98 in^2. At this drift, the braced-altered subassemblage attains a strength of only 1.5 times that of the original frame.

It is still possible to achieve twice the strength of the original structure in the braced-altered frame at 0.39% drift by simply increasing the area of the cable braces. Assuming beam alteration scheme 2, Eqn 2.3 can be modified to predict the brace area required,

$$A_c = [(n-0.6)(V_u)(L)]/[(C)(E)(delta_{fu})(Cos^2\theta)] \qquad (4.3)$$

Similar expressions can be derived for beam alteration schemes 1, 3, and 4. The variables V_u and $delta_{fu}$ refer to the lateral strength and drift, respectively, of the original frame at ultimate. Expressions can be developed similarly to predict brace area required at any specified drift level.

Using Eqn 4.3 and n=2, the cable brace area required is 1.4 in^2. The response of the braced-altered subassemblage with brace cross sectional areas of 1.4 in^2 is plotted in Fig. 4.14. For comparison, the response of the braced-unaltered subassemblage of Fig. 4.10 is repeated in Fig. 4.14. At a drift of 0.39%, both the braced-altered and braced-unaltered curves reach the desired strength of twice that of the original unaltered subassemblage. To achieve the desired stiffness and strength at 0.39% drift, the area of the cable braces was increased by nearly 43%. The additional brace area in effect increases the stiffness of the braced-altered frame by nearly 25%. The ultimate strength of the braced-altered subassemblage increases to nearly four times the strength of the original structure at drifts in excess of 0.9%. The overall objective of the retrofitting project as well as specific design criteria given by the user and governing building codes will weigh heavily on the designer when deciding whether increased cable brace area is a just trade off for increased frame stiffness.

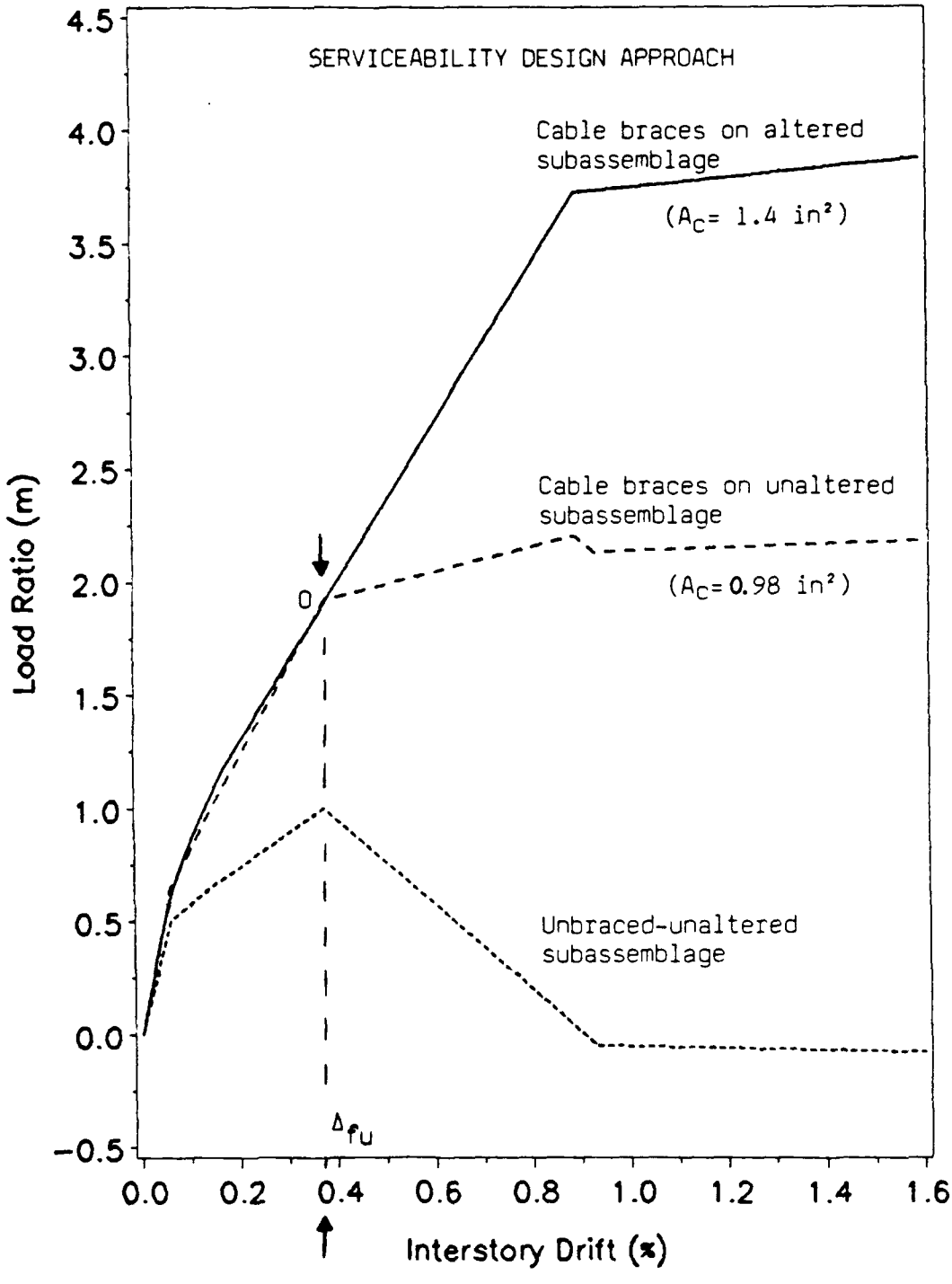

Fig. 4.14 Matching response of the altered subassemblage with response of the braced only subassemblage at a specified drift. Serviceability design approach, 0.5Py prestress force, n=2, cable area = 1.4 in²

CHAPTER 5

PRESTRESSED CABLE BRACES APPLIED TO A SIX STORY SUBASSEMBLAGE OF THE PROTOTYPE FRAME

In this chapter the focus of the study is expanded to examine the global behavior of a six story version of the prototype frame to retrofit strengthening. The investigation is limited to the response of the frame along a typical column line. The design of the prototype frame introduced in Sec. 2.3 was first completed. The frame design was conducted in such a way as to represent common design practice in effect when such structures were originally designed. Applicable design codes as well as typical hand calculation techniques of the time were utilized.

Once the prototype frame was designed, unique single story subassemblages were developed for each level of the frame. A typical six story subassemblage was also introduced to model the global behavior of the frame along a typical interior column line of the perimeter frame.

The single story subassemblages were useful in studying the response of the six story prototype frame on a story by story basis. The purpose of studying the six story subassemblage is as follows. The hypothesis was developed in references 2 and 3 that for geometrically uniform frames, the global behavior of the retrofitted frame can be predicted by analysis of a generic single story subassemblage. To evaluate this hypothesis the response curves obtained from the six story subassemblage under several bracing schemes were compared to those

obtained from analysis of a generic single-story subassemblage. The advantages and limitations of the hypothesis are discussed. Finally a discussion is presented on how one might develop a practical design strength ratio scheme for the prototype frame based on the requirements of current building codes.

5.1 MODELING THE SIX STORY SUBASSEMBLAGE

5.1.1 Design Of The Prototype Frame

The prototype frame was introduced in Sec. 3.2 as being seven stories high and eleven bays long. For the purpose of conducting the experimental tests discussed in Sec. 2.3 [7], only the third, fourth, and fifth levels of the frame were fully designed (see Fig. 2.8). In order to examine the behavior of a multi-story version of the prototype frame to retrofit strengthening, the frame design for the remaining floors had to be completed.

Gravity and seismic loads for the design were obtained from the 1955 edition of the Uniform Building Code [12]. The portal method was used for frame analysis, and design was carried out using working stress design in accordance with the 1951 edition of the ACI Building Code [10]. Gravity and seismic loads were the same as those utilized by the designers of the original prototype frame shown in Figs. 2.7 and 3.2.

Design values of total story shear force for a six story prototype frame were calculated using the 1955 Uniform Building Code and are summarized in Table 5.1. Also shown in the table are the nominal

(unfactored) story shear forces obtained using the 1988 edition of the Uniform Building Code [15].

TABLE 5.1

Comparison Of 1955 and 1988 Total Story Shear Forces For A Six Story Prototype Frame

(values shown in kips)

Story	V(1955)	V(1988)	% Increase
1	956	2188	129
2	837	2076	148
3	703	1852	163
4	552	1517	175
5	397	1069	169
6	191	509	166
		Average	158

In the initial design calculations performed for the experimental study [7], the prototype frame was assumed to be seven stories tall. Grade Fy = 60 ksi steel was assumed for the spandrel reinforcement and Fy = 50 ksi steel was assumed for the column longitudinal reinforcement. The grades of steel ultimately used in the experimental and analytical analysis of the prototype frame were Fy = 60 ksi for the column

longitudinal reinforcement and Fy = 40 ksi for all other reinforcement. Using these revised steel grades and assuming a seven story frame, initial calculations revealed that the spandrel reinforcement shown in Fig. 3.2 for levels two and four were inadequate. Revision of building height downward from seven stories to six stories reduces the spandrel moments at levels 2 and 4 sufficiently that resizing of reinforcement at those levels is not necessary. This action was taken so as to not change the structural characteristics of the original prototype frame at levels three, four, and five which correspond to the region of the frame tested experimentally [7].

Frame design was completed assuming the prototype frame to be a six story structure. A plan and profile of the revised six story prototype frame is shown in Fig. 5.1. Spandrel reinforcement for the complete frame is summarized in Fig. 5.2. The sections shown depict longitudinal reinforcement typical at the spandrel ends. For simplicity, spandrel reinforcement in the exterior bays was assumed the same as that provided for the interior bays. The reduction of frame height from seven to six stories necessitated a revision downward in column axial loads due to gravity forces at each story. As a result, column lateral strength for any given story was also reduced (see lateral shear strength equation for short columns in Fig. 3.7). Nevertheless, longitudinal reinforcement for the third and fourth floor columns (those modeled for the experimental study) remained unchanged (see Fig. 2.7). A summary of column reinforcement details is shown in Fig. 5.3. Minimum tie spacing provisions governed for all six stories, therefore a constant tie spacing of 18 inches was used over the full height of the building.

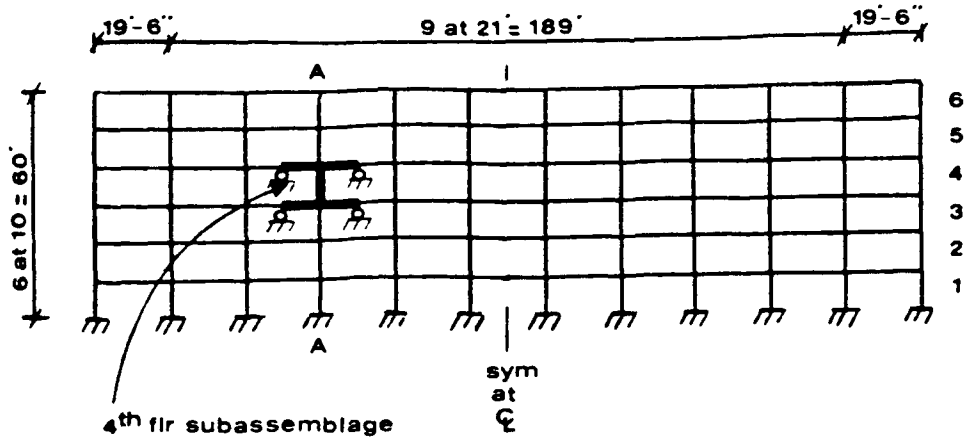

ELEVATION

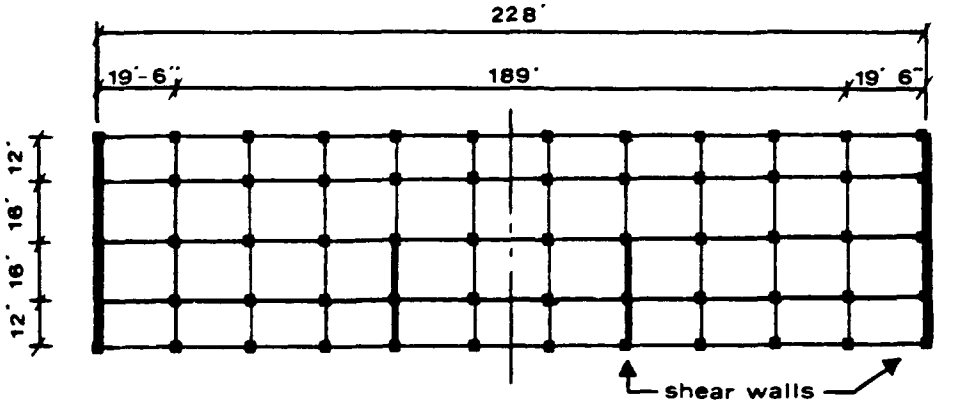

PLAN

Fig. 5.1 Plan and profile of the six story prototype frame

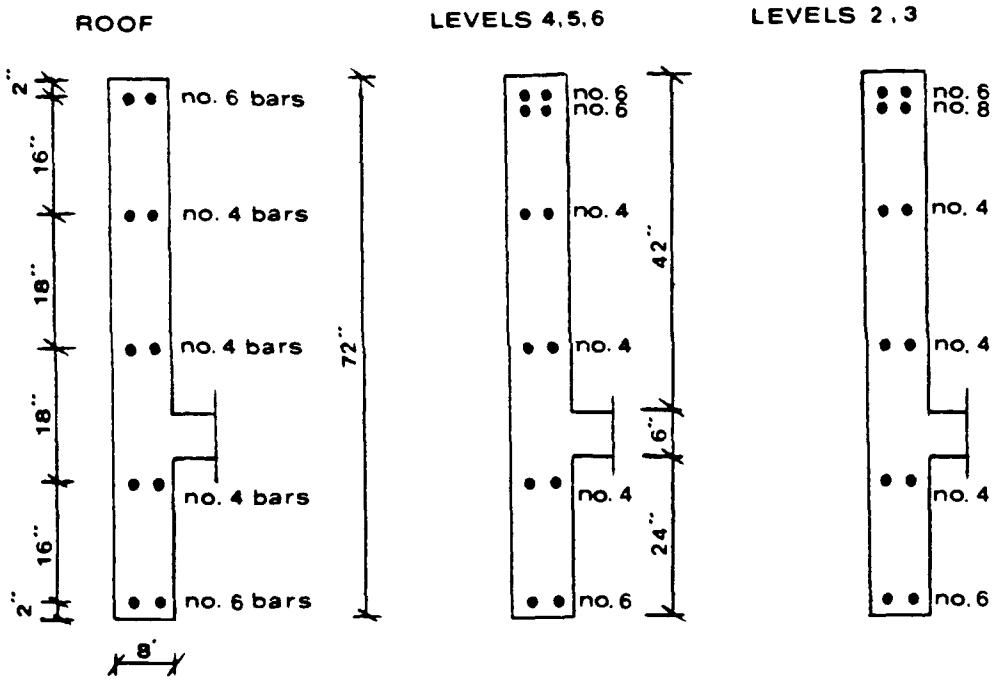

Fig. 5.2 Spandrel reinforcement for the six story prototype frame

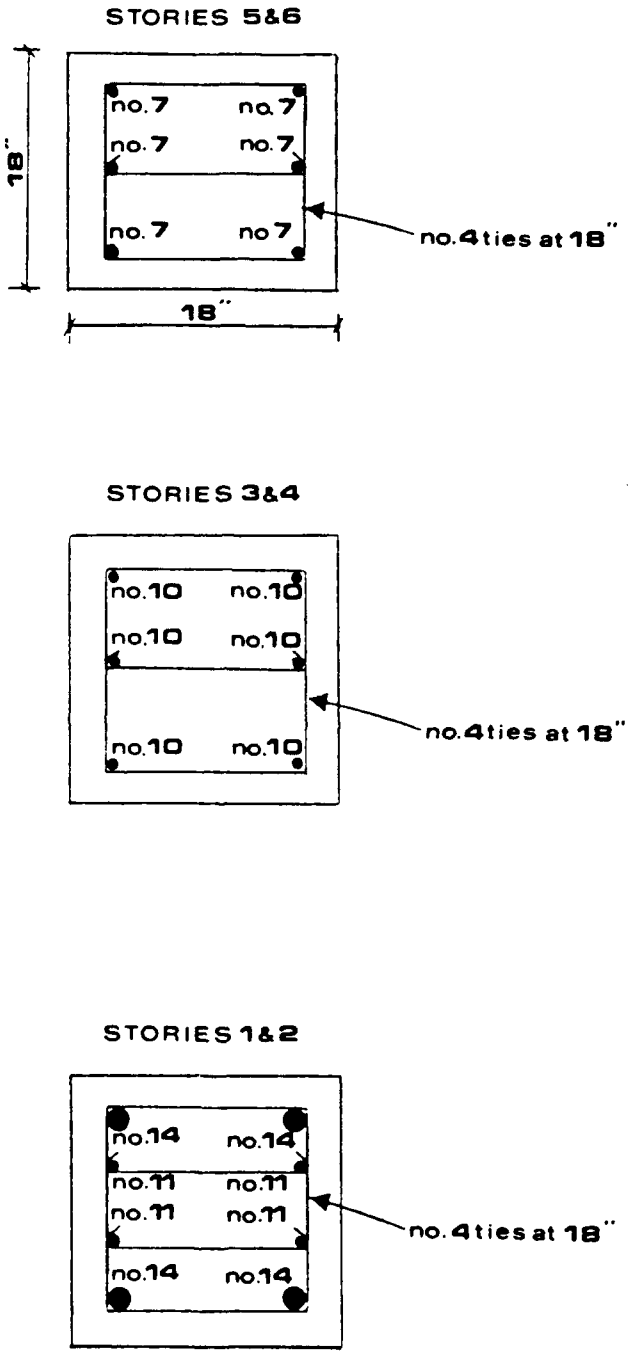

Fig. 5.3 Column reinforcement for the six story prototype frame

Longitudinal column reinforcement was assumed to be the same for all frame columns in a given story.

5.1.2 Selection Of Typical Six Story Subassemblage Of The Prototype Frame

The six story subassemblage chosen for this study is located along column line A-A in Fig. 5.1. The subassemblage represents a typical interior column line in the prototype frame. The analytical model of the six story subassemblage is shown in Fig. 5.4. The assumptions made in modeling the prototype frame were discussed previously in Sec. 3.2 and are applicable to the six-story subassemblage. As discussed in Sec. 3.2 axial inextensibility of the columns and beams has been assumed. As a result, one horizontal degree of freedom is established per story. Roller supports are assumed for the boundary conditions at midspan of the spandrel beams as shown in the figure. Displacements are applied at the beam column joint at each story.

Single-story subassemblages for each story have also been established along column line A-A. The location of a typical single-story subassemblage established for the fourth floor is shown in Fig. 5.1. The fourth floor subassemblage has been designated as the generic single story subassemblage used in the discussion of Sec. 5.3. The choice of generic subassemblage was made for several reasons. First, the fourth floor subassemblage most closely resembles the subassemblage studied in previous studies [2, 3] as well as chapters 3 and 4. Reinforcement, strength, stiffness, axial force, location in the frame,

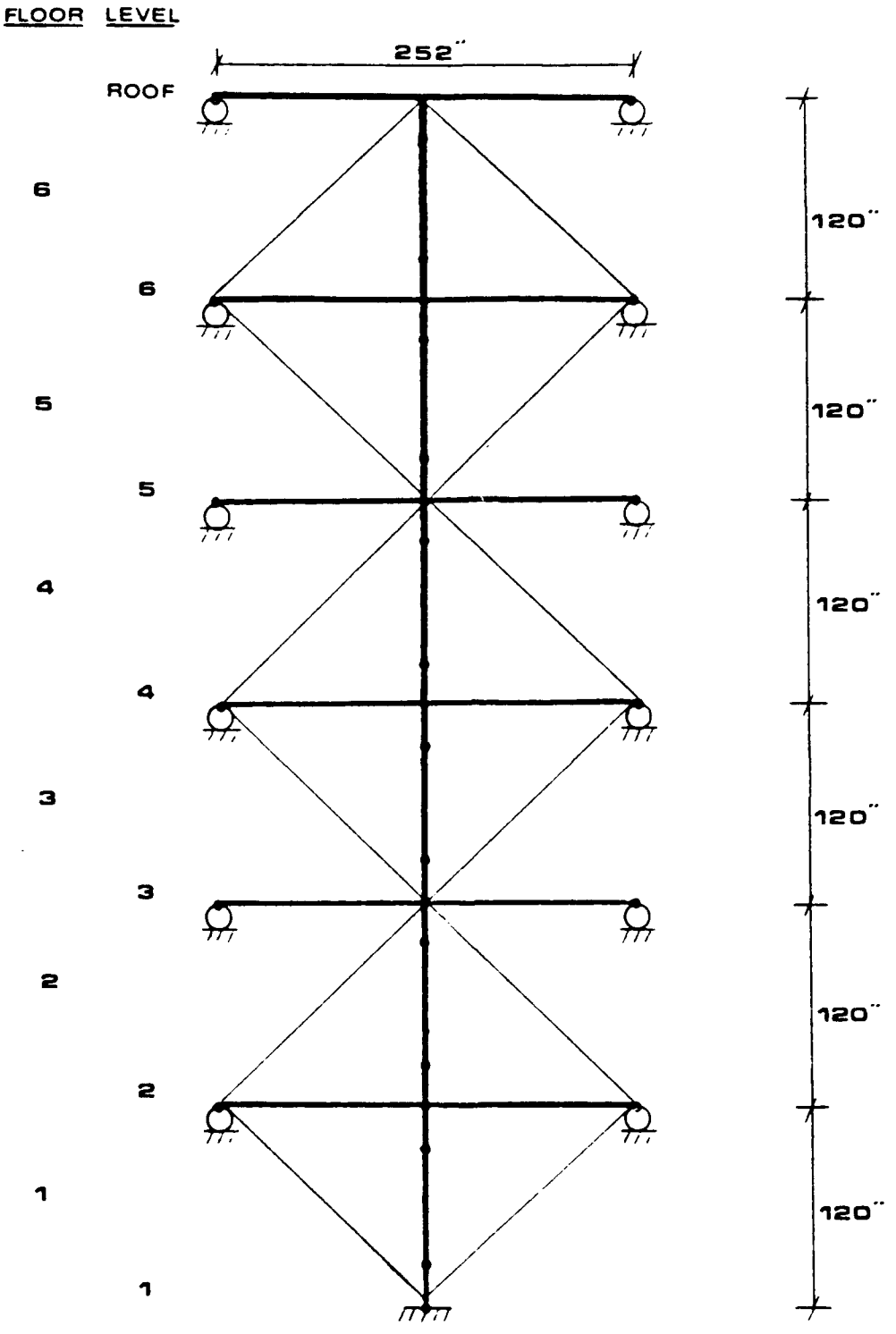

Fig. 5.4 Analytical model for the six story subassemblage of the prototype frame

and response history most closely match the original subassemblage of the seven story frame. Secondly, the subassemblage is located near the center of the frame away from the frame boundaries.

5.1.3 Prestressed Cable Brace And Beam Alteration Schemes Used In The Study

It was shown in chapter 4 that there are advantages to using beam alteration in conjunction with prestressed cable bracing systems. As a result, the designer of a retrofit strengthening scheme may wish to utilize both prestressed cable braces and beam alteration. In Sections 5.2 and 5.3 several prestressed cable bracing schemes are examined as well as a beam alteration scheme to support the study. These retrofit strengthening schemes are presented next.

In Sec. 4.5.3 it was demonstrated how an engineer can utilize the serviceability design approach and Eqn. 2.3 to design a retrofitted structure which will achieve a desired strength at a specified drift. Once the response of the unstrengthened frame is determined, the designer can derive equations similar to Eqn. 4.3 for selected beam weakening schemes. This approach was followed in determining required cable brace areas.

A design strength ratio of n=2 was arbitrarily chosen for each story. Further, n=2 strength was to be attained at a drift corresponding to shear failure of the columns in each story of the unstrengthened frame. For example, the ultimate lateral strength of story 6 was determined to be 52.4 kips at a relative interstory drift of 0.34% (0.407 in.) from single story subassemblage analysis. The

response of the unstrengthened subassemblage is normalized with respect to 52.4 kips and plotted as the solid line in Fig. 5.5. With n=2, the desired retrofitted strength is 2(52.4) = 104.8 kips. From Eqn. 2.3 the required cable area was found as:

$$A_c = [(2-1)(52.4k)(174in)]/[(1)(26,000ksi)(.407in)Cos^2(43.6)] = 0.82\ in^2$$

If beam alteration is also part of the retrofitting scheme, a larger cable brace area is required to achieve n=2 strength at 0.34% drift (see discussion in Sec. 4.5.3). The response of the story six subassemblage to beam alteration (u = 16 in., v = 16 in.) is normalized to 52.4 kips and plotted as the dashed curve in Fig. 5.5. Observe that at a drift of 0.34%, the strength of the altered subassemblage is 50% that of the unaltered subassemblage. The cable brace area required to reach n=2 strength in a braced-altered subassemblage is calculated as:

$$A_c=[(2-0.5)(52.4k)(174in)]/[(1)(26,000ksi)(0.407in)Cos^2(43.6)]= 1.23in^2$$

Cable brace areas were similarly calculated for each story of the six story prototype building. The cable brace area schemes utilized in this chapter are summarized in Table 5.2. Bracing schemes A, B, and C were developed for application without beam alteration. Scheme A1 was developed in conjunction with beam alteration.

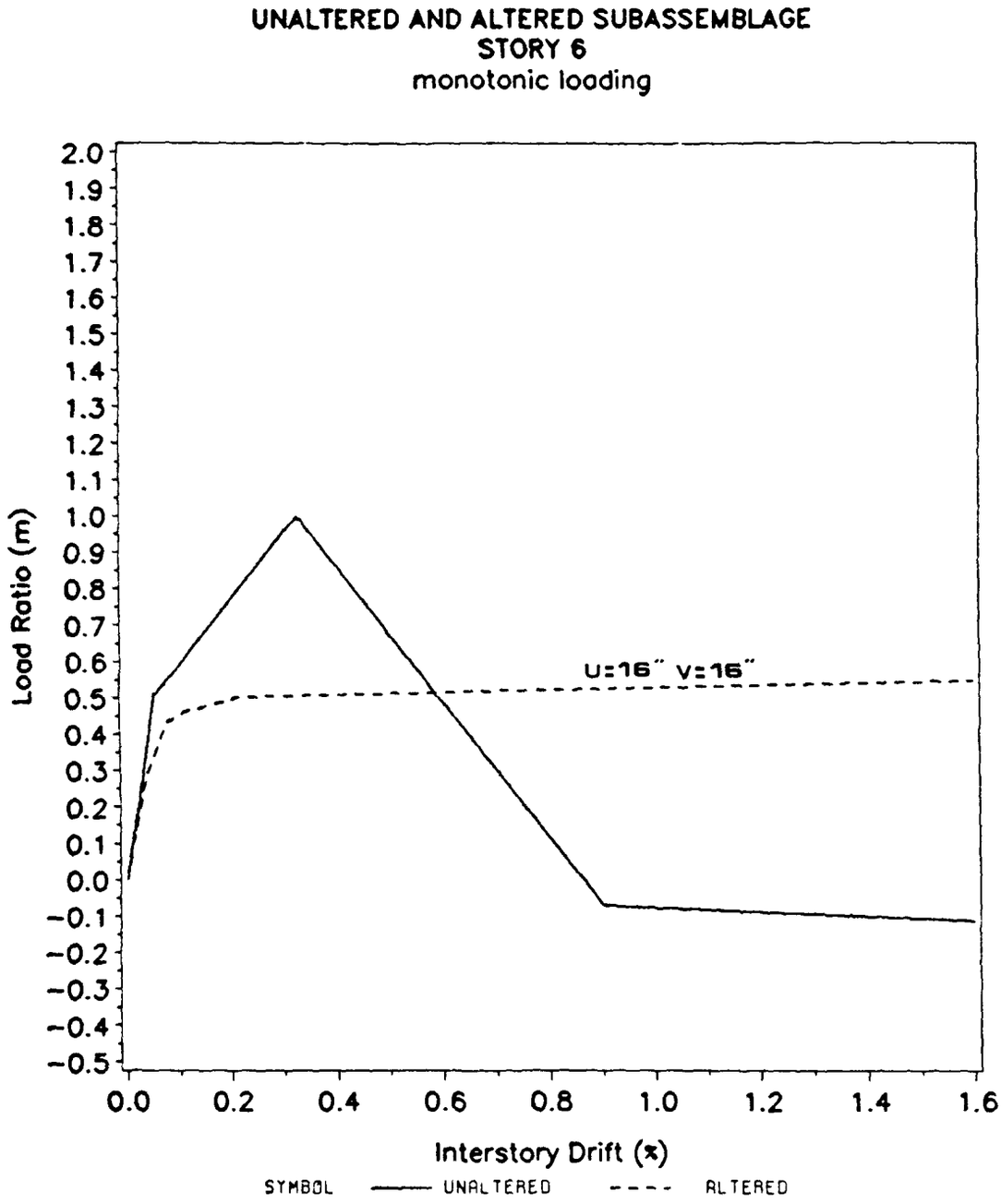

Fig. 5.5 Response of unaltered and altered single story subassemblages for story 6, monotonic loading, u=16 in., v=16 in.

TABLE 5.2

Prestressed Cable Brace Area Schemes

(areas in square inches)

Floor	Scheme A	Scheme A1	Scheme B	Scheme C
1	1.49	2.07	1.49	1.49
2	1.21	1.84	1.49	1.49
3	1.09	1.39	1.09	1.49
4	1.05	1.44	1.09	1.49
5	0.93	1.50	0.93	1.49
6	0.82	1.23	0.93	1.49

Notes:
Scheme A : Bracing area changes every story on unaltered frame
Scheme A1: Bracing area changes every story on altered frame
Scheme B : Bracing area changes every other story on unaltered frame
Scheme C : Bracing area held constant for all stories on unaltered frame

There are many factors which affect a designer's choice of cable brace area schemes for a structure. Among the most influential factors are: 1) the importance of achieving specified lateral strengths at each story level, 2) minimization of labor and material costs, and 3) frame geometry. Careful consideration of the relative importance of these factors may lead a designer to any number of prestressed cable brace area schemes.

Suppose the designer's overriding objective is to double the lateral capacity of each story at a drift level corresponding to the ultimate strength of that story in the unstrengthened frame. The designer would choose a design ratio of n=2 and calculate the cable

brace area required for each story as shown above. If this was the only concern, either prestressed cable brace area scheme A or A1 shown in Table 5.2 would be arrived at. In designing prestressed cable brace scheme A and A1, the designer assumes it is practical to specify different cable brace areas for each story. The number of connections and prestressing points as well as the manhours required to install and prestress each cable is assumed to be of secondary concern. The advantage of such a scheme is that the designer can closely control the design strength of each story as desired.

The designer might be primarily concerned with controlling installation costs, thus desiring to minimize the number of connections, prestressing points and cable sizes utilized. A bracing area scheme similar to scheme C shown in Table 5.2 might then be specified. In scheme C the assumption is that only one cable size is to be used for the entire structure. The cable brace areas shown represent the largest area required by any story in the structure to reach twice its unstrengthened capacity, or n=2.

Scheme B represents a compromise between schemes A, and C. In designing scheme B costs are limited by changing cable sizes every other story. The number of connections and prestressing points, as well as installation manhours, are greatly reduced over those required by schemes A and A1. Meanwhile greater control over frame response is achieved over that provided by scheme C.

In chapter 4, four beam alteration schemes were evaluated for the fourth story subassemblage of the original seven story prototype frame. It was shown that beam alteration scheme 2 provided optimum results.

Recall that in scheme 2 the first layer of negative and positive reinforcement was cut (refer to Fig. 3.2 and Table 4.1). The conclusion was drawn that scheme 2 provides optimum results for the fourth story subassemblage analyzed. Alteration scheme 2 might not necessarily be optimal if, for example, one evaluates the response of a two story subassemblage consisting of floors three and four. For such a case, scheme 1 might be appropriate for level 4 spandrels and scheme 2 appropriate for level 3.

For a six story structure, it becomes apparent that a great number of beam weakening schemes can be developed. In an effort to limit the scope of this study, only one beam alteration scheme for the six story subassemblage was considered. Using the identical approach utilized in chapter 4, the optimum beam alteration scheme for each level of the six story frame was determined by single-story subassemblage analysis. The optimum beam weakening scheme for each level is summarized in Table 5.3. The combination of all six beam weakening schemes shown will be used in the discussion of Sec. 5.2 in conjunction with prestressed cable brace scheme A1.

5.2 RESPONSE OF THE SIX STORY FRAME USING UNIQUE SINGLE STORY SUBASSEMBLAGE ANALYSES

5.2.1 Response Of The Unstrengthened Frame

As discussed in Sec. 5.1.2, unique single story subassemblages were developed for each story of the prototype frame. A monotonic static incremental displacement analysis was conducted on unstrengthened

TABLE 5.3

Beam Alteration For The Six Story Subassemblage

Level	U	V	W	r	Reinforcement Cut	
					negative	positive
2	6"	0"	36"	2.06	2-#6 2-#8	none
3	6"	0"	36"	1.93	2-#6 2-#8	none
4	3"	3"	36"	1.64	2-#6	2-#6
5	6"	6"	36"	2.84	4-#6	2-#6
6	6"	6"	36"	2.50	4-#6	2-#6
Roof	16"	16"	36"	1.65	2-#6	2-#6

versions of each subassemblage. The incremental displacements were applied in such a manner that for any load step the prescribed relative story displacements at each level were identical. The applied displacements varied linearly with the height of the frame. The maximum applied interstory drift was 1.6%.

The response curves for each story are plotted in Fig. 5.6. All six response curves are dominated by shear failure of the reinforced concrete short columns. The lateral capacity of each subassemblage is shown in kips force. This value represents the lateral capacity each subassemblage contributes to total story strength. The total story strength at any level is attained by multiplying the strength of the corresponding subassemblage by the number of bays (11) times 2, or 22.

An identical analysis was conducted on the six story subassemblage of Fig. 5.4. A plot of the relative story response curves for the six story subassemblage provides very close agreement to the curves obtained from the individual subassemblages and therefore is not repeated.

When interpreting the curves of Fig. 5.6, it is important to recognize how the shear dominated column behavior is reproduced by the analytical model. Recall that nonlinear rotational springs at the column ends are used to produce the overall nonlinear lateral load-displacement curve of the column element (refer to Sec. 3.3). The moments at the ends of the column element establish behavioral states of each spring. As long as the column end moments are equal, the rotational springs exhibit simultaneous behavior, and the desired overall column load-displacement curve is represented exactly as seen in the curves for stories 2, 4, and 5.

If, however, the column end moments are not equal, different nonlinear behavior is exhibited by the two rotational springs. Behavioral changes occur for each spring independently at various column drifts. This causes a deviation in behavior from the desired column load-displacement curve. One end of the column may "fail" earlier than the other. This behavior is seen in the curves for stories 1, 3 and 6. Such behavior is an anomaly unique to the analytical model since the actual column displays a global shear failure at a unique drift.

The general shape of the response curves for stories 2, 4, and 5, as well as their failure mechanisms, are identical to the subassemblage discussed in detail in Sec. 3.7.1. The stiffness and strength of the spandrel beams framing into the bottom of the column is the same as for

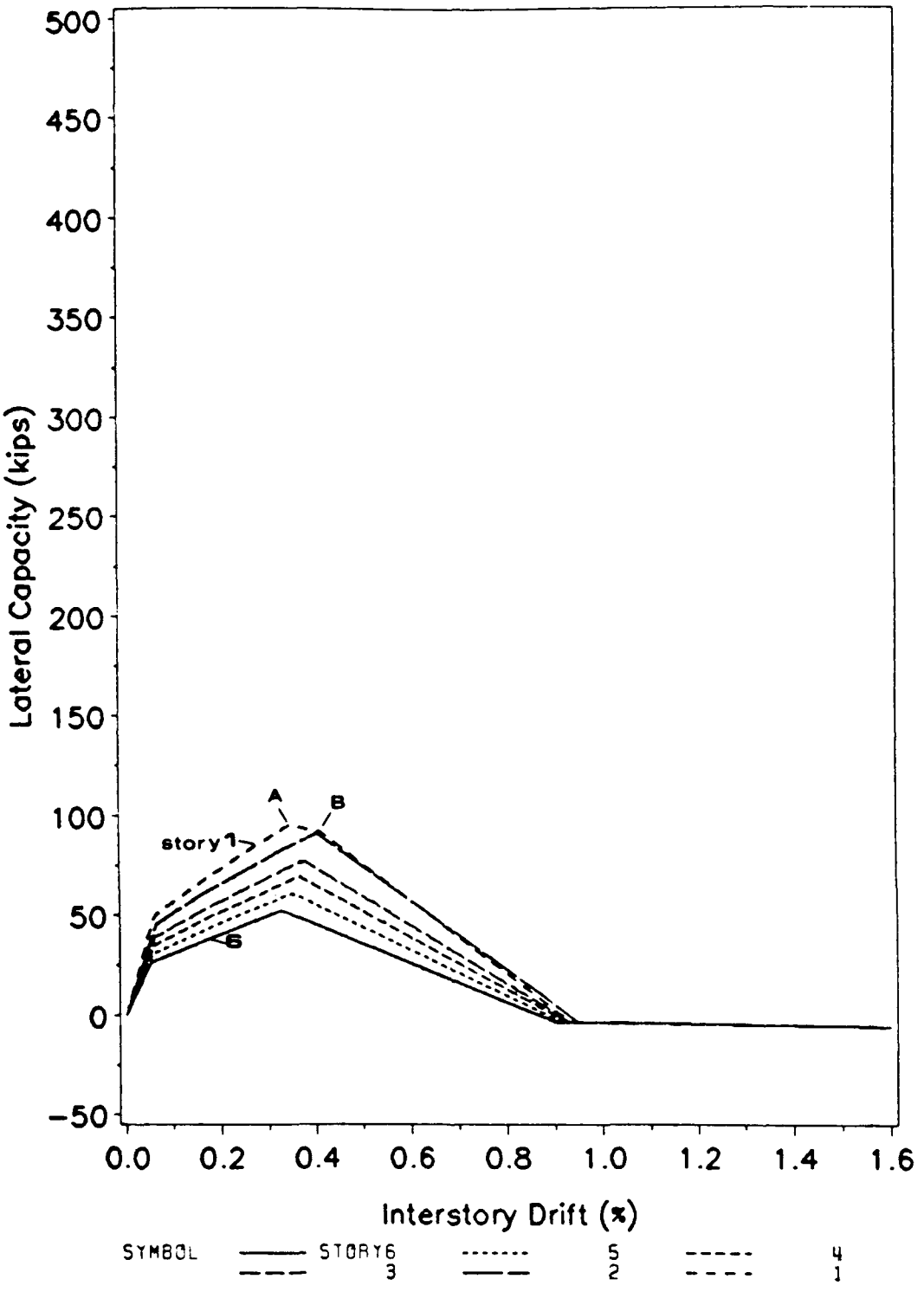

Fig. 5.6 Response curves for unstrengthened single story subassemblages to monotonic loading

the top of the column in the cases of stories 2, 4, and 5. Since the member properties of these subassemblages are symmetrical, an inflection point is located at mid-height of the column. This results in equal end moments for the column. When the column reaches its ultimate shear capacity, simultaneous behavior of the nonlinear springs (due to the equal end moments) causes both ends of the column to "fail" at the same time.

Failure mechanisms for stories 1, 3, and 6 are slightly different. The member properties for the spandrel framing in at the bottom of the subassemblage column are not the same as they are at the top of the column. Since the subassemblage no longer has symmetrical member properties, the inflection point in the column moves away from the center. A larger moment develops at the bottom of the column where the beam-column joint is stiffer. As a result, the lower column spring "fails" first. The upper column spring "fails" at a slightly higher drift. This condition is of little significance in stories 3 and 6; however, it is quite prevalent in story 1. The bottom of the first story column is assumed fixed in the computer model. This is equivalent to framing the column into infinitely stiff spandrel beams at the column base. A larger end moment therefore develops in the bottom of the column than at the top. It follows that the ultimate capacity of the inelastic spring is reached first at the base. This occurs at a drift of 0.35% and is labeled as point A in the figure. Ultimate capacity of the inelastic spring at the top of the column is reached at a drift of 0.40% shown as point B. Actual shear failure of the column should occur at approximately 0.4% drift with a lateral load of 99 kips.

The observed ultimate lateral strengths of each story and their corresponding ultimate drifts are summarized in Table 5.4. Observe that the lower stories achieve a higher ultimate lateral capacity than the upper stories. This is attributable to increased axial load on the lower story columns as well as increased transverse shear reinforcement in stories 1 and 2.

TABLE 5.4

Ultimate Lateral Capacity Of The Unstrengthened Frame By Story

Story	Lateral Capacity (kips)	% Drift at Ultimate
1	95.0	0.35
2	89.2	0.40
3	77.3	0.36
4	69.3	0.36
5	60.9	0.34
6	52.4	0.32

5.2.2 Response Of the Braced-Unaltered Frame

Bracing scheme A was next applied to the single story subassemblages and the six story subassemblage. Monotonic incremental displacements were applied to both the single story and multi-story models. The resulting curves for the single story subassemblages are

presented in Fig. 5.7. The corresponding response curves obtained from analysis of the six story subassemblage are identical to those in Fig. 5.7 and are therefore not repeated.

Recall that for bracing scheme A the size of cable bracing was changed at every story level. Further, the objective was to double the lateral strength for any story at a drift corresponding to shear failure of the columns in the original unstrengthened frame. Comparison of the unstrengthened and braced curves confirm that this objective was met. Note that the failure mechanism of each story is still dominated by shear failure of the columns. Further, column shear failure occurs at the same drift in both the unstrengthened and braced versions of the frame.

At drifts beyond those causing shear failure of the columns, response is dominated by characteristics of the cable braces as described in detail in Sec. 3.7.2. The reader is reminded here that these results rely on the validity of the assumption that the columns maintain their ability to carry the gravity loads even though the column has failed in shear. Ultimate story strength at each floor is reached at a common drift of 0.88%. This drift corresponds to simultaneous yielding and slackening of cable braces in each story.

5.2.3 Response Of The Braced-Altered Frame

Prestressed cable bracing scheme A1 and the beam alteration scheme shown in Table 5.3 were applied to the single story subassemblages and the six story subassemblage. Monotonic incremental displacements were again applied as in the previous unstrengthened and braced-unaltered

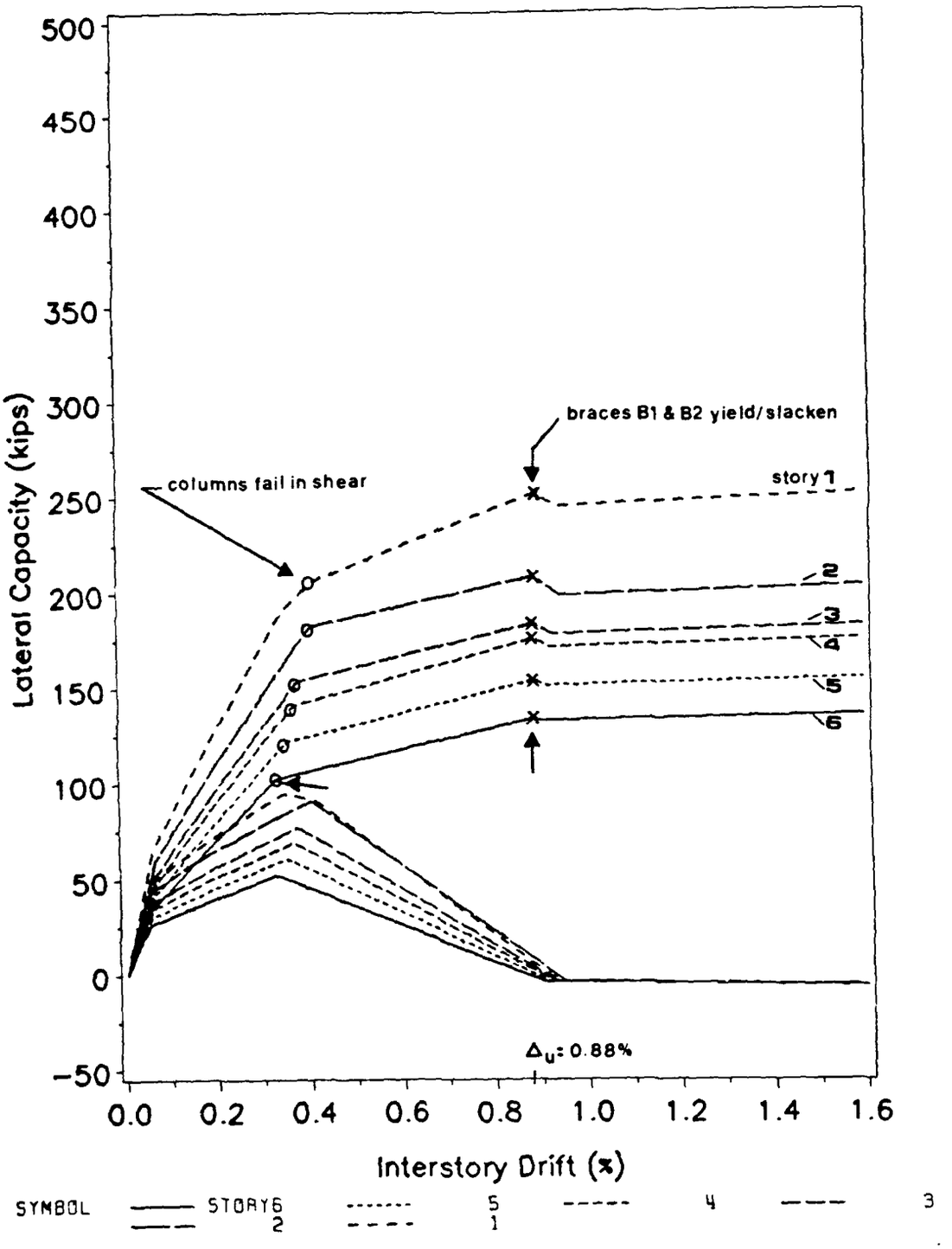

Fig. 5.7 Response curves for braced-unaltered single story subassemblages to monotonic loading, prestressed cable brace scheme A

runs. The resulting curves obtained from the single story subassemblages are presented in Fig. 5.8. The response curves obtained from the six story subassemblage analysis once again confirm good agreement with analysis using single story subassemblages.

In bracing scheme A1 the size of cable bracing was again changed at every story level. As with scheme A, the objective was to double the lateral strength at each story at a drift corresponding to shear failure of the columns in the unstrengthened frame. To achieve this objective the larger cable brace sizes indicated in Table 5.2 were required as explained in the discussion of Sec. 4.5.3. Comparison of the unstrengthened braced-altered curves of Fig. 5.8 at the appropriate drift confirms that this objective was met.

With the exception of story 1, the failure mechanisms of each story is no longer dominated by shear failure of the columns. Beam weakening at level 2 spandrels was successful in moving failure away from the top of the first story column and into the beams. Beam weakening may not, however, prevent shear failure from eventually occurring in the story 1 column. The "failure" of the inelastic spring at the base of the story 1 column is delayed from occurring until a drift of 0.48%. Even with a reduced end moment transferred to the top of the column in an altered frame, the story 1 column may still fail in shear because of the large end moment at the base of the column. A design engineer may in this case elect to utilize one of the more traditional seismic retrofitting techniques discussed in chapter 1 to strengthen the first floor columns.

Plastic hinges formed in the weakened spandrel beams at drifts shown in the figure. Beyond these drifts, response was again dominated

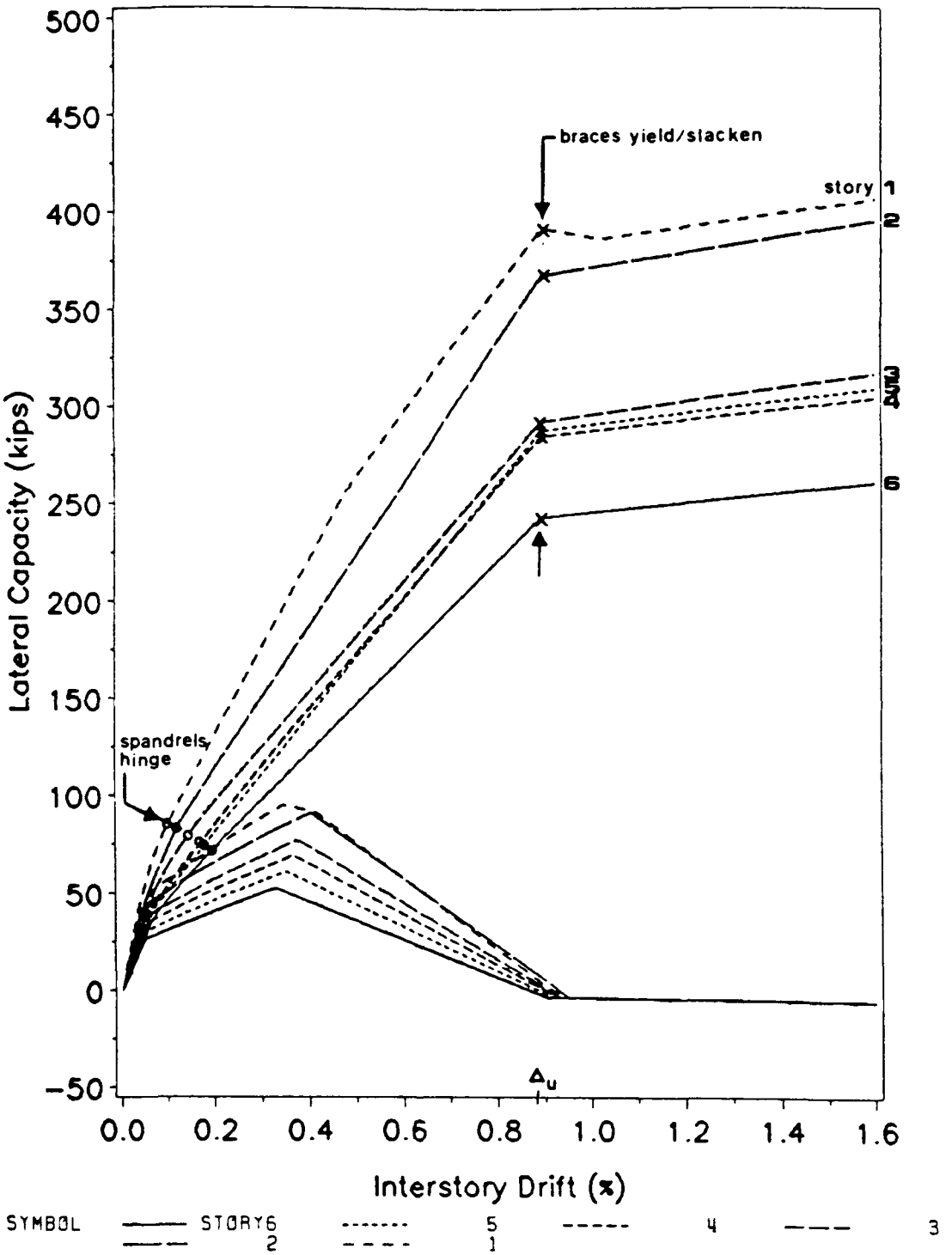

Fig. 5.8 Response curves for braced-altered single story subassemblages to monotonic loading, prestressed cable brace scheme A1

by behavior of the prestressed cable bracing system. Ultimate story strength at each floor was again reached at a common drift of 0.88%.

5.3 EVALUATION OF THE SINGLE STORY GENERIC SUBASSEMBLAGE HYPOTHESIS BY CONTRAST WITH RESULTS OF A SIX STORY SUBASSEMBLAGE ANALYSIS

In the previous prestressed cable brace study [2], it was hypothesized that global behavior of the retrofitted frame could be adequately represented by modeling and analyzing the generic single story subassemblage. In this section the hypothesis is evaluated. The six story subassemblage was fitted and analyzed with bracing schemes A, B, and C of Table 5.3. The resulting normalized response curves for each scheme were compared and contrasted to the normalized response curve obtained from a generic single story subassemblage.

The location of the generic single story subassemblage is shown in Fig. 5.1. The generic subassemblage is identical to the unique single story subassemblage developed for story 4 in Sec. 5.2. The choice of generic subassemblage was made for the following reasons. First, the fourth floor subassemblage most closely resembles the subassemblage studied in previous studies [2, 3] as well as chapters 3 and 4. Reinforcement, strength, stiffness, axial force, location in the frame, and response history most closely match the original subassemblage of the seven story frame. Secondly, the subassemblage is located near the center of the frame away from the frame boundaries.

The cable brace area used was 1.05 in^2 which is the same cable brace area specified for story 4 in bracing scheme A. The monotonic response of unstrengthened and braced-unaltered versions of the

subassemblage are plotted in Fig. 5.9. The generic subassemblage hypothesis is based on the premise that the normalized response curve of Fig. 5.9 adequately represents the global behavior expected of the complete frame. The critical unstated assumption was that every bay of the frame is braced uniformly and that cable brace areas are selected based on a common design ratio n throughout the structure.

Relative response curves for the unstrengthened six story subassemblage and a braced-unaltered version with bracing scheme A are presented in Fig 5.10. The relative response curves have been normalized with respect to the ultimate strength of the unstrengthened frame at each story (load ratio m as defined in Sec. 2.4.2).

The monotonic response curves for the unstrengthened frame shown in Fig. 5.10 fall within a fairly tight band as expected. The response of the generic subassemblage is the same as that for story 4 and falls in the center of the family of curves.

Recall that in bracing scheme A the size of the cable braces was changed at every level of the frame. The family of curves representing response of the braced frame with bracing scheme A falls within a relatively tight band. The curves have a range of 0.31 at 0.88% drift and a deviation of 0.13 using the generic subassemblage response as the basis. The response of the braced generic subassemblage is identical to the response of story 4 and falls near the center of the family of curves. The generic subassemblage model underestimates the ultimate strength of story 1 by 4.8% and overestimates the ultimate strength of story 2 by 8.8%. For bracing scheme A the generic subassemblage hypothesis seems reasonable.

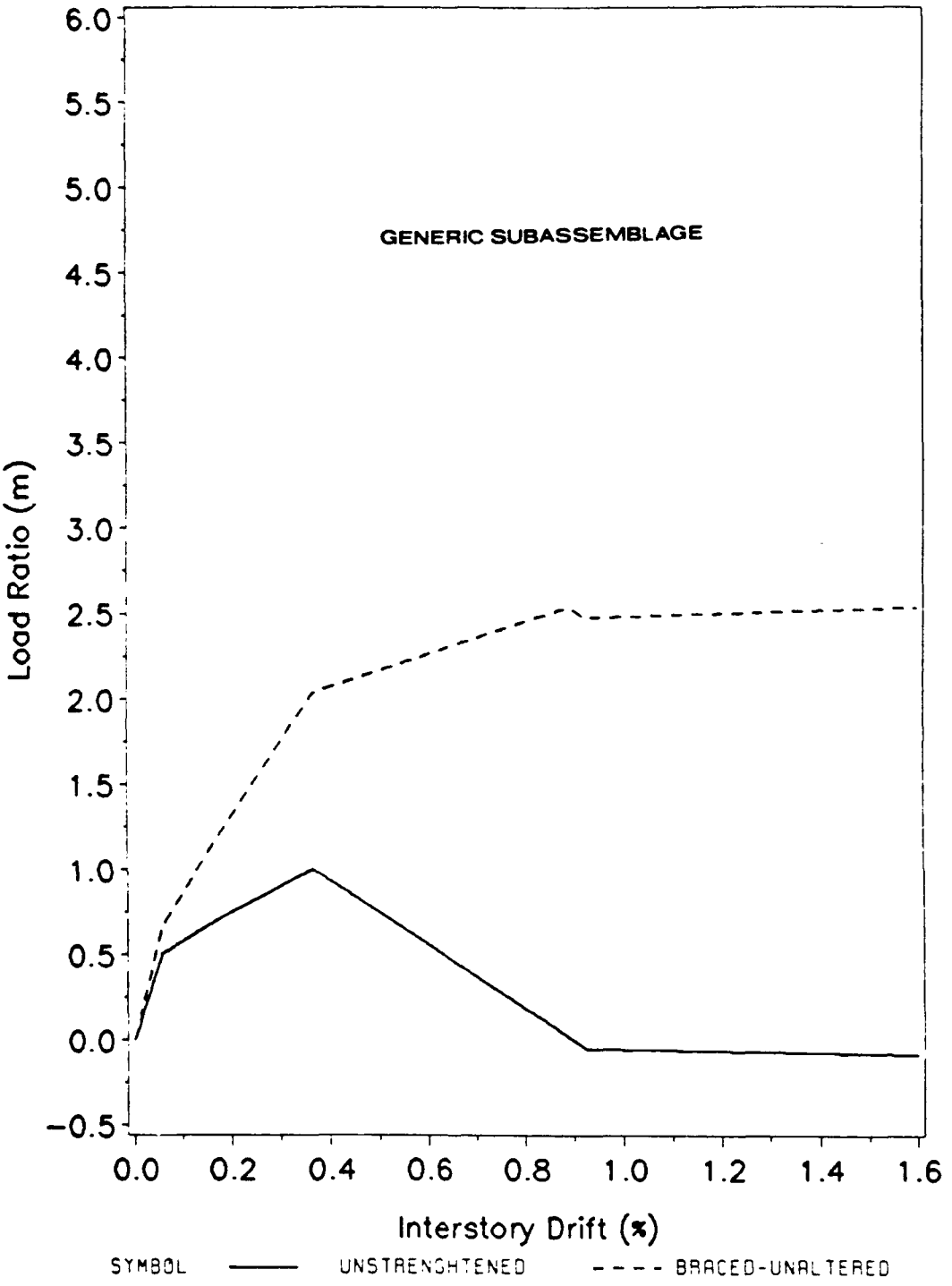

Fig. 5.9 Monotonic response of unbraced and braced versions of the generic single story subassemblage, n=2, Ac=1.05 in²

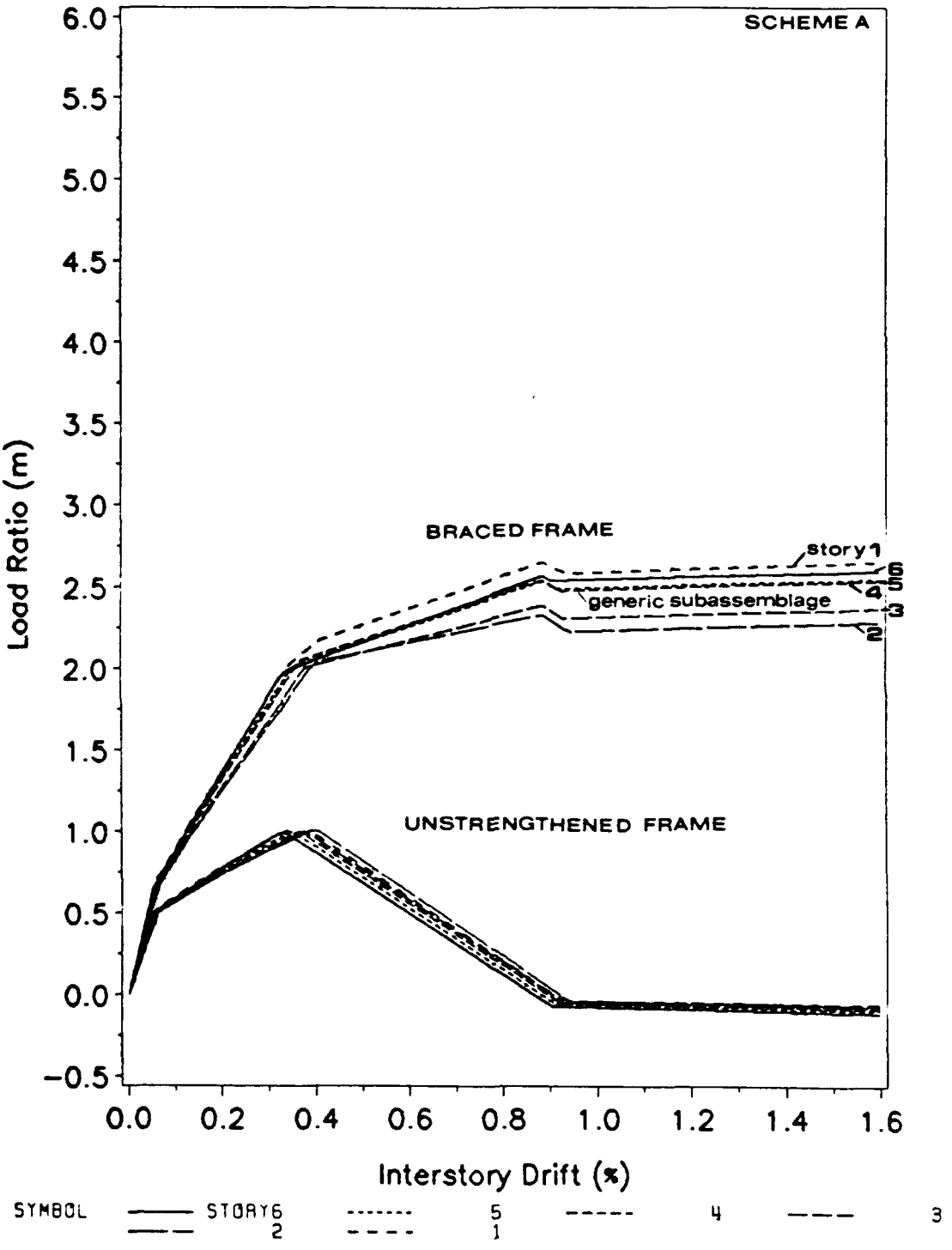

Fig. 5.10 Relative monotonic response of unbraced and braced versions of the six story subassemblage changing size of cable braces every story, scheme A

Using bracing scheme B the cable brace size was changed every other story (at levels 3, and 5). The relative response curves for bracing scheme B are plotted in Fig. 5.11. The response of the generic subassemblage is presented as well and plots on top of the story 5 curve. The dispersion of the response curves is more apparent in this bracing scheme and falls into roughly two distinct bands as expected since the cable brace size was changed every other story. One band contains the curves for the odd numbered stories 1, 3, and 5. The second band contains curves for the even numbered stories 2, 4, and 6. The range of the curves is 0.52 at 0.88% drift. The deviation from that of the generic subassemblage response increases to 0.23. The generic subassemblage model underestimates the ultimate strength of story 6 by 14.7% and overestimates the ultimate strength of story 3 by 6.0%.

In bracing scheme C the cable brace size is held constant for the entire height for the structure. The response of the six story subassemblage with bracing scheme C is plotted in Fig. 5.12. The response of the generic subassemblage is presented in the figure as well for comparison. The family of braced response curves are dispersed to the maximum extent under this bracing scheme. The range of the curves is 2.06 and the deviation from the generic subassemblage model is 1.33. The generic subassemblage model underestimates the ultimate strength of story 6 by 86.9%.

The generic subassemblage model becomes progressively less accurate in representing the global response of the frame as the bracing scheme employed deviates from one in which the cable brace area is changed at every story level. In a practical bracing scheme, cable brace area

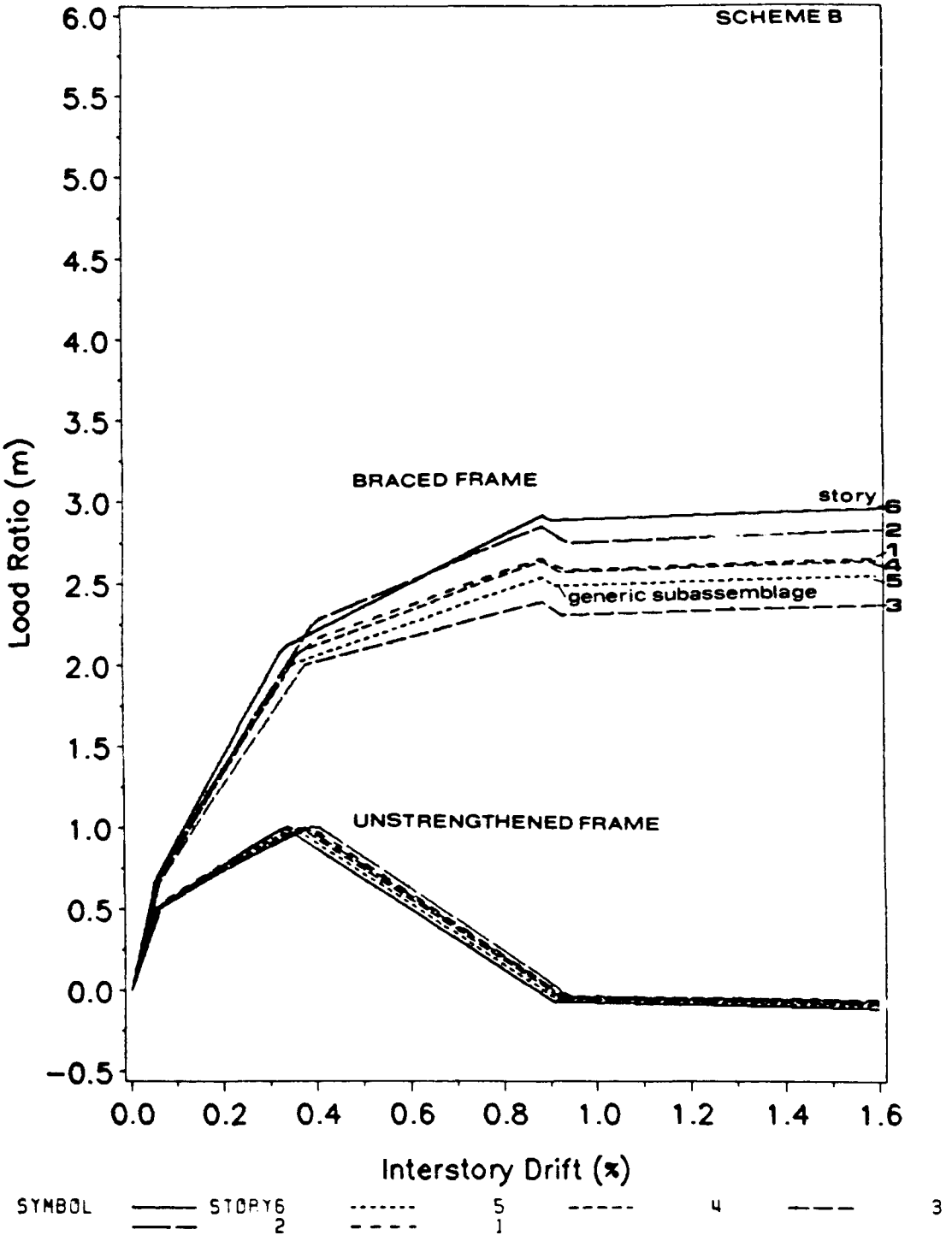

Fig. 5.11 Relative monotonic response of unbraced and braced versions of the six story subassemblage changing size of cable braces every other story, scheme B

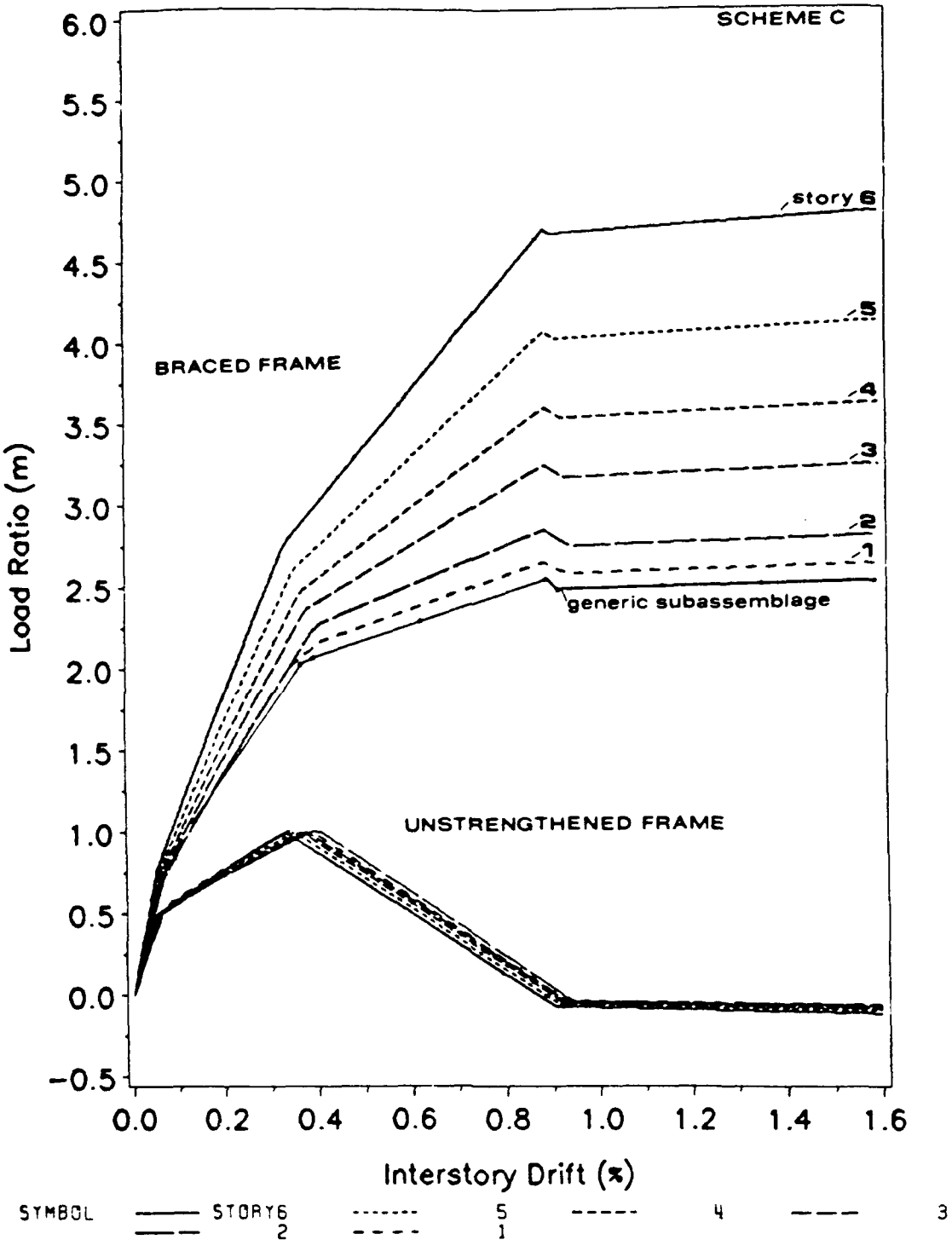

Fig. 5.12 Relative monotonic response of unbraced and braced versions of the six story subassemblage holding size of cable braces constant scheme C

might change every other story or at some other feasible interval. The generic subassemblage model is therefore of little practical value in designing bracing schemes of this type. In Sec. 5.2 it was shown that unique single story subassemblages and the six story subassemblage produce nearly identical results. As a minimum, one should employ either a combination of unique single story subassemblages or a multi-story subassemblage if one wants to accurately represent global behavior of a frame under practical bracing schemes.

5.4 DISCUSSION OF PRACTICAL DESIGN STRENGTH RATIO SCHEMES FOR THE PROTOTYPE FRAME

In the previous two sections, the response curves for the six story subassemblage were studied under the four bracing schemes of Table 5.2. To put the results into practical perspective, it is of interest to evaluate the adequacy of these bracing schemes for bringing the prototype frame up to current building code standards.

In Sec. 5.1 the prototype frame was designed using seismic design loads recommended by the 1955 edition of the Uniform Building Code. In order to examine the level of retrofit strengthening which would actually be required for the prototype frame, the recommended design story shears were recalculated using the method specified in the 1988 edition of the Uniform Building Code. From these results the ultimate load ratio m required for each story in order to meet present code standards was calculated and presented in column 2 of Table 5.5.

TABLE 5.5

Ultimate Load Ratios Attained By Various Bracing Schemes

Story	m required to meet 1988 UBC code	ultimate m attained with TABLE 5.3 bracing schemes Scheme A	Scheme A1	Scheme B	Scheme C
1	2.77	2.63	4.11	2.63	2.63
2	2.63	2.29	4.09	2.80	2.83
3	2.66	2.36	3.75	2.36	3.23
4	2.18	2.51	4.14	2.62	3.57
5	1.53	2.51	4.65	2.51	4.05
6	0.73	2.53	4.58	2.88	4.69

The ultimate m ratio achieved for each of the four bracing schemes obtained from Figures 5.8, 5.10, 5.11, and 5.12 are presented as well in Table 5.5. Recall that all four bracing schemes were developed utilizing the serviceability design approach with an arbitrarily chosen n = 2. Using the serviceability design approach, the stated objective was to double the lateral strength for a given story at a drift corresponding to shear failure of that story in the original frame.

Use of bracing scheme A results in deficient levels of retrofit strength in stories 1, 2, and 3 by 5.3%, 12.9%, and 11.3% respectively. Execution of scheme A, however, results in attainment of unnecessarily high lateral strengths in stories 4, 5, and 6. The required ultimate load ratios in stories 4, 5, and 6 are exceeded by 15.1%, 64%, and 246% respectively. Similarly, use of schemes B and C come closer than scheme

A to matching required strengths in the first three stories, however retrofit strengths achieved by both schemes remain deficient by 5.3% in story 1. Scheme A1 bracing was applied in conjunction with the beam alteration scheme of Table 5.3. As seen in Table 5.5, the required ultimate load ratio provided is far exceeded in all six stories.

From these results it is evident that any practical bracing scheme will most likely make use of a unique design strength ratio n estimated for each story based on current seismic design loads. Additionally, because considerably higher ultimate m ratios are obtained by using beam alteration in conjunction with the cable bracing, lower design ratio n values for each story may be selected.

CHAPTER 6

INSTALLATION OF PRESTRESSED CABLE BRACING SYSTEMS AND CONNECTION DESIGN

6.1 PRACTICAL CONSIDERATIONS FOR APPLICATION OF PRESTRESSED CABLE BRACING SYSTEMS

In chapters 4 and 5 the benefits of retrofit strengthening with prestressed cable bracing and beam alteration were analytically demonstrated. Practical implementation of beam alteration may be accomplished by simply cutting or coring into the beam. Although the operation is labor intensive, material costs are small and execution difficulty is manageable. The greatest concerns in beam alteration involve accurately determining the placement of reinforcing steel prior to cutting, and obtaining adequate operating clearance for concrete saws and/or drills. Care must be taken to cut only the desired layers of longitudinal steel while preserving the integrity of the shear reinforcement. Applications of beam weakening techniques have already been successfully implemented in conjunction with traditional steel bracing systems. Installation of prestressed cable bracing systems, however, are not so straight forward. To the knowledge of this author, no practical applications of prestressed cable bracing systems have been implemented or tested to date.

Modeling a prestressed cable bracing system analytically has been discussed extensively in this study. Actual installation of prestressed cable braces to a structure such as the prototype building introduces many additional problems not considered in the present study. In this section some of these considerations are identified and discussed in

light of how they may affect practical application of prestressed cable braces.

Types And Sizes Of Standard Prestressing Tendons. There are four common types of tendon systems: monostrand, single bar, multi-wire, and multi-strand tendons. The most widely used type of prestressed tendon used for post-tensioning applications is the seven wire strand [13]. In this study grade 270 seven wire strand tendons were assumed for the cable brace model. Standard nominal diameters and cross-sectional areas available for grade 270 tendons are given in Table 6.1.

TABLE 6.1 Standard Seven Wire Prestressing Cable Sizes, Grade 270

Nominal Diameter (in.)	Nominal Cross-Sectional Area ($in.^2$)
3/8	0.085
7/16	0.115
1/2	0.153
0.6	0.216

Any number of seven wire strands can be combined into a multi-strand tendon as needed to achieve larger cross-sectional areas. For the purpose of this study the assumption was made that any size multi-strand cable required would be available. In practical applications the

exact theoretical cable brace area required would in general not be available. It is not practical to mix strand sizes within a cable to reach a certain cross-sectional area. Cross-sectional areas can be obtained reasonably close to the theoretical area required, however, by choosing an appropriate number of seven wire strands shown in Table 6.1.

Post-Tensioning Techniques. Throughout this thesis the generic term "prestressed cable braces" has been used to describe the bracing system. In the prestressed concrete industry, prestressing operations are generally divided into two classifications: pretensioning and post-tensioning. In pretensioning the tendon is stressed prior to casting the concrete, while in post-tensioning the tendon is tensioned after the concrete has been cast. For application to cable bracing, standard techniques developed for post-tensioning tendons would most likely be appropriate.

Various proprietary post tensioning systems are available. These systems differ in the type of tendon that they employ, in the manner in which the tendons are tensioned, and in the anchorage devices which are used. The Freyssinet K-Range and the VSL multi-strand post tensioning systems are discussed below.

The Freyssinet K-Range System is illustrated in Fig. 6.1. The Freyssinet K-Range System is a multi-strand system in which each strand is individually gripped by three conical jaws that seat into tapered holes inside an anchorage block. The stressing is performed by a center-hole jack which simultaneously tensions all strands in a tendon. Upon release of the jack, pull in of the strands engages the wedge like jaws that anchor the strands. There is a certain loss of cable

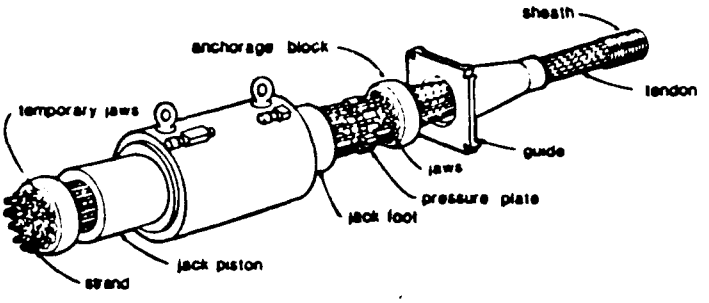

(a) Jacking and anchorage components

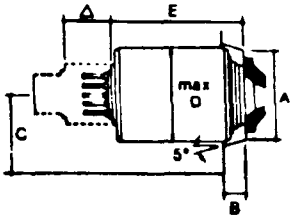

jack type	A in (mm)	B in (mm)	C in (mm)	D in (mm)	E in (mm)
4/.5	5.38 (140)	4.5 (100)	4.5 (100)		
7/.5 4/.6	6.26 (160)	4.5 (100)	6.0 (136)	13 (326)	25 (630)
12/.5 7/.6	7.26 (250)	4.5 (120)	7.0 (176)	13 (326)	25 (630)
12/.6	8.00 (300)	4.5 (126)	8.0 (200)	16 (390)	29 (760)
19/.6	11.00 (500)	5.0 (140)	9.0 (250)	20 (510)	35 (900)

(b) Jacking details

unit	range in no of strands	sheath inside dia in. (mm)	tendon force, kips (kN) 0.7 $A_{ps}f_{pu}$
1/.5	1	1.0 (26)	29.0 (129)
7/.5	5 7	2.1 (54)	57.8 (257) 203.4 (900)
12/.5	8 12	2.6 (66)	231.3 (1028) 346.9 (1543)
19/.5	13 19	3.3 (84)	375.8 (1671) 549.3 (2443)
27/.5	20 27	3.7 (94)	578.2 (2572) 780.5 (3472)
37/.5	28 37	4.4 (113)	808.4 (3600) 1069.8 (4756)
55/.5	38 55	5.0 (128)	1098.5 (4886) 1590.0 (7072)

(c) 1/2 in. (13mm)-270K series

unit	range in no of strands	sheath inside dia in. (mm)	tendon force, kips (kN) 0.7 $A_{ps}f_{pu}$
1/.6	1	1.4 (36)	41.8 (182)
4/.6	2 4	2.1 (55)	82.0 (365) 164.0 (730)
7/.6	5 7	2.6 (70)	205.0 (912) 287.0 (1277)
12/.6	8 12	3.2 (80)	328.0 (1458) 492.0 (2188)
19/.6	13 18	4.3 (100)	533.0 (2371) 770.0 (3466)
27/.6	20 27	4.7 (120)	820.0 (3648) 1107.0 (4924)
37/.6	28 37	5.1 (130)	1148.0 (5107) 1517.0 (6748)

(d) 0.6 in. (15mm)-270K series

Fig. 6.1 The Freyssinet K-Range post tensioning system [13]

elongation that takes place before the conical jaws engage the cable strands. This loss of cable pretension must be accounted for in design. Detailers of post-tensioning anchor blocks must ensure that there is sufficient clearance for erectors to thread cables as well as maneuver and operate the center hole jack.

The VSL multi-strand post tensioning system is illustrated in Fig. 6.2. Jacking and anchoring devices for the VSL multi-strand system are similar to those developed previously for the Freyssinet System. Multi-strand tendons can be jacked from both ends to reduce frictional losses or can be jacked from one end with the other end of the tendon terminating in a dead end anchor. Both the Freyssinet and the VSL systems utilize 1/2 or 0.6 in. seven wire strand tendons and have jacks available which can prestress up to 55 strands simultaneously. Either system can probably be adapted to post-tension cable braces.

Location Of Post-Tensioning Anchors. Drawing from conclusions developed in Ref. 2, there are two general X bracing patterns practical enough to be considered for use with prestressed cable braces. These two patterns are shown in Fig. 6.3. In the subassemblage models studied in chapters 4 and 5 only Pattern 1 braces were analyzed. Similar conclusions are drawn if the study is conducted using Pattern 2 braces. If Pattern 2 bracing is used, additional braces and post-tensioning connectors are needed over that required by use of Pattern 1 bracing; however, the area required for each cable is less.

In Pattern 1 the prestressed cable braces are assumed to extend from the beam column joint of the upper story to the center of the

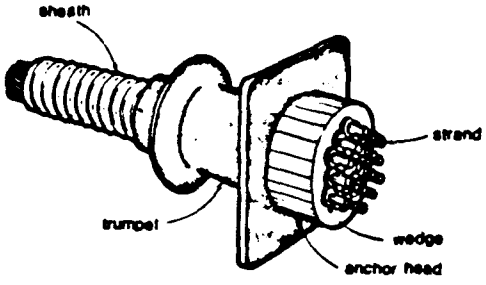

(a) Stressing anchorage details

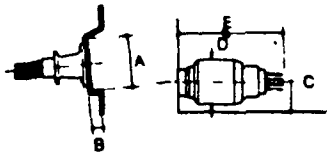

Jack type	A in. (mm)	B in. (mm)	C in. (mm)	D in. (mm)	E in. (mm)
E5-3	14 (356)	5 (127)	7 (178)	13 (330)	51 (1296)
E5-7 E6-3	16 (406)	5 (127)	9 (229)	16 (406)	52 (1321)
E5-12 E6-7	18 (457)	5 (127)	10 (254)	18 (457)	52 (1321)
E5-19 E6-12	22 (559)	7 (178)	10 (254)	18 (457)	55 (1397)
E5-31 E6-19	27 (686)	7 (178)	11 (279)	20 (508)	57 (1448)
E5-55 E6-31	36 (914)	10 (254)	18 (457)	30 (762)	70 (1778)

(b) Jacking details

unit	range in no of strands	sheath inside dia in. (mm)	tendon force, kips (kN) 0.7 $A_{ps}f_{pu}$
E5-3	2	1.25 (31)	57.0 (257)
	3	1.50 (38)	86.7 (386)
E5-4	4	1.63 (41)	115.6 (514)
E5-7	5	1.75 (44)	144.5 (643)
	7	2.00 (50)	202.4 (900)
E5-12	8	2.00 (50)	231.3 (1029)
	12	2.50 (63)	346.9 (1543)
E5-19	13	2.63 (66)	375.8 (1671)
	19	3.13 (78)	549.3 (2442)
E5-22	20	3.25 (81)	578.2 (2571)
	22	3.38 (85)	636.0 (2828)
E5-31	23	3.50 (88)	664.9 (2957)
	31	4.00 (100)	896.2 (3985)
E5-55	55	5.49 (139)	1590.4 (7070)

(c) VSL 1/2 in.(13mm)-270K 'E series'

unit	range in no of strands	sheath inside dia in. (mm)	tendon force, kips (kN) 0.7 $A_{ps}f_{pu}$
E6-3	2	1.50 (38)	82.0 (365)
	3	1.50 (38)	123.1 (547)
E6-4	4	2.00 (50)	164.1 (730)
E6-7	5	2.25 (57)	205.1 (912)
	7	2.25 (57)	287.1 (1277)
E6-12	8	2.81 (71)	328.2 (1459)
	12	3.00 (76)	492.2 (2189)
E6-19	13	3.25 (81)	533.3 (2371)
	19	3.75 (95)	779.4 (3468)
E6-22	20	4.00 (100)	820.4 (3648)
	22	4.00 (100)	902.4 (4012)
E6-31	23	4.50 (114)	943.5 (4196)
	31	5.00 (126)	1271.8 (5654)
E6-55	55	6.50 (165)	2256.1 (10033)

(d) VSL 0.6 in. (15mm)-270 K 'E series'

Fig. 6.2 The VSL multi-strand post tensioning system [13]

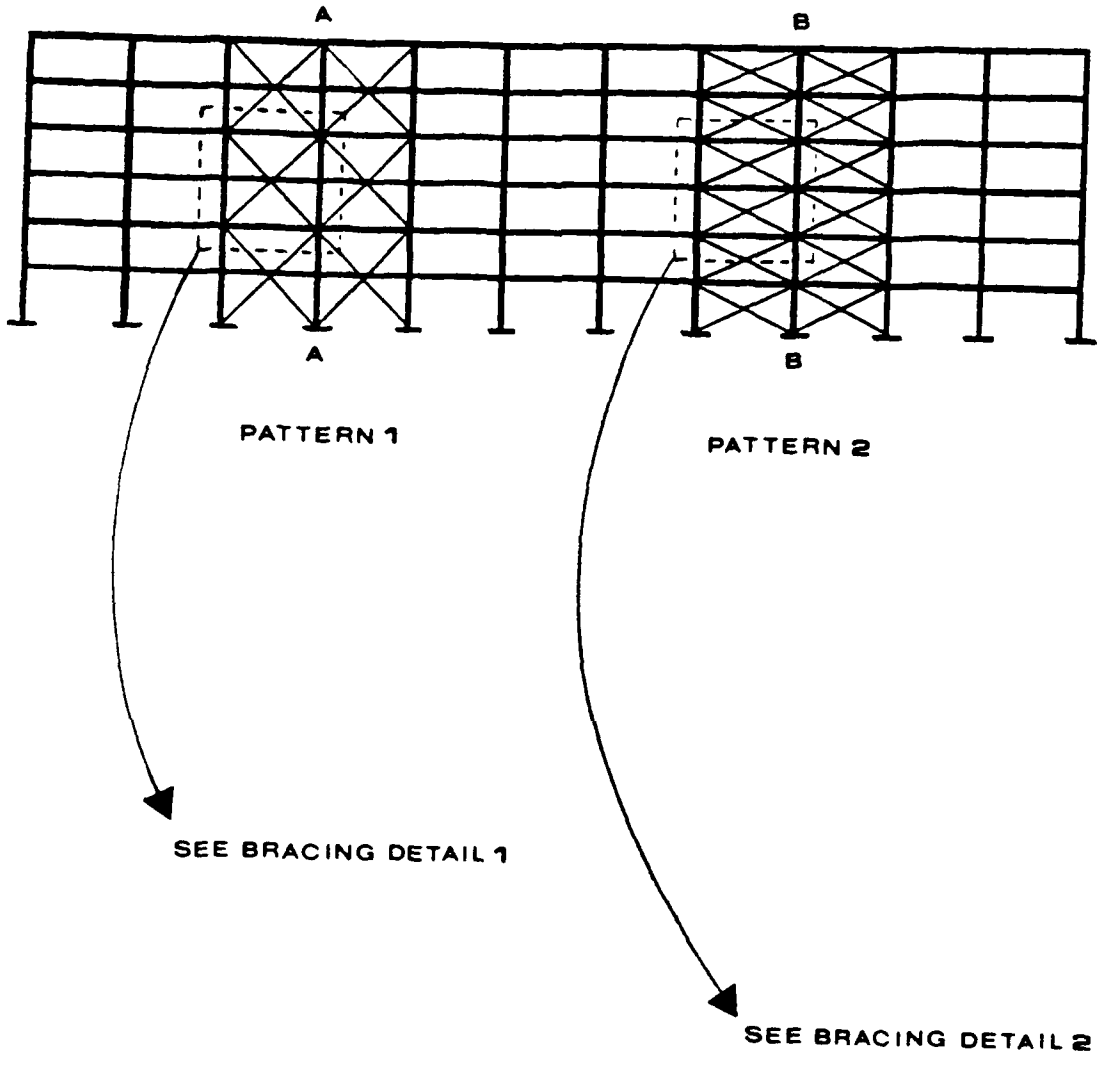

Fig. 6.3 Prestressed cable bracing patterns

spandrel beam of the lower story. This assumption carries with it several design considerations which affect the feasibility of installing cable braces using Pattern 1. A cross section of the prototype frame is shown in Fig. 6.4. For the prototype frame shown, notice that the spandrel beams are not flush with the face of the column. Any post-tensioning connector attached to the center of the spandrel beam must project a distance Z as shown in Fig. 6.4. Z is the distance from the face of the spandrel beam to the plane of action for the prestressed cables. Z is a measure of the eccentricity the spandrel beam-cable brace connection would have to be designed for. In the case of the prototype frame, this eccentricity will be in the neighborhood of 15 to 17 inches. Such a connection block would most likely be very bulky in order to accommodate post-tensioning and terminating of tendons at this location.

A more practical approach would be to limit post-tensioning points to the beam-column joints as shown in Fig. 6.4. The post-tensioning connectors shown are bolted to the face of the column and centered over the centroid of the beam-column joint. All initial post-tensioning of cables can take place at such post-tensioning connectors. Connectors placed at the spandrel beam-cable brace joints could be of a sleeve type that simply pass the tendons through to the next beam-column connector prior to post-tensioning. After post-tensioning, such connections might be clamped or grouted. Because of the impracticality of post-tensioning tendons at the spandrel beam-cable brace joint for Pattern 1, it is consequently not possible to specify different cable brace areas for every story as in bracing schemes A and A1 of Table 5.2.

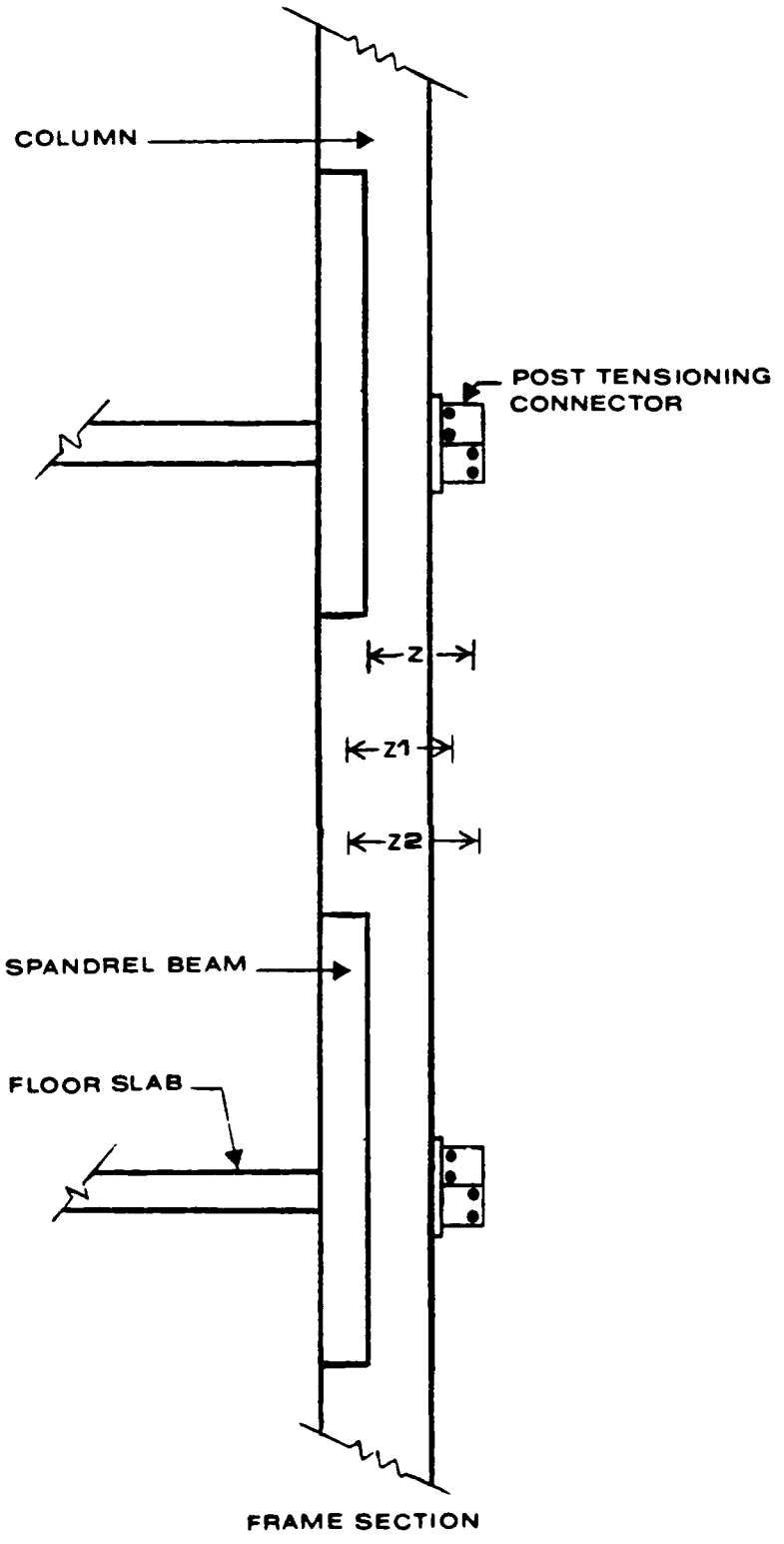

Fig. 6.4 Frame section showing a profile view of Pattern 2 Type B post-tensioning connectors

Post-Tensioning Sequence. The analytical research presented thus far begins with the post-tensioned cables already in place. Static analysis of the braced frame with DRAIN-2D confirms that the additional forces imposed by the prestressed cable braces do not yield any of the members or joints of the original unstrengthened frame. However, this may not be true during the installation and initial post-tensioning of the cable brace system. Careful attention must be given to the post-tensioning sequence for the bracing system. Simultaneous and or incremental post-tensioning of several cables may be necessary in order to avoid overstressing the structure during the retrofitting operation.

Out-Of-Plane Forces. Significant out-of-plane forces are imposed on the frame with the installation of a prestressed cable brace system. For the purpose of the present analytical study the assumption was made that all forces associated with the retrofitted frame are in-plane. The distances Z1 and Z2 in Fig. 6.4 illustrate the incorrectness of this assumption. Z1 and Z2 are the distances between the planes of action for the beam forces and the bracing system. The maximum distance Z2 can be as high as 21 inches for the prototype frame. Such eccentricities will impose torque on the frame columns. This problem will be predominate during the post-tensioning operation on all bays; however, it will persist on columns adjacent to unbraced bays even after post-tensioning is completed. The magnitude of such out-of-plane forces must be evaluated and considered with respect to the capacity of the frame to carry these forces.

6.2 CONCEPTS FOR POST-TENSIONING CONNECTOR DESIGNS

In this section some concepts for post-tensioning connector blocks and their installation are discussed. The sketches presented are to be taken as conceptual and not final designs. Number, location, size, and spacing of bolts as well as need for stiffeners has not been considered. Connection blocks for Patterns 1 and 2 of Fig. 6.3 were considered.

Bracing Detail 1 for bracing Pattern 1 is shown in Fig. 6.5. In general three distinct connector types will be required for this bracing scheme. Types A and B connectors are located at the slab level of the beam column joints. These connectors must be capable of anchoring two or more tendons stressed to $0.5P_y$. The type A connector is for use on columns adjacent to unbraced bays. Type B connectors are used on columns with two or more adjacent bays braced. Type C connectors are located at spandrel beam-cable brace joints. As discussed in Sec. 6.1, type C connectors are used to clamp the cable braces in place after the completion of post-tensioning operations.

Details for both type A and B connectors are conceptually illustrated in Fig. 6.6. The steel base plate is located over the centroid of the beam column joint. The plate would probably be bolted to the column. It may be possible to drill completely through the column, fix a base plate on the inside face of the beam-column joint as well and prestress the bolts to ensure a good connection. The cable anchor blocks are fixed to the steel base plate either by bolting or welding. The cable terminations must be secured or epoxied in some manner to prevent possible unseating during cyclic loading.

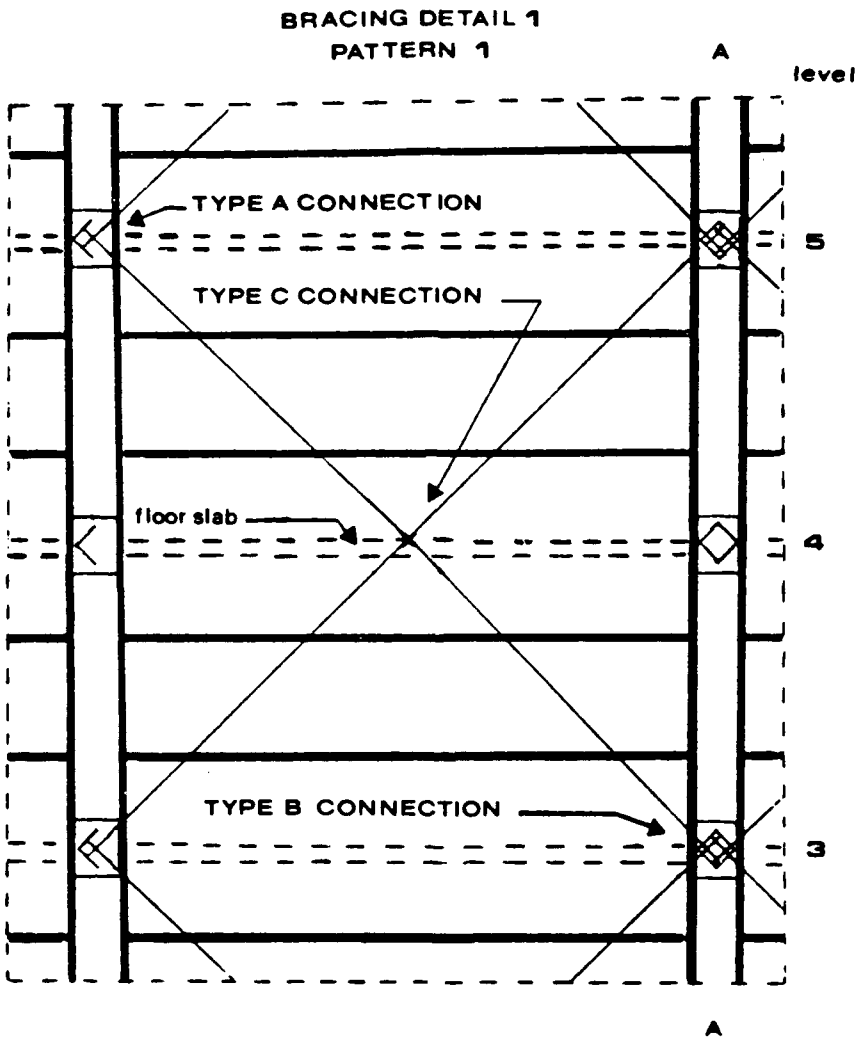

Fig. 6.5 Prestressed cable bracing detail 1

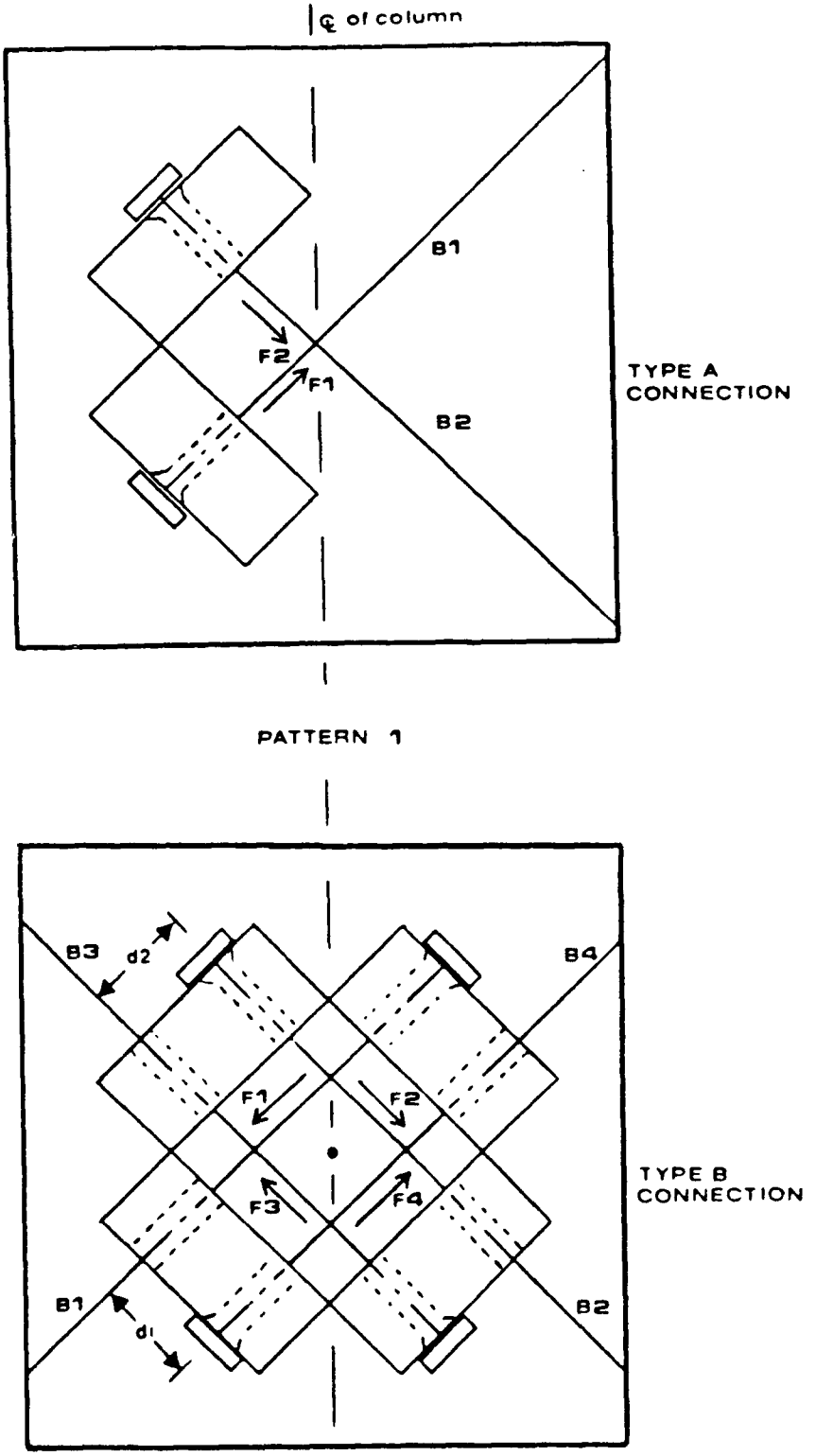

Fig. 6.6 Conceptual sketch of Pattern 1 Type A and B connectors

In the type A connection, the prestressed cable force passes concentrically through the beam column joint as assumed in the computer model of the analytical study. Since both F1 and F2 are tensile forces, there is a net horizontal force (horizontal component of F1 + F2) which must be resisted by the beam-column joint. As pointed out in the previous section, the eccentricity of this force may be as high as 21 inches for the prototype frame. The designer must look at whether or not the frame can handle the combined torque and bending. If the torque is too high, it may be feasible to attach prestressed cable braces to both the inside and outside faces of the frame, thus eliminating the torque and reducing the problem to one of pure bending. Attaching cable braces to the inside face of the frame will require cutting cable troughs in the floor slabs. This is necessary to pass the cables from one story to the other. With modern concrete cutting and coring equipment, placing cable braces on both sides of the frame is quite feasible. The labor involved, inconvenience to building occupants, and aesthetics, however, may eliminate cable braces as a desirable retrofitting scheme.

In a type B connection, forces do not pass exactly through the centroid of the beam-column joint as shown. If braces B1, B2, B3, and B4 are all the same size and carry the same prestress force, the joint will be in equilibrium under static load. If B1, B2, B3, and B4 are not the same, the unbalanced force will have to be carried by the frame. The cable termination points are located such that the moment F1*F4*d1/2 should be roughly canceled by the moment F2*F3*d2/2. The type B connection does not experience the same combined torque and bending

forces at rest that the type A connection does, except possibly during post-tensioning operations and cyclic loading. The possibility of overstressing during post-tensioning can be reduced or eliminated by carefully considering the post-tensioning sequence.

Sizing type A and type B anchor blocks will be fairly straight forward. Under static load the anchor blocks for both type A and B connections experience primarily shear force; however, the height of the blocks may be great enough that bending may become a concern. The cable spacings, d1 and d2, are dependent on the clearance requirements of the center hole jacks used to post-tension the cables as well as minimum spacing and edge distance requirements.

The effect cable brace orientation has on design of type A and type B connectors is shown in Figs. 6.7 and 6.8. The cable brace areas required by Pattern 2 bracing schemes are significantly less than those required by Pattern 1 bracing schemes. As a consequence, the forces seen by the connectors in Fig. 6.8 are correspondingly less than the connectors of Fig. 6.6. This fact may significantly influence the decision of which bracing pattern is ultimately chosen for the retrofitting scheme.

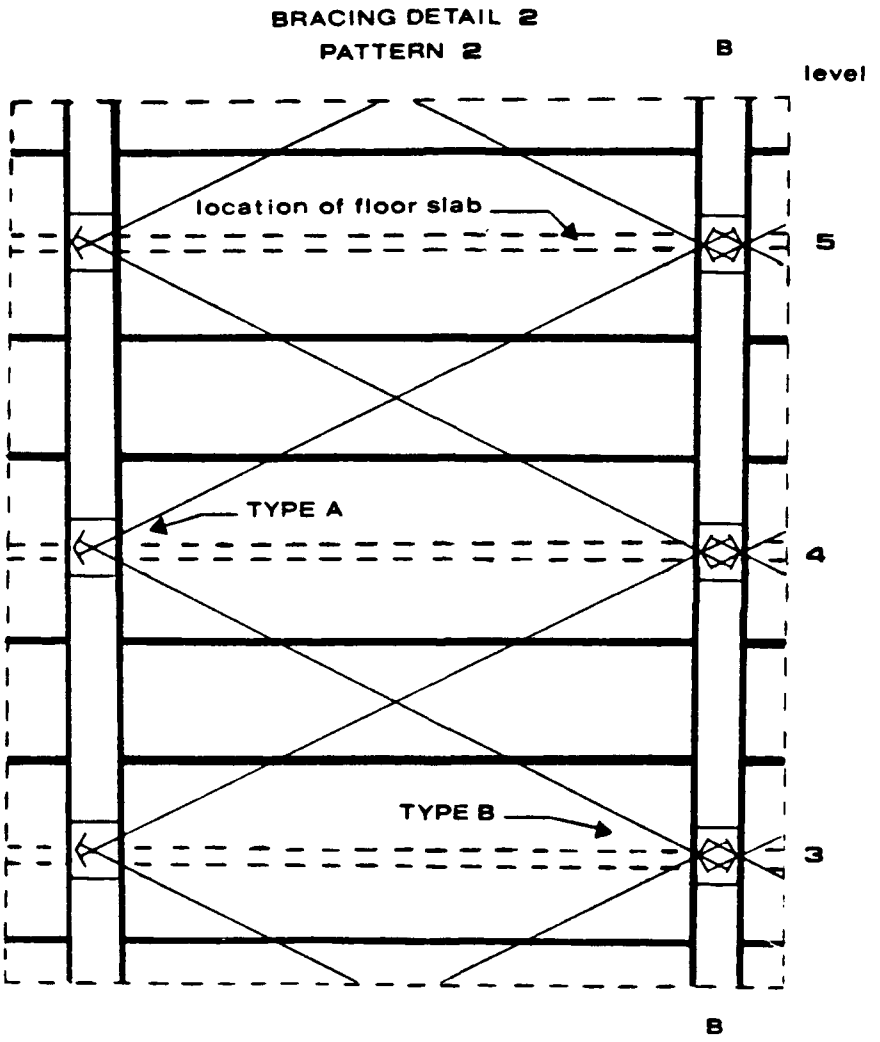

Fig. 6.7 Prestressed cable bracing detail 2

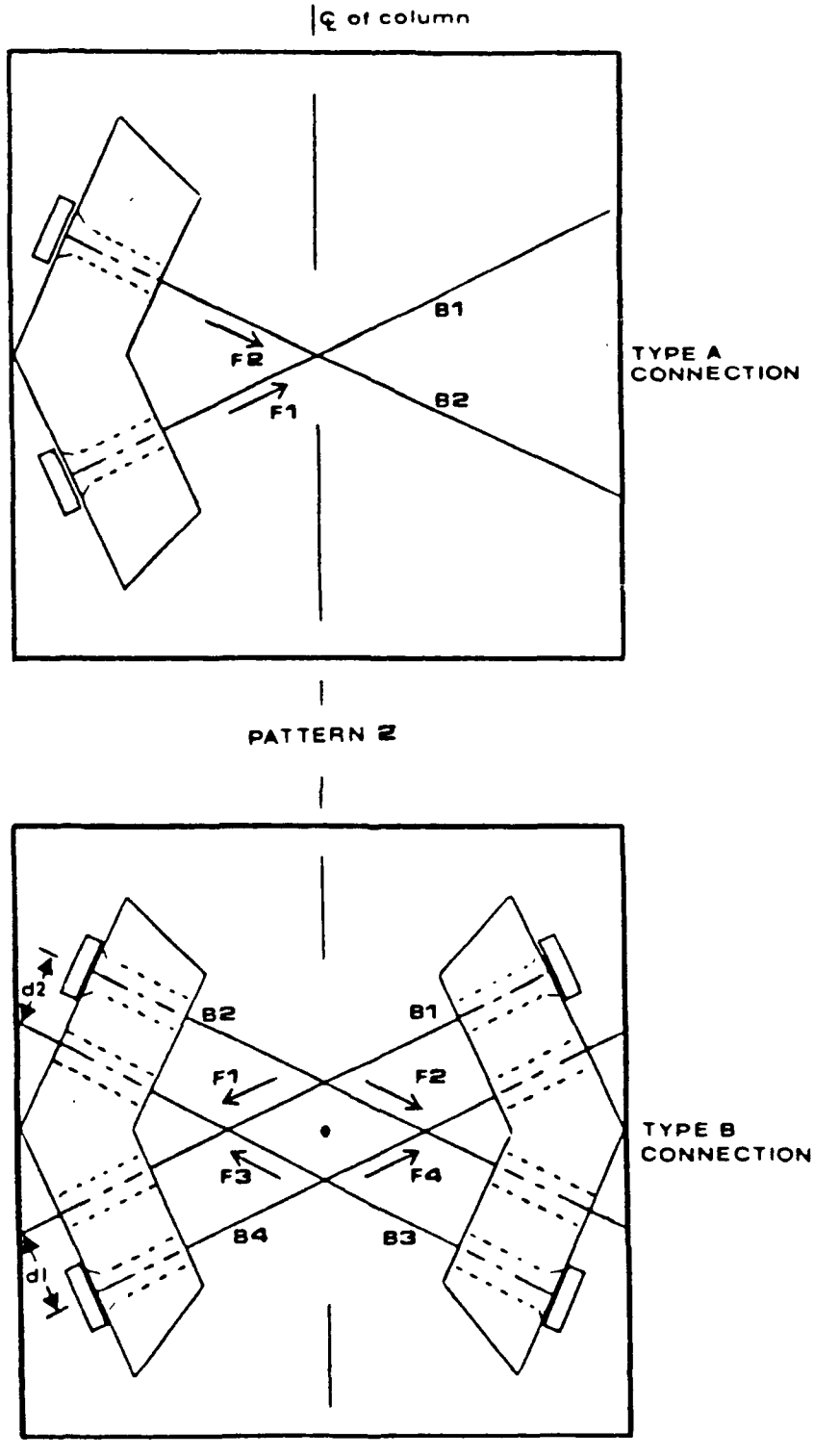

Fig. 6.8 Conceptual sketch of Pattern 2 Type A and B connectors

CHAPTER 7

SUMMARY AND CONCLUSIONS

7.1 SUMMARY

The objective of this thesis is to study analytically the effectiveness of prestressed cable bracing systems in conjunction with beam alteration as a viable retrofit strengthening scheme for seismically inadequate structures. Structures which are likely candidates for seismic retrofitting are inadequate for two primary reasons: 1) their lateral load carrying capacity is insufficient to sustain seismic loading specified in current building codes and/or, 2) the unstrengthened structures feature an undesirable failure mechanism such as failure of the columns in shear.

The prototype frame studied in this thesis is typical a class of building commonly constructed during the 50's and 60's in California and elsewhere. The reinforced concrete prototype frame features deep spandrel beams and short columns. The structure is six stories high and eleven bays long. The external frames are adequate to carry gravity loads but are deficient in lateral capacity. The prototype frame's failure mechanism is non-ductile and is dominated by shear failure of the reinforced concrete short columns.

The analytical study was carried out using DRAIN-2D. DRAIN-2D is a general purpose computer program for the dynamic analysis of inelastic plane frame structures. The current version of the program features element EL7, a reinforced concrete element with degrading stiffness. With EL7 one is able to model the negative lateral stiffness exhibited

by a reinforced concrete short column once its shear capacity has been reached. An option has been added to the program which utilizes the program's existing dynamic analysis algorithm to perform static incremental displacement analysis.

In the first part of the study the effectiveness of prestressed cable braces applied to a single story subassemblage of the prototype frame was re-examined. The concept of beam alteration or beam weakening was then introduced. A single story subassemblage was studied under several beam alteration schemes. The affect of systematically weakening the spandrel beams on the frame's failure mechanism was determined. An optimum beam alteration scheme was selected for the subassemblage. The response of unstrengthened, braced-unaltered and braced-altered subassemblages were studied under both monotonic and cyclic loading.

The second part of this research expanded on the first part by focusing on the behavior of a six story subassemblage of the prototype frame to retrofit strengthening. The remaining four levels of the prototype frame were designed in accordance with building codes and design procedures in common use when such structures were originally constructed.

The response of unstrengthened, braced-unaltered, and braced-altered unique single story subassemblages were studied and compared to the response predicted by a six story subassemblage. The influence of changing brace areas at various elevations of the frame was evaluated by contrasting the response of a generic subassemblage to the response obtained from analyzing a six story subassemblage retrofitted with different brace area schemes (with and without beam alteration). The

retrofit schemes studied were also evaluated with respect to their adequacy for meeting current building code seismic strength requirements.

The third part of this thesis focused on examination of some practical aspects of designing and installing prestressed cable bracing systems. Several design considerations were introduced which must be addressed to practically implement prestressed cable bracing. Finally, conceptual connection details were presented which illustrated how prestressed cable braces might be attached to a structure in a retrofitting operation.

7.2 CONCLUSIONS

The following conclusions can be drawn from this study of retrofitting seismically deficient reinforced concrete frames with prestressed cable bracing systems and beam alteration:

1) A prestressed cable bracing system applied to the weak column-strong beam frame studied is effective in increasing lateral strength. Following either the ultimate strength or serviceability design approach, any reasonable desired strength can be attained by choosing an appropriate design ratio n for use in determining cable areas required.

2) The use of prestressed cable bracing alone on the prototype frame improves the ductility of the strengthened system (assuming the columns can maintain gravity load capacity). The additional ductility is solely attributable to the bracing, as the frame's failure mechanism is unaltered.

3) Beam alteration is an effective means of altering the failure mechanism of the original frame studied. Failure can be shifted from the columns to the beams by selectively reducing the strength and stiffness of the beams. It was determined that the moment capacity of the prototype spandrel beams at midspan, as well as shear capacity at the spandrel ends, were sufficient to carry gravity loads even if all primary positive and negative reinforcement is severed. As a result, it is possible to weaken the beams sufficiently to ensure that plastic hinges form in the beams prior to the columns reaching their ultimate shear capacity. Ultimate strength of the original frame is greatly reduced by weakening the beams. The improvement in frame ductility, however, is dramatically improved.

4) The cyclic behavior of the prototype frame is dramatically improved with use of beam weakening. Evaluation of the hysteretic behavior of the original and altered frames indicates the altered frame will dissipate significantly more energy during a seismic event.

5) The consequential reduction in frame lateral strength resulting from beam weakening can be restored by supplemental use of prestressed cable braces. Combination of prestressed cable bracing and beam alteration results in dramatic improvements in strength, ductility, and failure mechanism.

6) For a given cable brace area, ultimate lateral strength attained by the retrofitted prototype frame is significantly increased if beam weakening is part of the retrofitting scheme. The trade off is that the increased ultimate strength is achieved at a much greater drift. The strength attained with the prestressed cable brace/beam

alteration scheme can be made to equal that attained by the bracing only scheme at lower drift levels by increasing the cable brace area. For the retrofit scheme studied, a 43% increase in cable brace area resulted in a 25% increase in stiffness in the retrofitted system.

7) For symmetric reinforced concrete frame structures with uniform bracing in every bay, global frame response can be predicted accurately by analysis of unique single story subassemblages established for each story, as well as by multi-story subassemblage models.

8) The value of using a single generic single-story subassemblage to represent the global behavior of a frame to retrofit strengthening is somewhat limited. Comparable results with analysis of a multi-story subassemblage can be obtained for a bracing scheme consisting of uniform bracing in all bays and cable brace size determined uniquely for each story using a constant design ratio n. For cases utilizing constant brace areas over several stories, unique single story subassemblages for each story in the frame should be developed.

9) Any practical retrofitting scheme will be based most likely on two types of objectives. The primary objective will likely be to increase the lateral strength capacity of the original frame at each story to that required to resist current building code design loads. The second objective might be a serviceability, or drift criteria. Such a criteria might be to prevent shear failure of the columns from occurring at low drifts as in the prototype frame studied. To meet such objectives, the required design ratio n can be established for each individual story. In the case the prototype frame studied, higher

design strength ratios are required for the first three stories than for the upper three stories.

10) Actual application of practical prestressed cable bracing systems introduces several design and installation considerations not investigated in this analytical study. Some of these considerations are briefly discussed below.

a) Location of post-tensioning anchors. The magnitude of the prestressing forces applied to the cable braces may introduce excessive internal stresses to the original frame. For the prototype frame examined in this study, the beam-column joints are more able to resist unbalanced prestress forces than connection points located at the midspan of the spandrel beams.

b) Post-tensioning sequence. Inattention to the post-tensioning sequence of the cable braces can also introduce excessive internal stresses to the original frame. The forces introduced at a typical interior joint by prestressed cable braces will balance or nearly balance each other after installation. Any resulting unbalance should be small and is transferred to the concrete frame. If post-tensioning of cables terminating at the joint is not executed either simultaneously or incrementally, the resulting unbalanced force, however temporary, is transferred directly to the concrete frame. Care must be taken to eliminate or minimize such situations. If not avoidable one must ensure that such induced stresses do not fail the concrete frame.

c) Out-of-plane forces. In the prototype frame studied the face of the columns and the spandrel beams are not flush. Installation of the bracing system therefore introduces additional out-of-plane forces to the system. Such eccentricities impose torque in addition to bending on the frame columns. This problem is predominant during the post-tensioning operation on all bays; however, it will persist on columns adjacent to unbraced bays even after post-tensioning is complete. The magnitude of such out-of-plane forces must be evaluated and considered with respect to the capacity of the frame to carry these forces.

7.3 RECOMMENDATIONS FOR FUTURE RESEARCH

EXPERIMENTAL RESEARCH: Experimental tests using prestressed cable braces and beam alteration are needed to verify the analytical conclusions made in this study. A single story subassemblage such as those developed in this study for the prototype frame could form the basis for an experimental study.

The most challenging task to be encountered in setting up an experimental study will lie in designing and fabricating the post-tensioning anchor blocks. The connections in the bracing system must not be the weak link in the system under cyclic loading.

Experimental research is necessary to confirm the effectiveness of improving the seismic performance of a prestressed cable braced frame with weak columns by weakening the beams. Various possible weakening

techniques including sawing and coring should be investigated. Guidelines for the design of weakening schemes should be developed.

ANALYTICAL RESEARCH: The research conducted in this study advances knowledge of prestressed cable bracing system behavior in conjunction with beam alteration. Analysis was limited to inelastic monotonic and cyclic incremental displacement analysis. The next step is to perform a dynamic analysis as well to assess the behavior of the retrofitted system to a more realistic loading scenario. A dynamic analysis may reveal some unforeseen problems not encountered in the static incremental analysis.

The global behavior of the prototype frame was studied with respect to vertical distribution of cable brace area. It would be interesting to expand the model to include the entire frame in order to study the effect of horizontal spacial distribution of prestressed cable braces. Such a study should be performed using a dynamic analysis. Further analytical work needs to focus on developing design guidelines for developing practical prestressed cable area and beam weakening schemes required to meet the designer's retrofitting objectives.

DRAIN-2D should be revised to increase its usefulness as a research tool. The program is written in out-dated FORTRAN language and is configured to run on main frame computer systems of vintage 1970 type. The numerous changes and additions made to the program by various users over the years has made troubleshooting the version of the program used for this study a nightmare. A project could be undertaken to rewrite the program, from the ground up, with modern FORTRAN language and state-of-the-art data storage and processing techniques. The rewritten

program should be well documented with a revised user's manual format and adequate comment statements within the program itself.

REFERENCES

1. Kanaan, A. and Powell, G., "DRAIN-2D, A General Purpose Computer Program For Dynamic Analysis Of Inelastic Plane Structures With User's Guide And Supplement," Earthquake Engineering Research Center, University of California Report No. EERC 73-6 and 73-22, August 1975.

2. Masroor, T., "Seismic Strengthening Of Reinforced Concrete Structures Using Prestressed Cable Bracing System," unpublished Masters thesis , The University of Oklahoma, May 1990.

3. Badoux, M., "Seismic Retrofitting Of Reinforced Concrete Structures With Steel Bracing Systems," unpublished Ph.D. dissertation, The University of Texas at Austin, May 1987.

4. Tang, X. and Goel, S., "DRAIN-2DM Technical Notes And User's Guide," Reasearch Report UMCE 88-1, Department of Civil Engineering, University of Michigan at Ann Arbor, January 1988.

5. Umehara, H., and Jirsa, J., "Shear Strength and Deterioration of Short Reinforced Concrete Columns under Cyclic Deformations," PMFSEL Report No. 82-3, The University of Texas at Austin, July 1982.

6. Woodward, K., and Jirsa, J., "Influence of Reinforcement on the Reinforced Concrete Short Column Lateral Resistance," ASCE Journal of Structural Engineering, Vol. 110, No. 1, January 1984.

7. Bush, T., "Seismic Strengthening of a Reinforced Concrete Frame," unpublished Ph.D. dissertation, The University of Texas at Austin, May 1987.

8. Sugano, S., and Fujimura, M., "Seismic Strengthening of Existing Reinforced Concrete Buildings," Proceedings of the Seventh World Conference on Earthquake Engineering, Part I, Vol. 4, Istanbul, Turkey, 1980, pp. 449-456.

9. American Concrete Institute, Building Code Requirements for Reinforced Concrete (ACI 318-89), Detroit, MI, 1989.

10. American Concrete Institute, "ACI Building Code," Journal of the American Concrete Institute, Detroit, MI, April 1951.

11. American Concrete Institute, Reinforced Concrete Design Handbook, 2nd Edition, American Concrete Institute, Detroit, MI, 1955.

12. Pacific Coast Building Officials Conference, Uniform Building Code 1955 Edition, Volume 3, Los Angeles, CA, 1955.

13. Collins, M. and Mitchell, D., Prestressed Concrete Structures, Prentice Hall, Englewood Cliffs, NJ 07632, 1991.

14. Keshavarzian, M., Schnobrich, W.C., Analytical Models for the Nonlinear Seismic Analysis of Reinforced Concrete Structures," Engineering Structures, 1985, Vol. 7.

15. International Conference Of Building Officials, Uniform Building Code, 1988 Edition, Whittier, CA, 1988.

APPENDIX A

REVISED USER'S GUIDE FOR DRAIN-2D MAIN PROGRAM WITH ELEMENTS EL7 AND EL1(m)

DRAIN-2D is a general purpose computer program for dynamic response analysis of planar inelastic structures under earthquake excitation. The program was originally developed by A. E. Kanaan and G. H. Powell in 1972 at the University of California at Berkeley [1]. The program has undergone several expansions and modifications since 1975 by various users at the University of Michigan at Ann Arbor [4], University of Texas at Austin [3], and the University of Oklahoma [2].

This appendix contains a complete user's guide for the program version used in this study. Data input specifications are given for elements EL7, reinforced concrete element with degrading stiffness, and EL1(m), truss element modified to model a prestressed cable brace. The reader is referred to the original user's manual found in reference [1] for data input instructions for other elements in the program library not used in this study.

INPUT DATA

The following input cards define the problem to be solved. Consistent units must be used throughout.

A. PROBLEM INITIATION AND TITLE

CARD A: Problem Initiation And Title (A5,3X,18A4). One card required.

Columns 1 - 5: Type "START"

6 - 8: Leave blank

16 - 80: Problem title (to be printed with output)

B: STRUCTURE GEOMETRY INFORMATION

CARD B1: Control Information (9I5,I10). One card required.

Columns 1 - 5: (NJTS) Number of nodes in the structure.

6 - 10: (NCONJT) Number of "control nodes" for which coordinates are specified directly. Equals number of B2 cards used.

11 - 15: (NCDJT) Number of B3 node coordinate generation cards used.

16 - 20: (NCDDOF) Number of B4 cards used to specify nodes with zero displacements.

21 - 25: (NCDDIS) Number of B5 cards used to specify nodes with identical displacements.

26 - 30: (NCDMS) Number of B6 cards used to specify EITHER lumped masses at the nodes if performing a dynamic analysis OR static loads or displacements at the nodes if performing a static incremental analysis.

31 - 35: (NELGR) Number of different element types used to describe the structure. See section E.

36 - 40: (KDATA) Data checking code. Leave blank or type a 0 to execute the program. Type 1 for a data checking run only. If the number of elements used in the structure does not exceed one, -1 can be typed to execute the program in core if desired.

41 - 45: (KODST) Structure stiffness storage code. A duplicate structural stiffness matrix must be retained and periodically updated. Leave blank or punch zero if this matrix is to be retained in the core. This will reduce input/output cost. Type 1 if the matrix is to be saved on scratch storage.

46 - 55: (TST) Blank COMMON length is assumed. If 0 or blank the value compiled into the program will be used. See discussion of capacity limitations in reference (1).

CARD B2: Control Node Coordinates (I5,2F10.0). One card for each control node. See NOTE 1 for more information.

Columns 1 - 5: *(IJT) Node number, in any sequence.*

6 - 15: X(IJT) X coordinate of node.

16 - 25: Y(IJT) Y coordinate of node.

CARD B3: Commands For Straight Line Generation Of Node Coordinates (415,F10.0). One card required for each generation command. Omit if there are no generation commands. See Note 1 for explanation.

Columns 1 - 5: (IJT) Number of the node at the beginning of the line to be generated.

6 - 10: (JJT) Number of the node at the end of the line to be generated.

11 - 15: (NJT) Number of nodes to be generated along the line.

16 - 20: (KDIF) Node number difference (constant value) between any two successive nodes on the line. If blank or 0, assumed to be equal to 1.

21 - 30: (PROP) Spacing between successive nodes on the generated line. If blank or 0, the nodes are automatically spaced uniformly along the generation line. If greater than 1.0, input value is assumed to be actual spacing. If less than 1, assumed to be the actual spacing divided by the length of the generation line.

CARD B4: Commands For Nodes With Zero Displacements (6I5). One line required for each command. Omit if no nodes are constrained to have zero displacements. See NOTE 2 for more information.

Columns 1 - 5: (IJT) Node number, or number of first node in a series of nodes covered by this command.

6 - 10: (KDOF(1)) Code for X displacement. Type 1 if X is constrained to zero, otherwise leave blank or type 0.

11 - 15: (KDOF(2)) Code for Y displacement.

16 - 20: (KDOF(3)) Code for rotation.

21 - 25: (JJT) Number of last node in the series. Leave blank if this command covers only a single node.

26 - 30: Node number difference (constant value) between successive nodes in the series. If blank or 0, the program assumes difference is 1.

CARD B5: Commands for Nodes with Identical Displacements (16I5). One line required for each command. Omit if no nodes are constrained to have identical displacements. See NOTE 3 for more information.

Columns 1 - 5: (KODOF) Displacement code as follows:

Type 1 for X displacement.

Type 2 for Y displacement.

Type 3 for rotation.

6 - 10: (NJT) Number of nodes covered by this command. Maximum is 14. See NOTE 3 for procedure when more than 14 nodes have identical displacements.

11 - 80: (IJOINT(I)) List of nodes in increasing numerical order. Up to 14 fields, I5 each.

CARD B6: Commands For Lumped Masses At The Nodes If Performing A Dynamic Analysis (I5,3F10.0,2I5,F10.0) OR Commands For Loads Or Displacements At The Nodes If Performing A Static Incremental Analysis (I5,3F10.0,2I5,F10.0). One line required for each command.

Columns 1 - 5: (IJT) Node number, or number of first node in a series of nodes covered by this command.

6 - 15: (FMAS(1))

If performing a dynamic analysis:

Mass associated with X displacement (may be zero)

If performing a static incremental analysis:

Portion of load or displacement associated with the X direction.

16 - 25: (FMAS(2))

If performing a dynamic analysis:

Mass associated with Y displacement. May be zero.

If performing a static incremental analysis:

Portion of load or displacement associated with Y direction.

26 - 35: (FMAS(3))

If performing a dynamic analysis:

Rotary Inertia. May be zero.

If performing a static incremental analysis:

Leave blank, not used.

36 - 40: (JJT) Number of last node in the series. Leave blank for a single node.

41 - 45: (KDIF) Node number difference between successive nodes in a series. If blank or 0, assumed to be equal to 1.

46 - 55: (SSCALE) Modifying factor.

If performing a dynamic analysis:

Factor by which the masses are divided. If blank or 0 the factor from the previous command is used. Typically the factor is g and the mass values are given as weights.

If performing a static incremental analysis:

Type 1.

C. LOAD INFORMATION

CARD C1: Load Control Information (3I5,6F10.0). One card required.

Columns 1 - 5: (KSTAT) Static load code OR static incremental analysis code. Type 1 if static loads are to be applied before the dynamic loads OR if static loads or displacements are to be applied before the static incremental loads or displacements. Leave blank or type 0 otherwise.

6 - 10: (NCDLD) Number of commands specifying static loads applied at the nodes before dynamic loads or before static incremental load analysis (if code in card C1(a) is 1). See CARD C2. Leave blank or type 0 if there are no static loads applied directly at the nodes.

11 - 15: (NSTEPS) Number of integration time steps to be considered in the dynamic analysis OR the number of static incremental load or displacement cycles to be performed in the static incremental analysis.

16 - 25: (DT) Integration time step for dynamic analysis. Increment for static incremental load or displacement analysis. Type 1 for static incremental analysis.

26 - 35: (FACAXH) Magnification factor to be applied to ground accelerations specified for the X direction. See Note 5 for additional explanation.

36 - 45: (FACTMH) Magnification factor to be applied to time scale of the record specified for the X direction. See Note 5.

46 - 55: (FACAXV) Magnification factor for ground accelerations in the Y direction.

56 - 65: (FACTMV) Magnification factor for time scale in the Y direction.

66 - 75: (DISMAX) Absolute value of the maximum displacement permitted before the structure can be assumed to have collapsed. The execution is terminated if this value is exceeded at any step. If zero or blank, value is assumed to be very high.

CARD C1(a). Static Incremental Analysis Information (format free, separate with commas).

Columns NA: (MSTAT) Static incremental load analysis code. Type 1 if analysis is required. Otherwise leave blank or type zero.

NA: (KSTDS) Static incremental displacement analysis code. Type 1 if analysis is required. Otherwise leave blank or type 0.

NA: (NCDDS) Number of commands specifying static displacements applied at the nodes before cyclic incremental displacement analysis. Leave blank or type 0 if there are no displacements applied. See CARD C2.

CARD C2: Commands For Static Loads Applied Directly At Nodes OR Commands For Static Loads Or Displacements Applied Directly at Nodes for Static Incremental Analysis (I5,3F10.0,2I5). One line required for each command. Omit if there are no static loads applied directly at the nodes (if static load code is 0 in card C1). Omit if there are no static loads or displacements applied directly at the nodes before the incremental analysis (if the static incremental analysis commands are 0 in card C1(a).

Columns 1 - 5: (IJT) Node number, or number of first node in a series of nodes covered by this command.

6 - 15: (FLD(1)) Load in the X direction, the same on all nodes in the series.

16 - 25: (FLD(2)) Load in Y direction, the same on all nodes in the series.

26 - 35: (FLD(3)) Moment load (right hand screw rule about the Z axis - hence counterclockwise positive as normally viewed).

35 - 40: (IJT) Number of last node in series. Leave blank for a single node.

41 - 45: (KDIF) Node number difference (constant) between successive nodes in series. If blank or 0, value assumed by the program is 0.

Note: A single node may appear in two or more commands if desired. In such a case, the total loads applied at the node will be the sum of the loads from the separate commands.

CARD C3: Acceleration Records For Dynamic Analysis Or Displacement Increments For Static Incremental Analysis.

CARD C3(a): Control Information (4I5,9A6). One card required.

Columns 1 - 5: (NPTH)

For dynamic analysis:

Number of time - acceleration pairs defining ground motion in the X direction. Type 0 or leave blank for no ground motion in this direction.

For static incremental analysis:

Number of load or displacement increments defining load or displacement history in the X direction (NPLDH). Type 0 or leave blank if there are no loads or displacements in this direction.

6 - 10: (NPTV)

For dynamic analysis:

Number of time - acceleration pairs defining ground motion in the Y direction. Type 0 or leave blank if no ground motion in this direction.

For static incremental analysis:

Number of load or displacement increments defining load or displacement history in the Y direction (NPLDV). Type 0 or leave blank if there are no loads or displacements in this direction.

15: (KFORM) Code for printing accelerations as input. Leave blank or type 0 for no output. Type 1 to get a listing of acceleration record.

20: Leave blank. Not used.

21 - 80: Title to identify records, to be printed with output.

CARD C3(b): Ground Acceleration Time History In X Direction For Dynamic Analysis Or Load / Displacement History For Static Incremental Analysis (12F6.0).

For Dynamic Analysis:

As many cards as needed to specify NPTH time - acceleration pairs, 6 pairs to a card, assumed to be in acceleration units (not multiples of the acceleration due to gravity). Omit if NPTH equals 0. Note that both the acceleration and time scales may be scaled if desired (see CARD C1). If the record is input in terms of the acceleration due to gravity, the accelerations must be multiplied by g to convert to acceleration units.

For Static Incremental Analysis:

As many lines as needed to specify NPLDH, number of increment - load / displacement pairs, 6 pairs to a line. Omit if NPLDH equals zero. The first specified step number must be zero, and the first load or displacement must be zero.

CARD C3(c): Ground Acceleration Time History In Y Direction For Dynamic Analysis Or Load / Displacement History For Static Incremental Analysis (12F6.0).

For Dynamic Analysis:

As many cards as needed to specify NPTV time - acceleration pairs. Omit if NPTV equals zero.

For Static Incremental Analysis:

As many lines as needed to specify NPLDV number of steps - incremental loads / displacement pairs, 6 pairs to a line. Omit if NPLDV equals zero. The first specified step number must be zero, and the first load or displacement must be zero.

CARD C4: DAMPING INFORMATION (4E10.0). One card. Refer to reference 4 for explanation.

Columns 1 - 10: Mass proportional damping factor, alpha.

11 - 20: Tangent stiffness proportion factor, beta.

21 - 30: Horizontal stiffness proportion factor, beta_o.

31 - 40: Structural damping factor, delta.

D. TIME HISTORY OUTPUT SPECIFICATION

Printed time histories of nodal displacements and element results may be obtained if desired. The printout is bulky and should not normally be requested.

CARD D1: Control Information (13I5). One card required.

Columns 1 - 5: (IPJ) Time interval for printout of nodal displacement time histories, expressed as a multiple of the time step delta t. Leave blank for no printout. The nodes for which the time histories are required are specified in CARDS D2, D3 and D4.

6 - 10: Time interval for printout of time histories of element results, expressed as a multiple of the time step delta t. Leave blank for no printout. The elements for which time histories are required are specified in CARD E.

11 - 15: (IENV) Output interval for results envelopes.

16 - 20: (NHOUT) Number of nodes (NHOUT) for which X displacement time histories are required.

21 - 25: (NVOUT) Number of nodes (NVOUT) for which Y displacement time histories are required.

26 - 30: (NROUT) Number of nodes (NROUT) for which rotation time histories are required.

Note: See program for additional input data required for more involved printouts.

CARD D2: List Of Nodes For X Displacement Time Histories (10I5). As many cards as needed to specify NHOUT node numbers, typed ten to a card. Omit if NHOUT equals 0.

CARD D3: List Of Nodes For Y Displacement Time Histories (10I5). As many cards as needed to specify NVOUT node numbers, typed ten to a card. Omit if NVOUT equals 0.

CARD D4: List Of Nodes For Rotation Time Histories (10I5). As many cards as needed to specify NROUT node numbers, typed ten to a card. Omit if NROUT equals 0.

CARD D5: List Of Pairs Of Nodes For Relative X Displacement History (10I5).

CARD D6: List Of Pairs Of Nodes For Relative Y Displacement History (10I5).

E. ELEMENT SPECIFICATION

For input and output, the elements must be divided into groups. All elements in any group must be of the same type, and typically all the elements of a single type will be included in a single group. However, elements of the same type may be subdivided into separate groups if desired.

Element groups may be input in any convenient sequence. Within any group, the elements must be numbered in sequence beginning with 1.

EL7. BEAM ELEMENT WITH NEGATIVE DEGRADING STIFFNESS. See reference 1 for complete description of the element. Number of words of information per element = 181.

CARD E7(a): Control Information For Group (7I5). One line required.

Columns 5: (I) Type 6 to indicate the group consists of EL7 elements.

6 - 10: Number of elements in the group.

11 - 15: Number of different element stiffness types (maximum of 40). See CARD E7(b).

16 - 20: Number of different end eccentricity types (maximum of 15). See CARD E7(c).

21 - 25: Number of different yield moment values for cross sections (maximum of 40). See CARD E7(d).

26 - 30: Number of different fixed end force patterns (maximum of 34). See CARD E7(e).

31 - 35: Number of different initial element force patterns (maximum of 30). See CARD E7(f).

CARD E7(b): Stiffness Types. Three lines for each stiffness type.

LINE 1: Beam Properties Data (I5,3F10.0,3F5.0).

Columns 1 - 5: (I) Stiffness type number, in sequence beginning with 1.

6 - 15: (FTYP(I,1)) Reference flexural stiffness, EI.

16 - 25: (FTYP(I,2)) Reference axial stiffness, EA.

26 - 35: (FTYP(I,3)) Effective shear stiffness, GA. If blank or 0, shear deformations are neglected.

36 - 40: (FTYP(I,4)) Flexural stiffness factor K_{ii}.

41 - 45: (FTYP(I,5)) Flexural stiffness factor K_{jj}.

46 - 50: (FTYP(I,6)) Flexural stiffness factor K_{ij}.

LINE 2: Hinge Stiffness Properties Data (I5,6F10.0). Refer to Fig. 3.10.

Columns 1 - 5: Stiffness type number, in sequence beginning with 1 and corresponding to the stiffness type number on the preceding Beam Properties Line.

6 - 15: Stiffness ratio of branch AB in proportion to the initial stiffness OA of the moment - rotation

relationship for inelastic - flexure at node i. If a non zero hinge stiffness is specified for node i on LINE 3, columns 6-15, then this ratio will apply directly to the hinge moment - rotation relationship or cantilever P-delta relationship.

16 - 25: Stiffness ratio of branch BC in proportion to initial stiffness OA of the moment - rotation relationship for inelastic - flexure at node i. Same for branch AB, a zero or nonzero hinge stiffness for node i on LINE 3, column 6-15 will control whether this ratio is directly applied to the hinge alone or to the beam as a whole. For column negative stiffness this value must be input as negative.

26 - 35: Stiffness ratio of branch CD in proportion to initial stiffness OA of the moment - rotation relationship for the inelastic - flexure at node i. Same as for branch AB, a zero or non zero hinge stiffness for node i on LINE 3, columns 6-15 will control whether this ratio is directly applied to the hinge alone or to the beam as a whole. For negative stiffness this value must be input as negative.

36 - 45: Stiffness ratio of branch AB in proportion to initial stiffness OA of the moment - rotation

relationship for inelastic - flexure at node j. If a non zero hinge stiffness is specified for node j on LINE 3, columns 16-25, then this ratio will apply directly to the hinge moment - rotation relationship or cantilever P-delta relationship.

46 - 55: Stiffness ratio of branch BC in proportion to initial stiffness OA of the moment - rotation relationship for inelastic - flexure at node j. Same for branch AB, a zero or nonzero hinge stiffness for node j on LINE 3, column 16-25 will control whether this ratio is directly applied to the hinge alone or to the beam as a whole. For column negative stiffness this value must be input as negative.

56 - 65: Stiffness ratio of branch CD in proportion to initial stiffness OA of the moment - rotation relationship for the inelastic - flexure at node j. Same as for branch AB, a zero or non zero hinge stiffness for node j on LINE 3, columns 16-25 will control whether this ratio is directly applied to the hinge alone or to the beam as a whole. For negative stiffness this value must be input as negative.

LINE 3: Hinge Stiffness Properties Data 2 (I5,4F10.0).

Columns 1 - 5: Stiffness type number, in sequence beginning with 1

and corresponding to the stiffness type number on the preceding Beam Properties line.

6 - 15: Hinge stiffness at node i. Leave blank or zero if the hinge properties are to be determined by the program. If blank or zero, the following field for node j must also be blank or zero. If non zero, the following field for node j must also be non zero.

16 - 25: Hinge stiffness at node j.

26 - 35: Unloading stiffness parameter for end i.

36 - 45: Unloading stiffness parameter for end j.

CARD E7(c): End Eccentricities (I5,4F10.0). One line for each eccentricity. Omit if there is no eccentricity. All eccentricities are measured from the node to the element ends. See reference 4.

Columns 1 - 5: End eccentricity type number, in sequence beginning with 1.

6 - 15: X_i = X eccentricity at end i.

16 - 25: X_j = X eccentricity at end j.

26 - 35: Y_i = Y eccentricity at end i.

36 - 45: Y_j = Y eccentricity at end j.

CARD E7(d): Cross Section Yield Interaction Surfaces (I5,6F10.0). Refer to Fig. 3.10.

Columns 1 - 5: Yield surface number, in sequence beginning with 1.

6 - 15: Positive moment at point A of the moment - rotation curve of the element.

16 - 25: Negative moment at point A of the moment - rotation curve of the element.

26 - 35: Positive moment at point B of the moment - rotation curve of the element.

36 - 45: Negative moment at point B of the moment - rotation curve of the element.

46 - 55: Positive moment at point C of the moment - rotation curve of the element.

56 - 67: Negative moment at point C of the moment - rotation curve of the element.

CARD E7(e): Fixed End Force Patterns (2I5,6F10.0). One card for each fixed end force pattern. Omit if there are no fixed end forces.

Columns 1 - 5: Pattern number.

10: Axis code, as follows:

Code = 0: Forces are in the element coordinate system. See reference 1.

Code = 1: Forces are in the global coordinate system. See reference 1.

11 - 20: Clamping force, F_i.

21 - 30: Clamping force, V_i.

31 - 40: Clamping force, M_i.

41 - 50: Clamping force, F_j.

51 - 60: Clamping force, V_j.

61 - 70: Clamping force, M_j.

CARD E7(f): Initial Element Force Patterns (I5,6F10.0). One card for each initial force pattern. Omit if there are no initial forces.

Columns 1 - 5: Pattern number, in sequence beginning with 1.

6 - 15: Initial axial force, F_i.

16 - 25: Initial shear force, V_i.

26 - 35: Initial moment, M_i.

36 - 45: Initial axial force, F_j.

46 - 55: Initial shear force, V_j.

56 - 65: Initial moment, M_j.

CARD E7(g): Element Generation Commands (12I5,2F5.0,I5,F5.0). One line for each generation command. Elements must be specified in increasing numerical order. Lines for the first and last elements must be included.

Columns 1 - 5: Element number, or number of the first element in a sequentially numbered series of elements to be generated by this command. See Note 6 for explanation of this generation procedure.

6 - 10: Node number at the element end i.

11 - 15: Node number at the element end j.

16 - 20: Node number increment for the element generation. If 0 or blank, assumed to be equal to 1.

21 - 25: Stiffness type number.

26 - 30: End eccentricity type number. Leave blank or zero if there is no end eccentricity.

31 - 35: Yield surface number for element end i.

36 - 40: Yield surface number for element end j.

45: Code for including geometric stiffness. Type 1 if geometric stiffness is to be included. Leave blank or type 0 if geometric stiffness is to be ignored.

50: Time history output code. If a time history of the element results is not required for the elements covered by this command, type 0 or leave blank.

If a time history printout, at the intervals specified on CARD D1, is required, type 1.

51 - 55: Fixed end force pattern number for static dead loads on the element. Leave blank if there are no dead loads. If the static load code, CARD C1, is 0, the fixed end force information is ignored.

56 - 60: Fixed end forces pattern number for the static live loads on the element. Leave blank if there are no live loads.

61 - 65: Scale factor to be applied to the fixed end forces due to static dead loads. Leave blank if there are no dead loads.

66- 70: Scale factor to be applied to fixed end forces due to static live loads. Leave blank or type 0 if there are no live loads.

71 - 75: Intial force pattern number. Leave blank or type zero if there are no initial forces.

76 - 80: Scale factor to be applied to initial element forces. Leave blank if there are no initial forces.

EL1(m): MODIFIED TRUSS ELEMENT. Number of words of information per element = 36.

CARD E1(a): Control Information For The Group (4I5). One line.

Columns 1 - 5: Type 1 to indicate that the group consists of truss elements.

6 - 10: Number of elements in the group.

11 - 15: Number of different element stiffness types (maximum is 40). See CARD E1(b).

16 - 20: Number of different fixed end force patterns (maximum is 40). See CARD E1(c).

CARD E1(b): Stiffness Types (I5,5F10.0,2I5). One line for each stiffness type.

Columns 1 - 5: Stiffness type number.

6 - 15: Young's modulus of elasticity.

16 - 25: Strain hardening modulus, as a proportion of Young's modulus.

26 - 35: Average cross sectional area.

36 - 45: Yield stress in tension.

46 - 55: Yield stress or elastic buckling stress in compression.

56 - 60: Buckling code. Type 1 if element buckles elastically in compression. Type 0 or leave blank if element yields in compression without buckling.

61 - 65: Prestressed cable bracing code. Type 1 for prestressed cable braces. Otherwise, leave blank or type 0.

CARD E1(c): Fixed End Force Patterns (2I5,4F10.0). One card for each fixed end force pattern. Omit if there are no fixed end forces.

Columns 1 - 5: Pattern number.

6 - 10: Axis code, as follows:

Code = 0: Forces are in the element coordinate system.

Code = 1: Forces are in the global coordinate system.

11 - 20: Clamping force F_i.

21 - 30: Clamping force V_i.

31 - 40: Clamping force F_j.

41 - 50: Clamping force V_j.

CARD E1(d): Element Generation Commands (9I5,2F5.0,F10.0). One line required for each generation command. Elements must be specified in increasing numerical order. Lines for the first and last elements must be included.

Columns 1 - 5: Element number, or number of first element in a sequentially numbered series of elements to be generated by this command. See Note 6 for explanation of generation procedure.

6 - 10: Node number at element end i.

11 - 15: Node number at element end j.

16 - 20: Node number increment for element generation. If 0 or blank, assumed to be equal to 1.

21 - 25: Stiffness type number.

26 - 30: Code for including geometric stiffness. Type 1 if geometric stiffness is to be included. Leave blank or type 0 if geometric stiffness is to be ignored.

31 - 35: Time history output code. If a time history of element results is not required for the elements covered by this command, type 0 or leave blank. If a time history printout (at the intervals specified on CARD D1) is required, type 1.

36 - 40: Fixed end force pattern number for static dead loads on the element. Leave blank or type zero if there are no dead loads.

41 - 45: Fixed end force pattern number for static live load on the element. Leave blank if there are no live loads.

46 - 50: Scale factor to be applied to fixed end forces due to static dead loads. Leave blank if there are no dead loads.

51 - 55: Scale factor to be applied to fixed end forces due to static live loads. Leave blank if there are no live loads.

56 - 65: Initial axial force on element, tension positive.

F. NEXT PROBLEM

The data for a new problem may follow immediately, starting with card A.

G. TERMINATION CARD (A4)

One card is needed to terminate the complete data set.

Columns 1 - 4: Type the word STOP.

NOTE 1. NODE COORDINATE SPECIFICATION

The "control node" coordinates must be defined with respect to the X, Y coordinate system. The coordinates of the remaining nodes may be generated using straight line generation commands (CARD B3). The number of nodes generated by each command may be one or any larger number. The coordinates of the two nodes at the beginning and end of the generation line must have been previously defined, either by direct specification or by previous straight line generation.

It is not necessary to provide generation commands for nodes which are (a) sequentially numbered between the beginning and end nodes of any straight line, and (b) equally spaced along that line. After all generation commands have been executed, the coordinates for each group of unspecified nodes are automatically generated assuming sequential numbering and equal spacing along lines joining the specified nodes immediately preceding and following the group. That is, any generation command with equal spacing and a node number difference of one is superfluous.

NOTE 2. NODES WITH ZERO DISPLACEMENTS

Each node of the structure may have up to three degrees of freedom,

namely X displacement, Y displacement and rotation. These are all displacements relative to the ground.

Initially the program assumes that all three degrees of freedom are present at all nodes (code = 0), and initializes the data arrays accordingly. If this assumption is correct, CARD B4 should be omitted. In some cases, however, either (a) certain nodes may be fixed relative to the ground in certain directions or (b) it may be reasonable to assume zero displacement. Any degree of freedom which is fixed is to be assigned a code = 1, and cards must be included to specify those nodes and degrees of freedom for which the codes are equal to 1.

If there is any doubt, it should be assumed that all nodes can displace with all three degrees of freedom (i.e. all codes = 0). If however, certain degrees of freedom can be eliminated, the computer time may be significantly reduced.

NOTE 3. NODES WITH IDENTICAL DISPLACEMENTS

It may often be reasonable to assume that certain nodes displace identically in certain directions. Identical displacements may be specified by the commands of CARD B5. The input format for this card limits to 14 the number of nodes covered by any single command. If more than 14 nodes are to be assigned identical displacements, two or more commands should be used, with the nodes in increasing numerical order in each command, and with the smallest numbered node common to all commands.

As with displacements which are constrained to be zero, greater computational efficiency may be achieved by specifying identical

displacements. However, whereas the specification of zero displacements will always decrease the structure stiffness band width or leave it unchanged, specification of identical displacements may increase this band width. The effect may be to increase the required structure stiffness storage and/or the computational effort required to solve the equilibrium equations. Identical displacements should therefore be specified with caution, and their effects on storage requirements and execution times should be investigated.

NOTE 4. SPECIFICATION OF LUMPED MASSES

The specification commands for lumped masses will generally permit the user to input the nodal masses with only a few cards. Any node may, if desired, appear in more than one specification command. In such cases the mass associated with any degree of freedom will be the sum of the masses specified in the separate commands. If certain nodes are constrained to have identical displacement, the mass associated with this displacement will be the sum of the masses specified for the individual nodes. Note that the masses are to be input in units of mass, not weight.

NOTE 5. SCALING OF EARTHQUAKE RECORDS

The acceleration scale factors may be used to increase or decrease the ground accelerations, or to convert them from multiples of the acceleration due to gravity to acceleration units. Modification of earthquake intensity by scaling the acceleration values is a common practice in research investigations, but should be undertaken cautiously

in practical applications. When the accelerations are scaled, the ground velocities and displacements are scaled in the same proportion.

Provision is also made to modify the time scale. If a time scale factor equal to, say, f, is specified, all input times are multiplied by f before obtaining the interpolated accelerations at intervals equal to the integration time step. If the ground accelerations remain unchanged, the effect is to increase the ground velocities by f and the ground displacements by f^2, and to alter the frequency content of the earthquake. Time scale modifications should not be made without carefully considering their influence on the ground motion.

NOTE 6. ELEMENT DATA GENERATION

In the element generation commands, the elements must be specified in increasing numerical order. Cards may be provided for sequentially numbered elements, in which each card specifies one element and the generation option is not used. Alternatively, the cards for a group of elements may be omitted, in which case the data for the missing group is generated as follows:

1. All elements are assigned the same stiffness, strengths, element load data and output code as the element preceding the missing group.
2. The numbers of the nodes for each missing element are obtained by adding the specified node number increment to the node numbers for the preceding element. The node number increment is that specified for the element preceding the missing group.

APPENDIX B

WORKED EXAMPLE WITH DRAIN-2D (BRACED SUBASSEMBLAGE)

In this section an example problem will be solved using the current version of DRAIN-2D. The revised user's manual given in Appendix A is applicable. Working this example will aid future researchers and interested readers to better understand the complicated data input required for this program. Additionally, the assumptions made by this researcher in modeling the subassemblage of the prototype structure will be made clear to those who may follow this research.

The problem worked here is that of the braced subassemblage of the prototype structure. The analytical model for the subassemblage is given in Fig. 2.10. The geometric and structural properties of the beam and column are given in Fig. 3.2. The input data is shown in Fig. B.1.

Cards A, B1, B2, B3, B4, B6, C1, C1a, C2, C3a, C3b, C4a, D1, D2, and E7a are self explanatory from the user's guide.

Card E7b. The initial column stiffness specified is calculated from data derived from the load deformation curve shown in Fig. 3.9 and $EI = (V)(L)^3/12(\Delta)$, where V = 38 kips, L = 72 inches, and Δ = .048 inches. EA and GA of the column are calculated based on the area of the uncracked transformed section, A_{tran} = 387.24 in^2. The option for having the program calculate the initial stiffness of the inelastic rotational springs is chosen in Card E7b(3) by inputing zeros in the appropriate fields for spring stiffnesses. As a result, the stiffness ratios specified in Card E7b(2) are simply the relative slopes of the load deformation curve in Fig. 3.9. The relative slopes of Fig. 3.9 are

also the relative slopes of the element moment rotation relationship. The moment rotation relationship for the column is obtained from the experimental load deformation curve of Fig. 3.9 by multiplying the load axis by 1/2 = 72/2, and dividing the drift axis by 1 = 72.

For the spandrel beams, the initial stiffness, EI/2, is calculated based on the uncracked transformed section. The uncracked transformed section includes a 48 inch length section of the 6 inch thick floor slab, EI/2 = (3122)(297,354)/2 = 464,169,594. Similarly, EA and GA are also calculated based on the area of the uncracked transform section, A_{tran} = 895.8 in^2. The program again calculates the initial stiffness of the inelastic rotational springs internally; therefore, the stiffness ratios specified in Card 7b(2) are the averaged ratios of the element's moment rotation relationship. The moment curvature diagram was first hand calculated for both positive and negative moment and used to derive the respective section moment rotation relationship at the beam ends. The curvature axis of the moment curvature relationship was multiplied by d/2 to obtain the moment rotation relationship. Because the spandrel beams are severely under reinforced (i.e. less than the minimum percentage of steel is provided) the positive cracking moment is larger than the positive yield moment. For simplicity, the model used by Badoux [3] for the beam element moment rotation relationship is utilized. The model is shown in Fig. 3.10. With this model, a reduced cracking moment is calculated based on the ultimate moment. Adjusting the cracking moments in this way makes it possible to specify the stiffness ratios of the moment rotation relationship in Card E7b(2) as applicable for both positive and negative moment.

Card E7d. The moments specified for the column are calculated again from the column load deformation curve in Fig. 3.9. The column is assumed to develop an inflection point at mid height. The moment is thus proportional to the shear force. The moment at points A, B, and C are then the shear at points A, B, and C of Fig. 3.9 multiplied by half the column effective height, 72/2 = 36 inches.

The moments specified for the spandrel beam are based on the hand calculated ultimate moment and Fig. 3.10. The calculated positive ultimate moment is 2013 kip-inches and the negative ultimate moment is 3186 kip-inches.

Card E7g, and G are self explanatory. A plot of the shear strength of the braced subassemblage vs cyclic lateral displacement at node 5 is shown in Fig. 4.11 with n = 2 and $0.5P_y$ prestress force.

```
START     BRACED SUBASSEMBLAGE (CYCLIC LOADING)(NON NORMALIZED)
    8     8    0    3    0    1    2
    1         0.         0.
    2       126.         0.
    3       252.         0.
    4         0.       120.
    5       126.       120.
    6       252.       120.
    7       126.        24.
    8       126.        96.
    1     0    1    0    4
    6     0    1    0    0
    2     1    1
    5        -1.         0.                                   1.
    0     0 4500          1.          1.                       1.
    0,1,1
    5     .00001
   14     0    1    1
    0.    0.0   10.   .050  100.   .090  250. -.140  400.   .250  600. -.27
 1200.   .610 1700. -.920 2200.  1.44 2600. -1.44 3000.  2.05 3400.-2.05
 4000.  2.16 4500. -2.16
        0.         0.         0.         0.
    1    0    0    1    0    0    0    0    2    0    0    0    0
    5
    6    7    4    0    3
    1 24624000.  1011528.   436000.   4.   4.   2.
    1   .149798  -.138158  -.003298   .149798  -.138158  -.003298
    1       0.0        0.0        0.1        0.1
    2464169594.  2796688.  1205747.   0.   3.   0.
    2   .091000   .091000   .000500   .091000   .091000   .000500
    2       0.0        0.0        0.1        0.1
    3464169594.  2796688.  1205747.   3.   0.   0.
    3   .091000   .091000   .000500   .091000   .091000   .000500
    3       0.0        0.0        0.1        0.1
    4999999999.999999999.         0.   4.   4.   2.
    4        1.         1.         1.         1.         1.         1.
    4      0.0        0.0        0.1        0.1
    1     1370.     -1370.     2700.     -2700.     -135.      135.
    2     1107.     -1752.     1560.     -2469.     2013.     -3186.
    3    10000.    -10000.    10000.    -10000.    11000.    -11000.
    1    1    2    3    2    0    2    2         1
    3    2    3    3    3    0    2    2         1
    5    7    8         1         1    1         1
    6    2    7         4         3    3         1
    7    5    8         4         3    3         1
    1    2    1    0
    1   26000.        .05       0.88       230.         0.    1    1
    1    1    5    0    1    0    1    0    0                   101.2
    2    3    5    0    1    0    1    0    0                   101.2
STOP
```

Fig. B.1 DRAIN-2D input data for the subassemblage